Institute of Thermoelectricity, Academy of Sciences and Ministry of Education and Science of Ukraine

Journal of THERMOELECTRICITY

International Research

Founded in December, 1993

published 6 times a year

No. 1 *2021*

Editorial Board

International Editorial Board

Founders – National Academy of Sciences, Ukraine
Institute of Thermoelectricity of National Academy of Sciences and Ministry of Education and Science of Ukraine

Certificate of state registration № КВ 15496-4068 ПР

Approved for printing by the Academic Council of Institute of Thermoelectricity of the National Academy of Sciences and Ministry of Education and Science, Ukraine

Address of editorial office:
Ukraine, 58002, Chernivtsi, General Post Office, P.O. Box 86.
Phone: +(380-372) 90 31 65.
Fax: +(380-3722) 4 19 17.
E-mail: jt@inst.cv.ua
http://www.jt.inst.cv.ua

Signed for publication 26.03.2021. Format 70×108/16. Offset paper №1. Offset printing.
Printer's sheet 11.5. Publisher's signature 9.2. Circulation 400 copies. Order 5.

Printed from the layout original made by "Journal of Thermoelectricity" editorial board
in the printing house of "Bukrek" publishers,
10, Radischev Str., Chernivtsi, 58000, Ukraine

CONTENTS

Rifert V.G., *doc. of techn. Sciences* [1]
Anatychuk L.I., *acad. of the NAS of Ukraine*[2,3]
Barabash P.O., *cand. of technical Sciences*[1]
Solomakha A.S. *cand. of technical Sciences* [1]
Usenko V.I., *cand. of technical Sciences* [1]
Petrenko V.G. *cand. of technical Sciences* [1]

[1]NTUU "Ihor Sikorskyi KPI", 6 Politekhnicheskaya str,
Kyiv, 03056, Ukraine, *e–mail: vgrifert@ukr.net*;
[2]Institute of Thermoelectricity of the NAS and MES of Ukraine,
1 Nauky str., Chernivtsi, 58029, Ukraine,
e–mail: anatych@gmail.com;
[3]Yuriy Fedkovych Chernivtsi National University,
2 Kotsiubynskyi str., Chernivtsi,
58012, Ukraine

JUSTIFICATION OF THERMAL DISILLATION METHOD WITH A THERMOELECTRIC HEAT PUMP FOR LONG-TERM SPACE MISSIONS

This article describes the main methods of thermal distillation that can be used for long-term space missions with humans. Their advantages and disadvantages are shown, the basic information on the characteristics of the systems, namely: productivity of the distillate, specific energy consumption per unit mass of the distillate and the quality of the distillate by evaporation (concentration) of aqueous NaCl solution, urine and mixtures – urine with condensate, with condensate and hygienic water. Restrictions that do not allow them to be used for flights and possible ways to solve them are indicated. Bibl. 36, Fig. 9, Table. 1.

Key words: thermoelectricity, heat pump, distiller.

Introducion

Wastewater treatment (liquid waste of human life) is critical for a successful human flight to the Moon and Mars [1 – 2]. Among all known wastewater regeneration systems, the most promising method is thermal distillation [3 – 4].

The principle of thermal distillation is based on the supply of heat to the initial solution, evaporation of water from the solution and condensation of the obtained steam. Thus, in the process of thermal distillation, there are stages of heat supply (evaporation) and heat removal (condensation), which makes it possible to use a heat pump to increase the efficiency of the system. In the conditions of weightlessness and rather small productivity the thermoelectric heat pump can work effectively. Its obvious advantage is the absence of moving parts, simplicity and reliability of construction.

A thermal vacuum compression centrifugal distiller has been installed at the only inhabited extraterrestrial object, the International Space Station (ISS), to regenerate wastewater. It has been operating

since 2008 and has processed more than 13 tons of water. This has significantly reduced the cost of its delivery (the cost of delivering 1 kg of cargo to the ISS is about $ 3.000. However, as already noted in many works, its design does not guarantee work in the case of long missions, and to eliminate this shortcoming is fundamentally impossible [5].

This article provides a brief overview and critical analysis of thermal distillation methods for operating conditions in weightlessness.

Static thermoelectric membrane distiller TIMES

This distiller was developed by Hamilton Seastrand Space Systems International in the 1970s [6-8].

The system uses a polymer membrane that selectively passes water from a wastewater source. Ideally, unwanted dissolved and undissolved solids do not pass through the membrane, and a high-quality distillate is obtained (Fig. 1). An important feature of TIMES is the overall recirculation of the feed stream, which becomes more and more concentrated during the distillation process. Energy consumption is minimized through the use of solid-state (immovable) heat pumps (thermoelectric devices).

The solution heated in the thermoelectric device is taken away by the circulating pump and passes through a special membrane, and the received water vapor condenses on the cold side of the thermoelectric device.

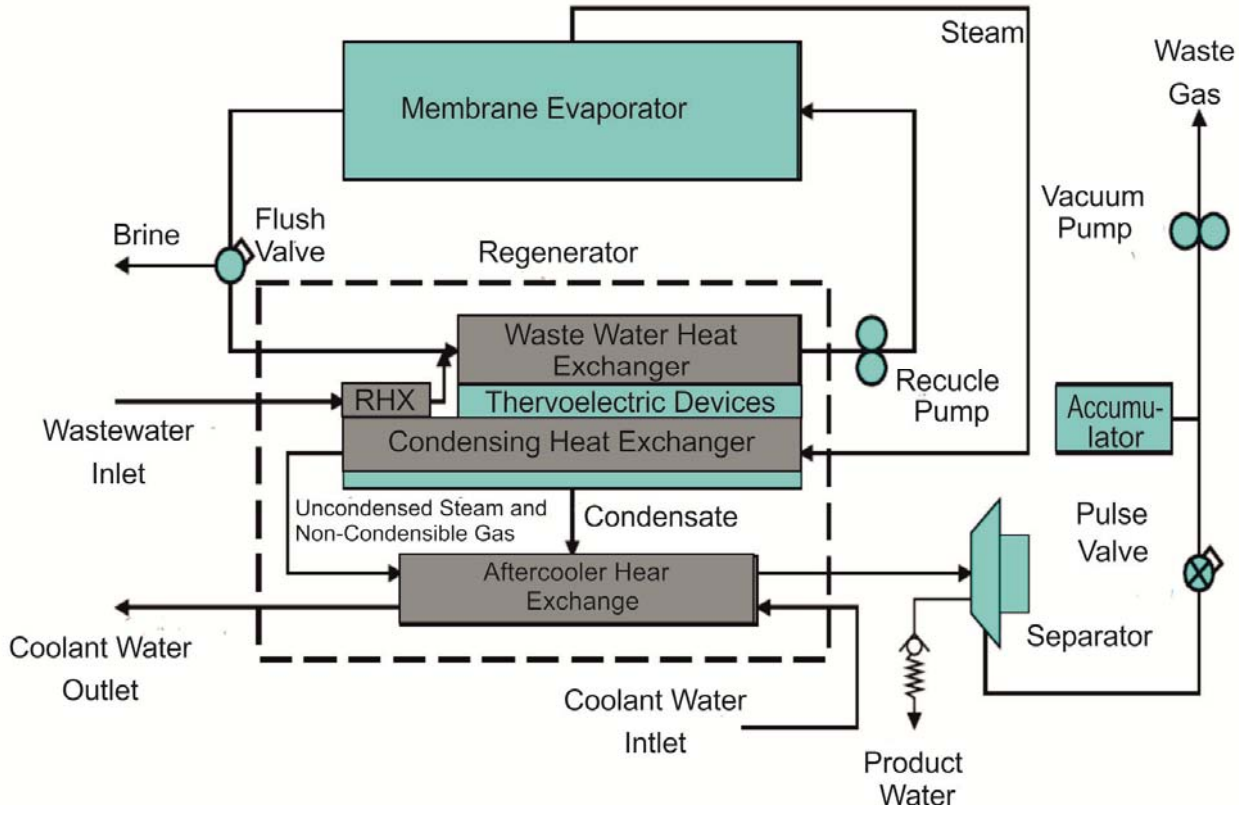

Fig. 1 Schematic diagram of TIMES

Based on the known equations and properties of semiconductors [7], a dimensionless diagram of thermoelectric characteristics was developed, which is shown in Fig.2.

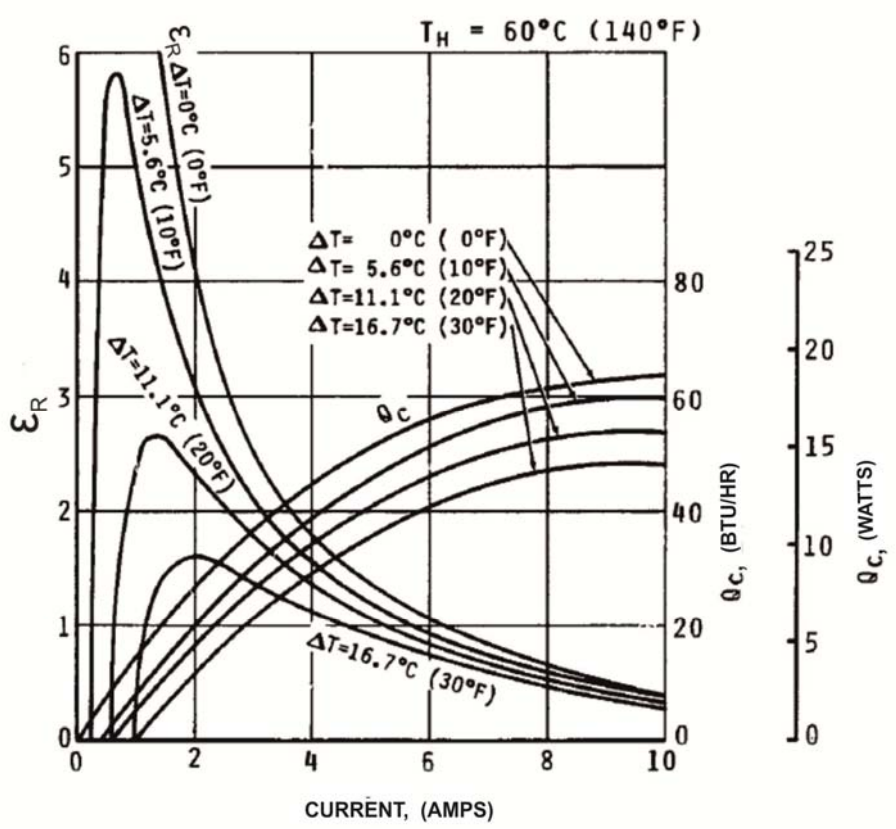

Fig. 2 Technical characteristics of the thermoelectric device

Thermoelectric efficiency (COP_R) is affected not only by the design of the condenser, but also by the area of the membrane, the rate of urine recirculation, the design of the urine heat exchanger, the thermoelectric current and the concentration of solids in wastewater, etc. As a result, in experimental trials in mild urine nominal COP_R approximately equaled 2.8. The main characteristics of the developed system are shown in Fig. 3.

Later TIMES was modified [8] to address the identified shortcomings: the membrane area was increased 2.6 times, the thermoelectric heat transfer area was increased 4.2 times, and the condenser was redesigned. The result of such modernization of the system was an increase in productivity when working on non-concentrated urine by 1.9 times and an increase in thermoelectric COP_R to 3.1 compared with the predicted theoretically $COP_R = 5$. Analysis of the system showed that the condensing heat exchanger is the main reason for this decrease in productivity. First, the flowing part of the condenser inefficiently removed water, which led to flooding of the heat exchange surface, resulting in the cessation of effective heat dissipation during condensation. Second, blocking all channels led to the accumulation of non-condensed gases in the condenser. This caused an increased thermal resistance of the condensation process, which further increased the thermoelectric temperature difference ΔT. Eventually, the pressure in the condenser increased until, at least through some of the channels, water was blown out, and the accumulation process began again. All this led to a very low energy efficiency of the system.

There were serious problems with the quality of the obtained water. Leaks were detected at the junction of the membranes and their collector. The second source of contamination is that dissolved solids inside the membranes are transported directly through the membrane walls when the membranes come into contact with the water condensate of the product inside the evaporator. The formation of condensate in the evaporator can occur during various transient modes of operation. The third reason for the decline in water

quality is the formation of water-soluble gases that can pass through membranes. The main undesirable gas is ammonia. Since the formation of ammonia depends on temperature, lowering the operating temperature of TIMES should lead to improved water quality. However, this required a transition to a lower operating pressure, and the design of TIMES condensing heat exchangers was sensitive to operating pressure, becoming less efficient at lower pressures.

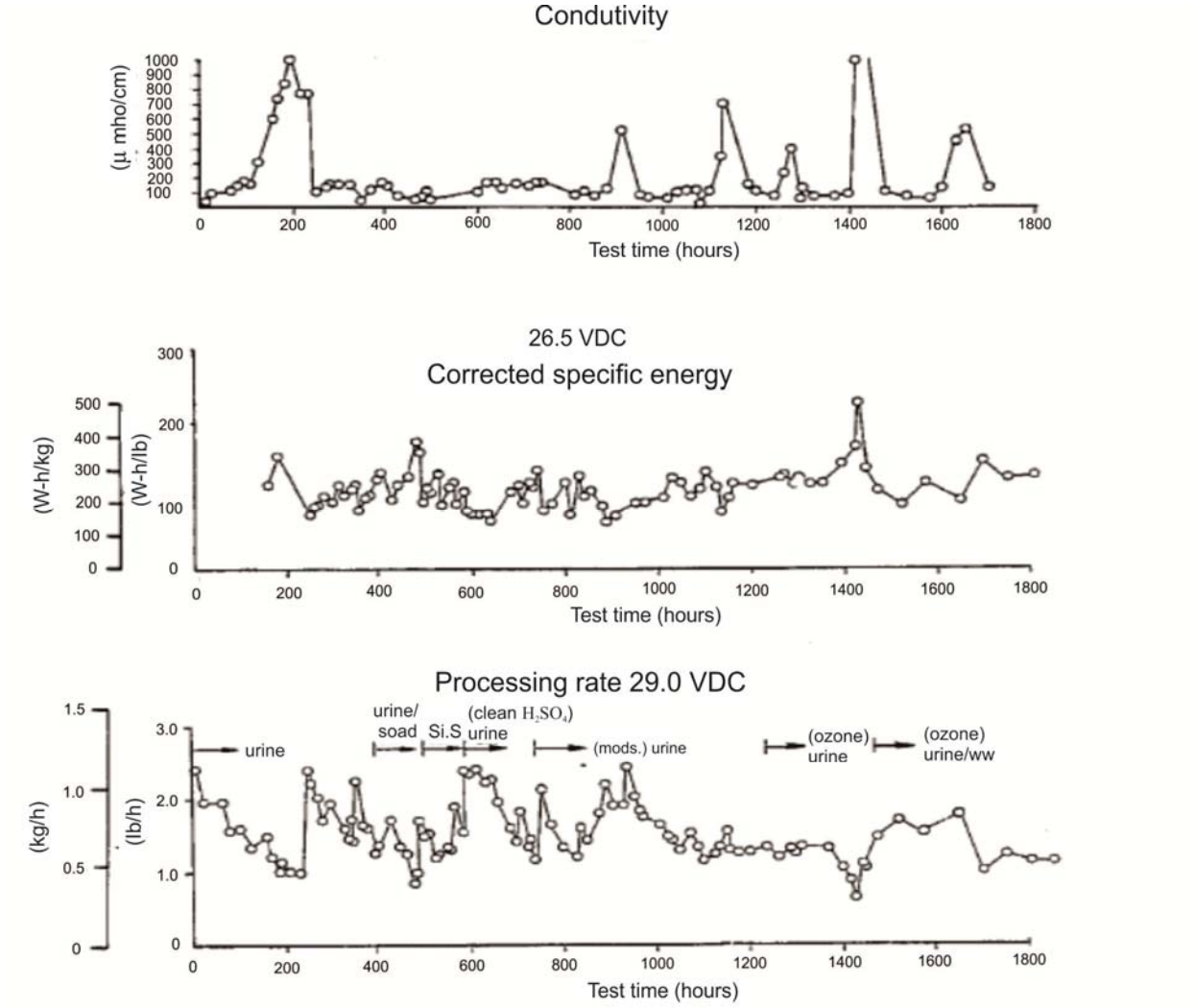

Fig. 3. Operating parameters of TIMES

In addition, the limiting concentration of liquid in the TIMES system is limited due to the deposition of salts in the pores of the membrane evaporator. Similar processes are observed in reverse osmosis membranes in the desalination of salt water with a concentration close to urine and a level of water up to 60 %.

Thus, despite an interesting idea, the TIMES system was unstable, especially in terms of energy efficiency and quality of the distillate. These shortcomings could not be eliminated without a radical change in the concept of the whole system. As a result, in the early 1990s, the development of the TIMES system virtually ceased, and for flight tests for urine processing on the International Space Station, a competitive VCD thermal distillation technology was chosen.

Centrifugal vapor compression distiller (VCD)

The steam compression centrifugal distiller (VCD) was created and manufactured in 1962 by order of NASA [9]. In 2008, the latest version of the VCD was installed on the ISS, where it continues to operate to this day. It produced more than 13 tons of distillate on the ISS [10].

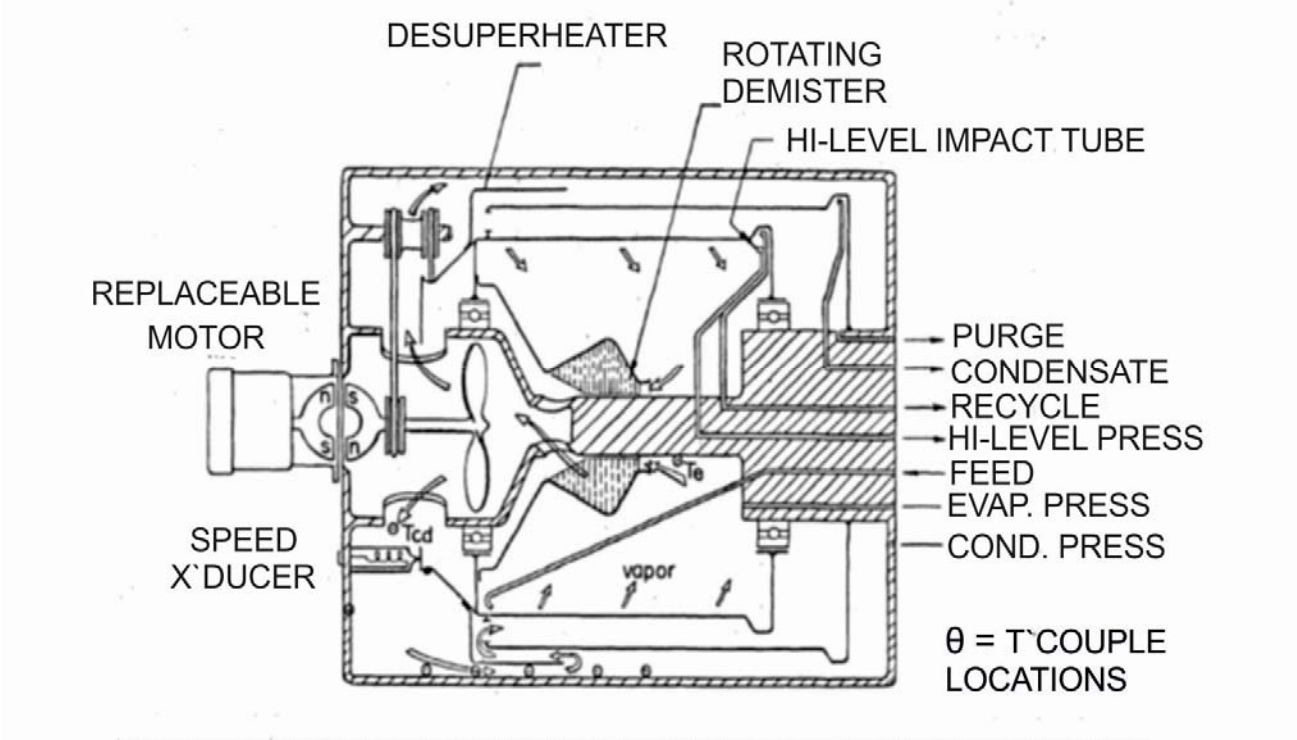

Fig. 4. Schematic diagram of VCD

Figure 5 shows the distillation unit, which is the main working component around which the VCD module is developed. Inside the distiller there are two main parts: a centrifuge for separating liquid and gas phases and a compressor. The centrifuge consists of two cylinders: an inner cylinder through which a film of evaporating liquid flows, and an outer cylinder designed to collect water droplets condensed on its surface. The compressor is designed to remove steam generated by evaporation, increase its temperature and pressure and supply it to the condenser. Not all liquid evaporates as it passes through the rotating cylinder; and the remainder, together with the solids that have been dissolved in the water, are discharged into an annular settler at the opposite end. The kinetic energy of the fluid is converted to static pressure, which is high enough to deliver fluid to the pump inlet without flashing. Similarly, the water condensed on the opposite side of the inner surface is collected in a rotating annular settling tank, taken by a stationary tube and sent to the inlet of the corresponding pump.

The compressor represents the two-rotor car with the drive from the electric motor, with a speed of 3600 rpm. To facilitate access, the engine is located outside the distiller. The synchronous magnetic coupling is used to transmit motor torque across the chamber boundary to the compressor inlet shaft without the need for dynamic shaft sealing. The centrifuge is driven by the compressor shaft through a belt and pulley system (centrifuge speed 290 rpm). A rotating demister is installed at the compressor inlet to exclude the ingress of liquid from the vapor stream. The distiller's water capacity when working on urine is about 1.3 l/h.

The specific energy consumption of the distillation unit significantly depends on the concentration of the solution (see Fig. 7).

More than 10 prototypes were manufactured for delivery to the station with detailed publication of the test results of these distillers [11]. Based on the results of operation on the ISS, information is provided on various damages in operation, both mechanical and problems with the quality of the distillate. Annually, reports at the ICES Life Support Conference provide information on the state of the system [10, 12 – 13].

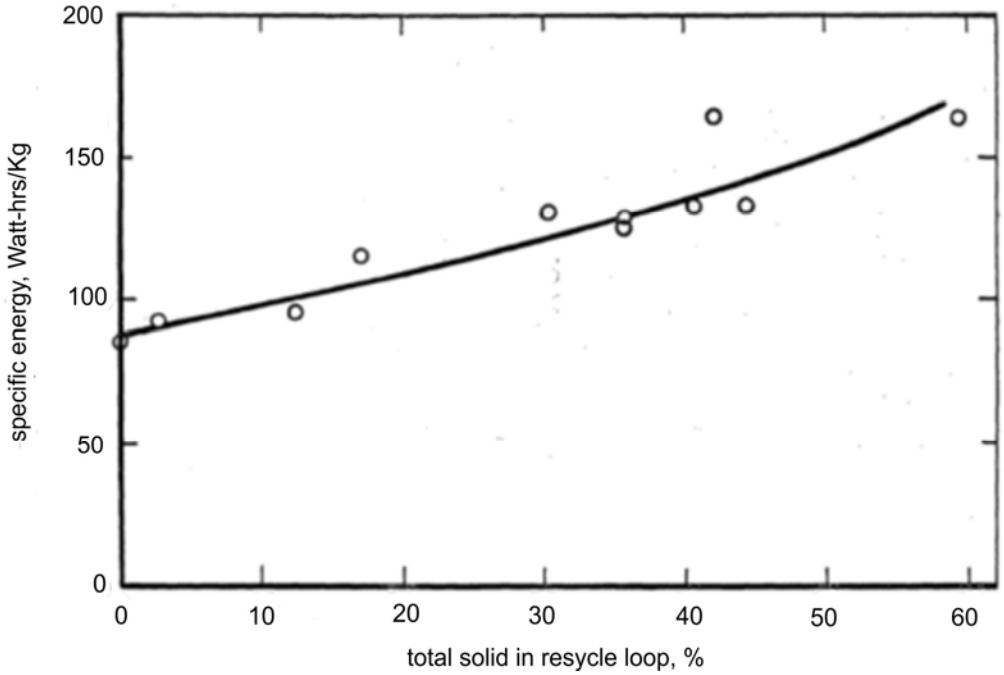

Fig. 5 The influence of concentration in the recirculation circuit on the specific energy consumption

Fig. 8 shows a graph of the total productivity of a vapor compression distiller in the period from 21.11.2008 to 21.11.2018 [10]. The average VCD productivity was 4 ... 5 l/day, did not exceed 1.8 l/h, the degree of water extraction was 75 %, and only after 2016 it was possible to increase it to 85 %. The main reason for low performance is the low heat transfer coefficient, which does not exceed 800 W/m^2. This is due to the low speed of the distiller centrifuge. Also in [9] it is noted that due to the peculiarity of the compressor, the inlet to the heat exchanger receives superheated steam. As a result, a significant part of the heat exchange surface is used for the inefficient process of cooling superheated steam and only then begins the condensation of steam.

As a result, despite the successful experience of VCD operation on the ISS, recent publications point to the impossibility of using this distiller for long space missions. For full-fledged space travel it has very low productivity (< 2 l/h), low efficiency (which also strongly depends on the solution being processed), in the design of the system there are inefficient peristaltic pumps for pumping liquid streams, the degree of regeneration 85 % is also insufficient for long missions. And what is very important, the presence of a complex steam compressor, in principle, does not allow guaranteeing uninterrupted operation for a long period of time, which is critically important for long space missions. These disadvantages cannot be eliminated without a complete restructuring of the distiller design.

Thus, there is a need to develop a system that would meet all the requirements for long flights.

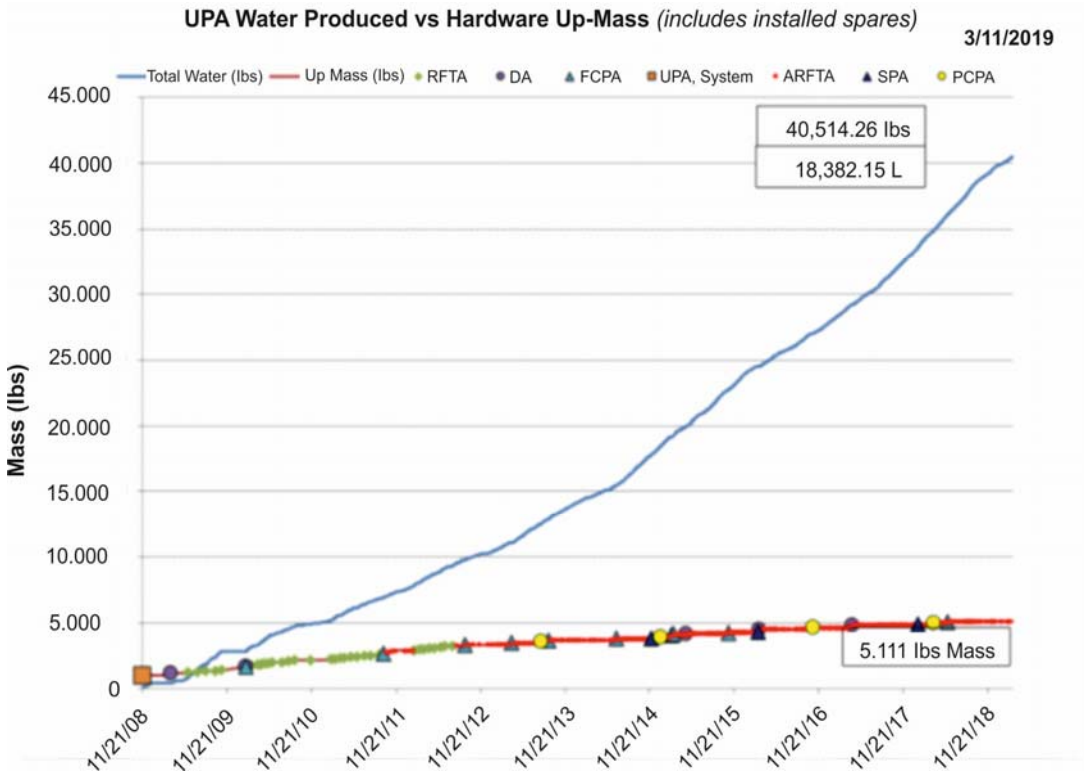

Fig. 6. Total and annual amount of distillate produced at ISS using VCD

Centrifugal wiped-film rotating disk distiller (WFRD)

The rotating disk evaporator was designed and tested at the UC Berkeley Water Technology Center [14 – 16].

Fig. 9*a* schematically shows the cross section of the distiller, and Fig. 9*b* is a schematic section of two pairs of disks. The rotor consists of disks connected together at the periphery to form cavities, and the cavities are also connected together at the periphery of the inner holes. The rotor is mounted on a hub closed at one end and open at the other. Steam is introduced through the open end and condenses on the inner surfaces of the rotary disks. The condensate formed on the inner surfaces of the discs is discharged to the periphery, where it enters the stationary product tubes (scoops) connected to the central tube and flows out of the evaporator as a distillate. The rotor rotates along a horizontal axis inside the chamber, into which an aqueous solution is fed along the length of stationary scrapers (Fig. 9*b*, and is distributed in the form of a thin uniform film on the outer surfaces of the rotary discs without the formation of dry spots. Non-evaporated liquid is discharged to the periphery of the discs and removed from the chamber. The use of centrifugal force and a scraper leads to a decrease in the thickness of the distillate film, which increases the heat transfer coefficient.

The system operated stably at an evaporation temperature of 60 °C, flat disks were made of copper with a thickness of 0.036 inches, the heat transfer coefficient reached 60 kW/m^2 at a temperature difference of 0.1 to 3 °C.

The initial solution was passed through a cartridge type filter, regenerative heat exchanger, degasser and then fed to the evaporator. Part of the liquid was evaporated from the initial solution, and the residue was pumped from the bottom of the chamber into a regenerative heat exchanger for cooling. The formed steam was removed by an external compressor, compressed to increase the pressure and saturation temperature, and then fed into the cavity for condensation.

The disadvantage of the proposed distiller (just as for VCD) is the presence of a compressor and the presence in the system of circulating pumps. In addition, there is no removal of the product (condensate) in weightlessness. In terms of technical characteristics, the distiller was also inferior to its competitors (see comparison below).

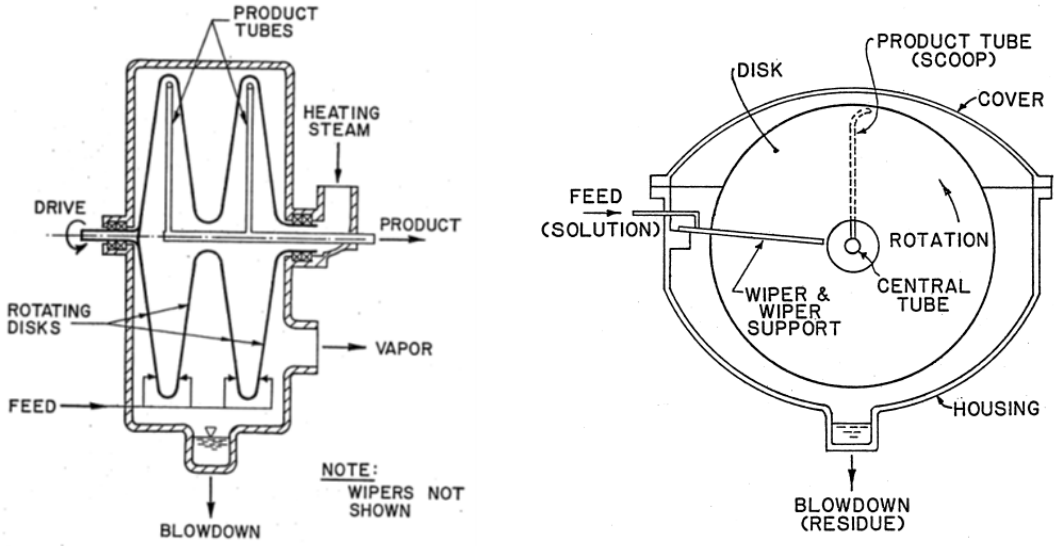

a) *b)*

Fig. 7. Schematic diagram of a centrifugal film scraper distiller (a) and a section of its evaporating section (b)

The system operated stably at an evaporation temperature of 60 °C, flat disks were made of copper with a thickness of 0.036 inches, the heat transfer coefficient reached 60 kW/m^2 at a temperature difference of 0.1 to 3 °C.

The initial solution was passed through a cartridge type filter, regenerative heat exchanger, degasser and then fed to the evaporator. Part of the liquid was evaporated from the initial solution, and the residue was pumped from the bottom of the chamber into a regenerative heat exchanger for cooling. The formed steam was removed by an external compressor, compressed to increase the pressure and saturation temperature, and then fed into the cavity for condensation.

The disadvantage of the proposed distiller (just as for VCD) is the presence of a compressor and the presence in the system of circulating pumps. In addition, there is no removal of the product (condensate) in weightlessness. In terms of technical characteristics, the distiller was also inferior to its competitors (see comparison below).

Thermal centrifugal distillers with thermoelectric heat pumps, developed at Kyiv Polytechnic Institute (KPI)

From 1974 to 1993, KPI scientists and engineers, on the instructions of a Russian company involved in the manufacture of equipment for space missions, developed and tested several types of centrifugal distillers with thermoelectric heat pumps for operating conditions in space.

Among them:

– thermoelectric centrifugal distiller, in which the heat exchange rotating surface was also a thermoelectric heat pump [17];

– centrifugal multistage distiller, which works in combination with a stationary thermopile.

Multistage centrifugal distiller with a heat pump

The cascade distillation system in a simplified form is shown in Fig. 10 [18 – 22]. The system consists of two main components: a multistage vacuum centrifugal distiller and a thermoelectric heat pump. The working liquid is fed to a multistage vacuum centrifugal distiller, where water evaporates and condenses. Several stages work in parallel to ensure high performance. Energy for the process comes from a heat pump in which the distillation water is cooled and the source working fluid is heated. Both streams circulate, respectively, through the cold and hot circuits of the heat pump and return to the distiller. The temperature in the hot circuit is 35 ... 45 °C and in the cold one is from 20 to 25 °C. The supply and removal of liquids is controlled by valves with adjustable pressure and does not require a digital controller. The working fluid is contained in the working tank and is supplied to the hot circuit through a pressure regulated valve. The system operates under vacuum, and when the volume of the hot circuit decreases during evaporation, the pressure in it decreases, and additional source liquid is sucked into the distiller. The product or condensate is fed into the product tank through a pressure-adjustable valve. The product tank is also maintained under vacuum. As the volume of the cold circuit increases, the pressure increases and the valve opens to drain the distillate (product).

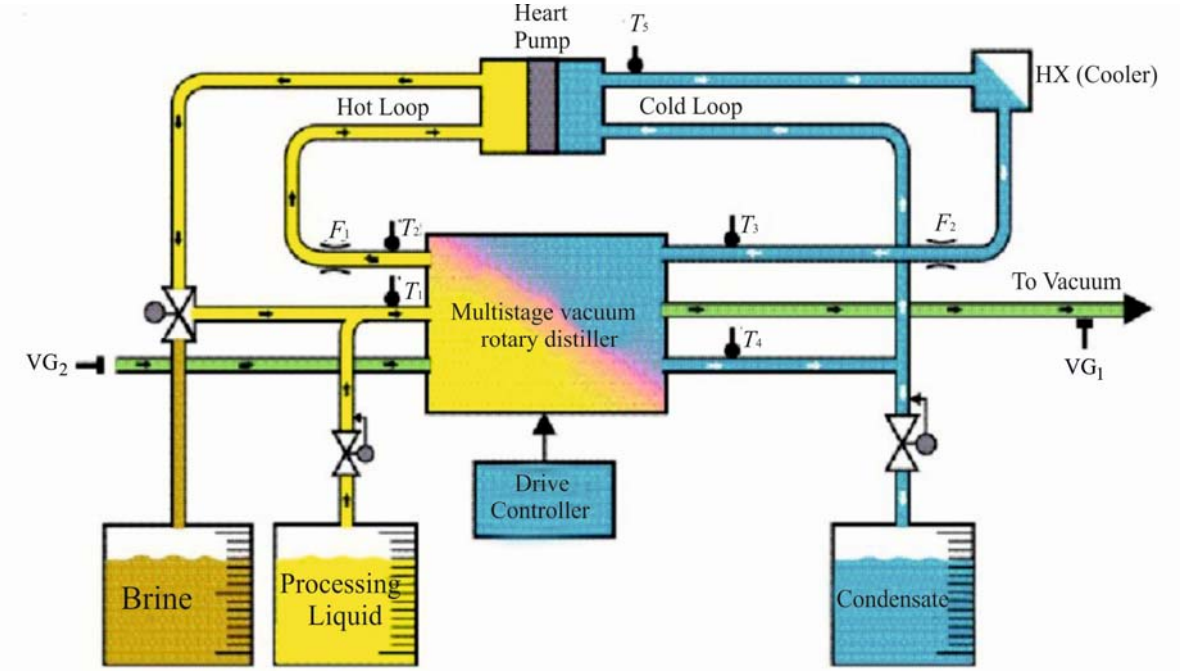

Fig. 8. Functional diagram of a cascade system

The process continues until the hot circuit is filled with concentrated brine and the evaporation temperature rises. At this point, the heat pump is turned off and the pressure is restored to atmospheric. This usually occurs when more than 90 % of the water is removed from the feed solution and collected in the product tank. The brine is then pumped out of the system into the brine tank and the distiller is turned off.

Two variants of the distiller were made: with three and with five stages.

Fig. 11 shows a diagram of a three-stage distiller. The five-stage device has a similar design, the main difference of which is only the number of steps.

The distiller has a sealed housing 1, in which the rotor 2 is mounted on bearings. The rotation of the rotor is provided by a drive through a sealed magnetic coupling. The rotor is divided by partitions into a number of distillation stages and a final condenser. Process (outlet) solution 3 is fed through channel 4,

where it is distributed according to the degrees of distillation. The solution is fed through channel 5 to the system heater, from which (in an overheated state) through channel 6 it returns to the device, where the overheating of the liquid is removed by self-boiling. The vapor of the last stage of evaporation is condensed in the final condenser at contact with the distillate cooled on the cold side of the heat pump and in the additional heat exchanger. The cooled distillate enters the device through channel 7, is heated and removed again for cooling by the built-in pump through channel 8. Excess condensate (distillate, product) is discharged by the Pitot tube into the storage tank through channel 10. Evacuation of the device is through channel 11.

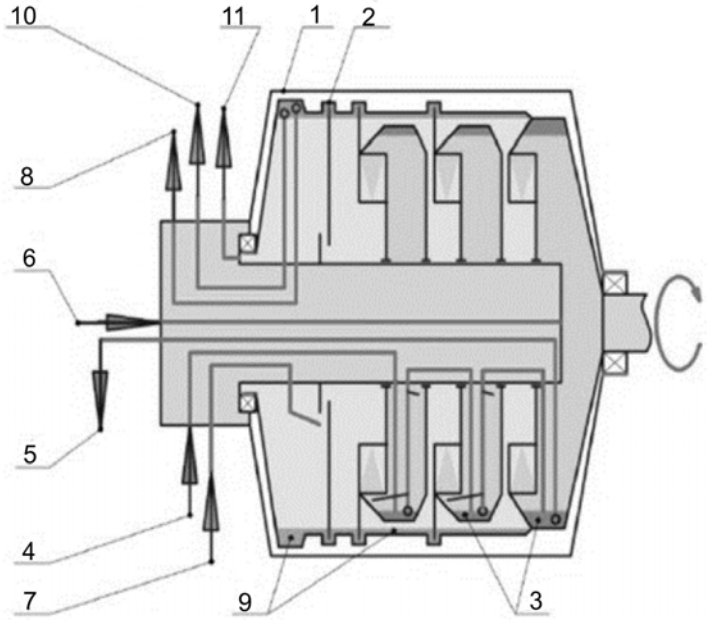

Fig. 9. The scheme of the centrifugal three-stage distiller:
1 - case; 2 - rotor; 3 - outlet solution 4 - inlet of the initial solution;
5 - outlet channel; 6 - supply channel; 7 - cooled condensate inlet; 8 - heated condensate outlet;
9 - condensate; 10 - the output of the distillate product; 11 - gas outlet

The advantages of CDS include:

1. High heat transfer coefficients (up to 104 W/(m^2 • K)) provide small temperature differences on the stages of the distiller.

2. The ability to achieve the degree of water extraction from the solution up to 96 % without deposits on the heat transfer surface.

3. Distillate quality is better than in VCD.

4. No external pumps with separate drives.

5. No seals with friction on a hard surface.

6. Self-regulation of the solution and condensate levels in the rotor cavities of the distiller.

In [23 – 32], a large number of different studies of CMED characteristics in the concentration of various types of wastewater [33], distiller modeling, system reliability issues [34 – 36], etc. were carried out.

Comparison of characteristics of the considered distillers

The initial (evaporated) liquids were two solutions [22], the amount was chosen based on the calculation for a 30-day mission. The first solution 1 consisted of pretreated urine and pretreated moisture

condensate. The second solution 2 included pre-treated hygienic wastewater (from shower, hand washing, brushing teeth, and wet shaving), as well as pretreated urine and pretreated moisture condensate. The summary characteristics based on the test results are shown in Table 1. For solution 1, the degree of water extraction for all systems was 93.5 %, and for solution 2 – 90 %.

The data in Table 1 show that each technology has proven itself well in the production of quality distillate. Overall, CDS was slightly better in terms of distillate quality, although all systems effectively removed over 99 % inorganic components and 98 % organic components. This efficiency minimizes the amount of post-treatment required to produce potable water.

Expert assessment of the test results: VCD system will be successful with a probability of 84 % – 90 % and a risk of 3 %; the CDS system will be successful with a probability of 84 % – 87 % and a risk of 5 %; the WFRD system will be successful with a probability of 52 % – 61 % and a risk of 7 %.

In [33], the characteristics of three centrifugal distillation technologies were compared: a vacuum compression distiller (VCD), a centrifugal distiller with a Wiped-Film Rotating Disk (WFRD), and a thermal centrifugal distiller with thermoelectric heat pumps (CDS).

Two solutions were used as working fluids [22], the amount was selected from the calculation for a 30-day mission. The first solution 1 consisted of pre-treated urine and pre-treated moisture condensate. The second solution 2 included pre-treated hygienic wastewater (from showering, hand washing, brushing teeth and wet shaving), as well as pre-treated urine and pre-treated moisture condensate. The total characteristics according to the test results are shown in Table 1. For solution 1, the degree of water extraction for all systems was 93.5 %, and for solution 2 – 90 %.

The data in Table 1 show that each technology has proven itself well in the production of quality distillate. Overall, CDS was slightly better in terms of distillate quality, although all systems effectively removed more than 99 % of inorganic components and 98 % of organic components. This efficiency minimizes the need for further processing to produce potable water.

Expert evaluation of test results: VCD system will be successful with a probability of 84 % – 90 % and a risk of 3 %; the CDS system will be successful with a probability of 84 % – 87 % and a risk of 5 %; the WFRD system will be successful with a probability of 52 % – 61 % and a risk of 7 %.

Table 1

Test results

Distiller	CDS		VCD		WFRD	
Solution	1	2	1	2	1	2
Productivity (kg/h)	3.7	4.88	1.63	1.87	16.1	16.8
Specific power consumption (Wh/kg)	109	110	188	163	85	86
Average power (W)	375	485	279	296	1252	1293

Data for WFRD showed an anomaly in the fact that the concentration of contaminants in the distillate is higher than for CDS and VCD. Analysis of the data shows that in the WFRD the streams of source liquid and distillate were partially mixed during operation.

The performance of CDS is about twice that of a VCD, and that of a WFRD is about 10 times that of a VCD. Therefore, although the input energy for WFRD and CDS is higher, the specific energy is less than for VCD. Values for VCD are also presented for the case when the heaters used to prevent condensation in the distiller housing are switched off.

Conclusions

Based on this review, it can be argued that the problem of providing astronauts with water during long flights is still very far from being solved. The VCD distillation system installed on the ISS is unsuitable in terms of reliability and stability. The TIMES and WFRD have a design unsuitable for working conditions in weightlessness. The CDS system shows the best results both in terms of energy efficiency and the quality of the distillate. However, the degree of water extraction is still insufficient.

Further research for future wastewater regeneration systems will be aimed at increasing the reliability and degree of water recovery.

References

1. Abney M. B., Perry J. L., Sanders G. B. (2018). A discussion of integrated life support and in situ resource utilization architectures for Mars surface mission. *48th International Conference on Environmental Systems Albuquerque, New Mexico, 8-12 July 2018, ICES-2018-23*
2. Jones H. W. (2017). Developing reliable life support for Mars. *47th International Conference on Environmental Systems, 16-20 July 2017, Charleston, South Carolina. ICES-2017-84*
3. McQuillan Jeff, Pickering Karen D., Anderson Molly, Carter Layne, Flynn Michael, Callahan Michael, Vega Leticia, Allada Rama and Yeh Jannivine (2010). Distillation technology down-selection for the exploration life support (ELS) water recovery systems element [Text].*The 40th International Conference on Environmental Systems, 2010, AIAA 2010-6125.*
4. Carter D. L. (2009). VCD ELS distillation down-select test final report [Text]. *Final Report, submitted to Online Project Information System (OPIS) for the Exploration Life Support Office.*
5. Gorensek Max B., Baer-Peckham David. Space station water recovery trade study – Phase change technology. *SAE paper 881015*
6. Thibaud-Erkey C., Fort J., and Edeen M. (2000). A new membrane for the thermoelectric integrated membrane evaporative subsystem (TIMES). *SAE Technical Paper 2000-01-2385 1999-01-1990*
7. Dehner G.F. (1984). TIMES regenerator redesign description Timothy D. Scull Hamilton Standard Space Systems International, Inc. Addendum development of a preprototype times wastewater recovery subsystem. *Prepared under contract no. nas 9-15471.*
8. Thibaud-Erkey Catherine and Hamilton James H.Fort 2000-01-2385 A new membrane for the thermoelectric integrated membrane evaporative subsystem (TIMES) Edeen Marybeth A. (1982). Sundstrand space systems international NASA-Johnson Space Center Water Recovery Technology, *SAE Technical Paper 820849*.
9. Vapor compression distillation module (*Contracts NAS9-13714 $ NAS9-14234*), Prepared by P. P. Nuccio, 1975
10. Carter L., Williamson J, Brown C.A., Bazley J., Gazda D., Schaezler R., Thomas F., Molina S. (2019). Status of ISS water management and recovery. *49th International Con- ference on Environmental Systems, 7-11 July 2019, Boston, Massachusetts. ICES-2019-36*

11. Noble Larry D., Schubert Franz H., Pudoka Rick J., Miernik Janie H. (1990). Phase change water recovery for the space station freedom and future exploration missions. *20th lntersociety Conference on Environmental Systems. Williamsburg, Virginia, July 9-12, 1990. SAE Technical Paper 901294.*
12. Carter L., Williamson J., Brown C.A., Bazley J., Gazda D., Schaezler R., Thomas Frank.(2018). Status of ISS water management and recovery. *48th International Conference on Environmental Systems. 8 - 12 July 2018, Albuquerque, New Mexico. ICES-2018-088.*
13. Carter L., Williamson J., Brown C.A., Bazley J., Gazda D., Schaezler R., Thomas Frank (2017). Status of ISS water management and recovery. *47th International Conference on Environmental Systems, 17 – 20 July 2017, Charleston, South Carolina. ICES-2016-036*
14. Tleimat B. (1982). Wiped-film rotating disc evaporator for water reuse.
15. Tleimat B., Tleimat M., *Grant No. 14-34-0001-0537.*Quinn G., Flynn M., Smith F. (2002). The development of the wiped-film rotating-disk evaporator for the reclamation of water at microgravity. *SAE TECHNICAL PAPER SERIES. 2002-01-2397*
16. Tleimat B.W., Tleimat M.C. (1996). Water recovery from and volume reduction of gray water using an energy efficient evaporator. *Desalination,* 107,111-119.
17. Raschetno-poiasnitelnaia zapiska k eskiznomu proektu tsentrobezhnogo termoelektricheskogo distilliatora [Calculation and explanatory note to the draft design of a centrifugal thermoelectric distiller], Kyiv, 1975. Access by link: https://drive.google.com/file/d/1Jab5d-FXBGdFRaofVGAFx77VcW9G5BLW /view?usp=sharingRifert V., Barabash P., Goliad N. (1990). Methods and processes of thermal distillation of water solutions for closed water supply systems. The 20th Intersociety Conference on Environmental Systems, Williamsburg, July 1990. SAE Paper 901249.
18. Rifert V., Barabash P., Goliad N. (1990). Methods and processes of thermal distillation of water solutions for closed water supply systems. *The 20th Intersociety Conference on Environmental Systems, Williamsburg, July 1990. SAE Paper 901249.*
19. Rifert V., Usenko V., Zolotukhin I., MacKnight A., Lubman A. (1999). Comparison of secondary water processors using distillation for space applications. *SAE Paper 99-70466, 29th International Conference on Environmental Systems, Denver, July 1999.*
20. Rifert V., Stricun A., Usenko V. (2000). Study of dynamic and extreme performances of multistage centrifugal distiller with the thermoelectric heat pump. *SAE Technical Papers 2000. 30th International Conference on Environmental Systems; Toulouse; France; 10-13 July 2000.*
21. Rifert V. G., Usenko V.I., Zolotukhin I.V., MacKnight A. and Lubman A. (2003). Cascaded distillation technology for water processing in space. *SAE Paper 2003-01-2625. 34st International Conference on Environmental Systems. Orlando, July 2003.*
22. Lubman A., MacKnight A., Rifert V., and Barabash P. (2007). Cascade distillation subsystem hardware development for verification testing. *SAE International, 2007-01-3177, July 2007.*
23. Samsonov N., Bobe L, Novikov V., Rifert V. and others (1994). Systems for water reclamation from humidity condensate and urine for space station. *The 24th International society Conference on Environmental Systems, June, 1994. SAE Paper 941536.*
24. Samsonov N.M., Bobe L.S, Novikov V., Rifert V.G., Barabash P.A et al. (1995). Development of urine processor distillation hardware for space stations. *The 25th International Conference on Environmental Systems, San Diego, July 1995. SAE Paper 951605*
25. Samsonov N.M., Bobe L.S, Novikov V., Rifert V.G., et al. (1997). Updated systems for water recovery from humidity condensate and urine for the International space station. *SAE Paper 972559, the 27th International Conference on Environmental Systems, Nevada, July 1997.*
26. Samsonov N.M., Bobe L.S, Novikov V., Rifert V.G., et al. (1999). Development and testing of a

vacuum distillation subsystem for water reclamation from urine. *SAE Paper 1999-01-1993, the 29th International Conference on Environmental Systems.*

27. Rifert V.G., Anatychuk L.I., Barabash P.A., Usenko V.I., Strikun A.P., Prybyla A.V.(2017). Improvement of the distillation methods by using centrifugal forces for water recovery in space flight applications. *J.Thermoelectricity*, 1, 71-83.
28. Rifert Vladimir G., Barabash Petr A., Usenko Vladimir, Solomakha Andrii S., Anatychuk Lukyan I., Prybyla A.V. (2017). Improvement the cascade distillation system for long-term space flights. *68th International Astronautical Congress (IAC), Adelaide, Australia, 25-29 September 2017*. IAC-17-A1.IP.25.
29. Rifert Vladimir G., Anatychuk Lukyan I., Solomakha Andrii S., Barabash Petr A., Usenko Vladimir, Prybyla A.V., Naymark Milena, Petrenko Valerii (2019). Upgrade the centrifugal multiple-effect distiller for deep space missions. *70th International Astronautical Congress (IAC), Washington D.C., United States, 21-25 October 2019.* IAC-19-A1,IP,11,x54316.
30. A.S.Solomakha, L.I.Anatychuk, V.G.Rifert, P.A.Barabash, V.Usenko, V.Petrenko (2020). Thermal distillation system for deep space missions: rationale for the choice. *71st International Astronautical Congress (IAC) – The CyberSpace Edition*, 12-14 October 2020. IAC-20-A1,VP,15,x61344. 7 pages.
31. Rifert, V.G., Anatychuk, L.I., Barabash, P.O., Solomakha A.S., Strykun A.P., Sereda, V.V., Prybyla, A.V. (2019). Evolution of centrifugal distillation system with a thermoelectric heat pump for space missions. *J.Thermoelectricity*, 3, 5 – 19.
32. Rifert V.G., Anatychuk L.I., Barabash P.O., Usenko V.I., Solomakha A.S., Petrenko V.G., Prybyla A.V., Sereda V.V. (2019). Comparative analysis of thermal distillation methods with heat pumps for long space flights. *J.Thermoelectricity*, 4, 5 – 18.
33. Jeff McQuillan, Karen D. Pickering, Molly Anderson, Layne Carter, Michael Flynn, Michael Callahan, Leticia Vega, Rama Allada and Jannivine Yeh (2010). Distillation technology downselection for the exploration life support (ELS) water recovery systems element. 40th *International Conference on Environmental Systems*, AIAA 2010-6125.
34. M. Callahan, A. Lubman, A. MacKnight, H. Thomas and K. Pickering (2008). Cascade distillation subsystem development testing. *SAE International*, 2008-01-2195.
35. M. Callahan, A. Lubman, and K. Pickering (2009). Cascade distillation subsystem development: progress toward a distillation comparison test. *SAE International*, 2009-01 -2401.
36. M. Callahan, V. Patel, and K. Pickering (2010). Cascade distillation subsystem development: early results from the exploration life support distillation technology comparison test. *American Institute of Aeronautics and Astronautics*, 2010-6149.

Submitted 10.02.2021

Ріферт В.Г., *док. техн. наук*[1]
Анатичук Л.І., *акад. НАН України*[2,3]
Соломаха А.С., *канд. техн. наук*[1]
Барабаш П.О., *канд. техн. наук*[1]
Усенко В.І., *канд. техн. наук*[1]
Петренко В.Г., *канд. техн. наук*[1]

[1]НТУ «КПІ», вул. Політехнічна, 6, Київ, 03056, Україна,
e–mail: vgrifert@ukr.net;
[2]Інститут термоелектрики НАН і МОН України, вул. Науки, 1,
Чернівці, 58029, Україна; *e–mail: anatych@gmail.com*
[3]Чернівецький національний університет ім. Юрія Федьковича,
вул. Коцюбинського 2, Чернівці, 58000, Україна

ОБГРУНТУВАННЯ МЕТОДУ ТЕРМІЧНОЇ ДИСТИЛЯЦІЯ З ТЕРМОЕЛЕКТРИЧНИМ ТЕПЛОВИМ НАСОСОМ ДЛЯ ТРИВАЛИХ КОСМІЧНИХ МІСІЙ

У статті описані основні методи термічної дистиляції, які можна використовувати для довготривалих космічних місій з людьми. Показано їх переваги та недоліки, наведено основні відомості щодо характеристик роботи систем, а саме: продуктивності по дистиляту, питомої витрати енергії на одиницю маси одержуваного дистиляту і якості дистиляту при випарюванні (концентруванні) водного розчину NaCl, урини й сумішей – урини з конденсатом, урини з конденсатом і гігієнічною водою. Вказано на обмеження, що не дозволяють їх використовувати для польотів та можливі шляхи їх вирішення. Бібл. 36, табл. 1, рис. 9.
Ключові слова: термоелектрика, тепловий насос, дистилятор.

Риферт В.Г., *док. техн. наук*[1]
Анатычук Л.И., *акад. НАН Украины*[2,3]
Соломаха А.С., *канд. техн. наук*[1]
Барабаш П.А., *канд. техн. наук*[1]
Усенко В.И., *канд. техн. наук*[1]
Петренко В.Г., *канд. техн. наук*[1]

[1]НТУ «КПІ», ул. Политехническая, 6, Киев, 03056, Украина,
e–mail: vgrifert@ukr.net;
[2]Институт термоэлектричества НАН и МОН Украины, ул. Науки, 1,
Черновцы, 58029, Украина; *e-mail: anatych@gmail.com*
[3]Черновицкий национальный университет им. Юрия Федьковича,
ул. Коцюбинского 2, Черновцы, 58000, Украина

ОБОСНОВАНИЕ МЕТОДОМ ТЕРМИЧЕСКОЙ ДИСТИЛЛЯЦИИ С ТЕРМОЭЛЕКТРИЧЕСКОЙ ТЕПЛОВОЙ НАСОС ДЛЯ ДЛИТЕЛЬНЫХ КОСМИЧЕСКИХ МИССИЙ

В статье описаны основные методы термической дистилляции, которые можно использовать для длительных космических миссий с людьми. Показано их преимущества и недостатки, приведены основные сведения о характеристиках работы систем, а именно: производительность по дистиллята, удельного расхода энергии на единицу массы получаемого дистиллята и качества дистиллята при испарении (концентрировании) водного раствора NaCl, урины и смесей - урины с конденсатом, урины с конденсатом и гигиенической водой. Указано на ограничения, не позволяющие их использовать для полетов и возможные пути их решения. Библ. 36, рис. 9, табл. 1.

Ключевые слова: Термоэлектричество, тепловой насос, дистиллятор.

References

1. Abney M. B., Perry J. L., Sanders G. B. (2018). A discussion of integrated life support and in situ resource utilization architectures for Mars surface mission. *48th International Conference on Environmental Systems Albuquerque, New Mexico, 8-12 July 2018, ICES-2018-23*
2. Jones H. W. (2017). Developing reliable life support for Mars. *47th International Conference on Environmental Systems, 16-20 July 2017, Charleston, South Carolina. ICES-2017-84*
3. McQuillan Jeff, Pickering Karen D., Anderson Molly, Carter Layne, Flynn Michael, Callahan Michael, Vega Leticia, Allada Rama and Yeh Jannivine (2010). Distillation technology down-selection for the exploration life support (ELS) water recovery systems element [Text].*The 40th International Conference on Environmental Systems, 2010, AIAA 2010-6125.*
4. Carter D. L. (2009). VCD ELS distillation down-select test final report [Text]. *Final Report, submitted to Online Project Information System (OPIS) for the Exploration Life Support Office.*
5. Gorensek Max B., Baer-Peckham David. Space station water recovery trade study – Phase change technology. *SAE paper 881015*
6. Thibaud-Erkey C., Fort J., and Edeen M. (2000). A new membrane for the thermoelectric integrated membrane evaporative subsystem (TIMES). *SAE Technical Paper 2000-01-2385 1999-01-1990*
7. Dehner G.F. (1984). TIMES regenerator redesign description Timothy D. Scull Hamilton Standard Space Systems International, Inc. Addendum development of a preprototype times wastewater recovery subsystem. *Prepared under contract no. nas 9-15471.*
8. Thibaud-Erkey Catherine and Hamilton James H.Fort 2000-01-2385 A new membrane for the thermoelectric integrated membrane evaporative subsystem (TIMES) Edeen Marybeth A. (1982). Sundstrand space systems international NASA-Johnson Space Center Water Recovery Technology, *SAE Technical Paper 820849*.
9. Vapor compression distillation module (*Contracts NAS9-13714 $ NAS9-14234*), Prepared by P. P. Nuccio, 1975
10. Carter L., Williamson J, Brown C.A., Bazley J., Gazda D., Schaezler R., Thomas F., Molina S. (2019). Status of ISS water management and recovery. *49th International Con- ference on Environmental Systems, 7-11 July 2019, Boston, Massachusetts. ICES-2019-36*
11. Noble Larry D., Schubert Franz H., Pudoka Rick J., Miernik Janie H. (1990). Phase change water recovery for the space station freedom and future exploration missions. *20th lntersociety Conference on Environmental Systems. Williamsburg, Virginia, July 9-12, 1990. SAE Technical Paper 901294.*

12. Carter L., Williamson J., Brown C.A., Bazley J., Gazda D., Schaezler R., Thomas Frank.(2018). Status of ISS water management and recovery. *48th International Conference on Environmental Systems. 8 - 12 July 2018, Albuquerque, New Mexico. ICES-2018-088.*
13. Carter L., Williamson J., Brown C.A., Bazley J., Gazda D., Schaezler R., Thomas Frank (2017). Status of ISS water management and recovery. *47th International Conference on Environmental Systems, 17 – 20 July 2017, Charleston, South Carolina. ICES-2016-036*
14. Tleimat B. (1982). Wiped-film rotating disc evaporator for water reuse.
15. Tleimat B., Tleimat M., *Grant No. 14-34-0001-0537.*Quinn G., Flynn M., Smith F. (2002). The development of the wiped-film rotating-disk evaporator for the reclamation of water at microgravity. *SAE TECHNICAL PAPER SERIES. 2002-01-2397*
16. Tleimat B.W., Tleimat M.C. (1996). Water recovery from and volume reduction of gray water using an energy efficient evaporator. *Desalination,* 107,111-119.
17. Raschetno-poiasnitelnaia zapiska k eskiznomu proektu tsentrobezhnogo termoelektricheskogo distilliatora [Calculation and explanatory note to the draft design of a centrifugal thermoelectric distiller], Kyiv, 1975. Access by link: https://drive.google.com/file/d/1Jab5d-FXBGdFRaofVGAFx77VcW9G5BLW /view?usp=sharingRifert V., Barabash P., Goliad N. (1990). Methods and processes of thermal distillation of water solutions for closed water supply systems. The 20th Intersociety Conference on Environmental Systems, Williamsburg, July 1990. SAE Paper 901249.
18. Rifert V., Barabash P., Goliad N. (1990). Methods and processes of thermal distillation of water solutions for closed water supply systems. *The 20th Intersociety Conference on Environmental Systems, Williamsburg, July 1990. SAE Paper 901249.*
19. Rifert V., Usenko V., Zolotukhin I., MacKnight A., Lubman A. (1999). Comparison of secondary water processors using distillation for space applications. *SAE Paper 99-70466, 29th International Conference on Environmental Systems, Denver, July 1999.*
20. Rifert V., Stricun A., Usenko V. (2000). Study of dynamic and extreme performances of multistage centrifugal distiller with the thermoelectric heat pump. *SAE Technical Papers 2000. 30th International Conference on Environmental Systems; Toulouse; France; 10-13 July 2000.*
21. Rifert V. G., Usenko V.I., Zolotukhin I.V., MacKnight A. and Lubman A. (2003). Cascaded distillation technology for water processing in space. *SAE Paper 2003-01-2625. 34st International Conference on Environmental Systems. Orlando, July 2003.*
22. Lubman A., MacKnight A., Rifert V., and Barabash P. (2007). Cascade distillation subsystem hardware development for verification testing. *SAE International, 2007-01-3177, July 2007.*
23. Samsonov N., Bobe L, Novikov V., Rifert V. and others (1994). Systems for water reclamation from humidity condensate and urine for space station. *The 24th International society Conference on Environmental Systems, June, 1994. SAE Paper 941536.*
24. Samsonov N.M., Bobe L.S, Novikov V., Rifert V.G., Barabash P.A et al. (1995). Development of urine processor distillation hardware for space stations. *The 25th International Conference on Environmental Systems, San Diego, July 1995. SAE Paper 951605*
25. Samsonov N.M., Bobe L.S, Novikov V., Rifert V.G., et al. (1997). Updated systems for water recovery from humidity condensate and urine for the International space station. *SAE Paper 972559, the 27th International Conference on Environmental Systems, Nevada, July 1997.*
26. Samsonov N.M., Bobe L.S, Novikov V., Rifert V.G., et al. (1999). Development and testing of a vacuum distillation subsystem for water reclamation from urine. *SAE Paper 1999-01-1993, the 29th International Conference on Environmental Systems.*
27. Rifert V.G., Anatychuk L.I., Barabash P.A., Usenko V.I., Strikun A.P., Prybyla A.V.(2017).

Improvement of the distillation methods by using centrifugal forces for water recovery in space flight applications. *J.Thermoelectricity*, 1, 71-83.

28. Rifert Vladimir G., Barabash Petr A., Usenko Vladimir, Solomakha Andrii S., Anatychuk Lukyan I., Prybyla A.V. (2017). Improvement the cascade distillation system for long-term space flights. *68th International Astronautical Congress (IAC), Adelaide, Australia, 25-29 September 2017*. IAC-17-A1.IP.25.
29. Rifert Vladimir G., Anatychuk Lukyan I., Solomakha Andrii S., Barabash Petr A., Usenko Vladimir, Prybyla A.V., Naymark Milena, Petrenko Valerii (2019). Upgrade the centrifugal multiple-effect distiller for deep space missions. *70th International Astronautical Congress (IAC), Washington D.C., United States, 21-25 October 2019*. IAC-19-A1,IP,11,x54316.
30. A.S.Solomakha, L.I.Anatychuk, V.G.Rifert, P.A.Barabash, V.Usenko, V.Petrenko (2020). Thermal distillation system for deep space missions: rationale for the choice. *71st International Astronautical Congress (IAC) – The CyberSpace Edition*, 12-14 October 2020. IAC-20-A1,VP,15,x61344. 7 pages.
31. Rifert, V.G., Anatychuk, L.I., Barabash, P.O., Solomakha A.S., Strykun A.P., Sereda, V.V., Prybyla, A.V. (2019). Evolution of centrifugal distillation system with a thermoelectric heat pump for space missions. *J.Thermoelectricity*, 3, 5 – 19.
32. Rifert V.G., Anatychuk L.I., Barabash P.O., Usenko V.I., Solomakha A.S., Petrenko V.G., Prybyla A.V., Sereda V.V. (2019). Comparative analysis of thermal distillation methods with heat pumps for long space flights. *J.Thermoelectricity*, 4, 5 – 18.
33. Jeff McQuillan, Karen D. Pickering, Molly Anderson, Layne Carter, Michael Flynn, Michael Callahan, Leticia Vega, Rama Allada and Jannivine Yeh (2010). Distillation technology downselection for the exploration life support (ELS) water recovery systems element. 40th *International Conference on Environmental Systems*, AIAA 2010-6125.
34. M. Callahan, A. Lubman, A. MacKnight, H. Thomas and K. Pickering (2008). Cascade distillation subsystem development testing. *SAE International*, 2008-01-2195.
35. M. Callahan, A. Lubman, and K. Pickering (2009). Cascade distillation subsystem development: progress toward a distillation comparison test. *SAE International*, 2009-01 -2401.
36. M. Callahan, V. Patel, and K. Pickering (2010). Cascade distillation subsystem development: early results from the exploration life support distillation technology comparison test. *American Institute of Aeronautics and Astronautics*, 2010-6149.

Submitted 10.02.2021

V.S. Zakordonets

V. S. Zakordonets, *cand. phys.-math. Science*

Ivan Pulyuy Ternopil National Technical University, 56,
Ruska str., Ternopil, 46001, Ukraine;
e-mail:wladim21@gmail.com

THERMOPOWER IN SEMICONDUCTOR SUPERLATTICES AT SCATTERING OF CURRENT CARRIERS BY PHONONS AND POINT DEFECTS

In the quasi-classical one-miniband approximation, the thermopower of semiconductor superlattices (SL) is investigated in the case of arbitrary statistics and at scattering of charge carriers by acoustic phonons, point defects, and nonpolar optical phonons, taking into account the change in the relaxation time as compared to bulk materials. An analytical dependence of the thermopower on the reduced width of the conduction band β in the direction of the superlattice axis is established. It is shown that the thermopower of the superlattice increases with an increase in the width of the conduction miniband, asymptotically approaching the limiting value at $\beta \geq 10$. Bibl. 17, Fig. 3.

Key words: Seebeck coefficient, superlattice figure of merit, thermoEMF.

Formulation of the problem.

The development of modern technique and technology is closely related to the search for new sources of energy, primarily electrical. The main requirement is to increase the generation power.

However, at the present time, additional conditions are coming to the fore: energy must be produced by environmentally friendly renewable sources that are not related to carbohydrates. Thermoelectric energy is one of the promising, and in some cases the only possible way to directly convert thermal energy into electricity. A significant limitation of thermoelectric energy conversion is the relatively low efficiency of conversion of thermal energy into electricity - from 3% to 8% [1].

The efficiency of thermoelectric conversion is determined by the ratio

$$\eta = \frac{\Delta T}{T_1}\frac{\sqrt{1+ZT}-1}{\sqrt{1+ZT}+1}, \tag{1}$$

where $\Delta T=T_1 - T_2$, $T=(T_1-T_2)/2$, T_1 is heater temperature, T_2 is refrigerator temperature,

$$Z = \frac{\alpha^2\sigma}{\kappa_e + \kappa_{ph}}, \tag{2}$$

is figure of merit of thermoelectric material, α is the Seebeck coefficient, σ, κ and κ_{ph} are coefficients of electric conductivity, electron and lattice thermal conductivity.

Analysis of recent research and publications.

High-efficiency thermoelectric energy converters require a large thermoelectric figure of merit, which for bulk materials has approached the limit value $ZT = 1$ [2]. However, low-size systems can overcome this limit. In [3-5], it was shown that the thermoelectric figure of merit of superlattices (SL) with rather narrow quantum wells (QWs) can significantly exceed the figure of merit of bulk semiconductor samples, the composition of which is similar to that of the SL material.

In this regard, special attention is paid to the study of transport phenomena in semiconductor superlattices. In particular, a large number of theoretical [6-9] and experimental [10,11] works are devoted to the study of thermopower. Superlattices include plane-layer crystals of transition metal dichalcogenides and their compounds, A_3B_6 semiconductors, polytypic semiconductor compounds, and others [11 – 13].

In [3 – 5], using a simple parabolic dispersion law in the one-miniband approximation, it was shown that in 2D structures a significant increase in thermopower is possible in comparison with 3D structures. It was assumed that dimensional quantization does not lead to a change in the relaxation time and carrier mobility in the direction perpendicular to the plane of the layers, as compared to bulk materials. The increase in the thermopower was associated only with an increase in the density of quantum states near the edges of dimensional quantization bands. The thermopower of SL with the use of a quasi-two-dimensional energy spectrum in the approximation of the relaxation time tensor for scattering of current carriers by phonons of various types using the cosine dispersion law and degenerate statistics was studied in [9]; however, the effect of the width of the conduction miniband on the magnitude of the thermopower in the direction of the SL axis was not considered.

The purpose of this work is to study the thermopower of semiconductor superlattices in the quasi-classical one-miniband approximation at scattering of charge carriers by acoustic phonons, point defects, and nonpolar optical phonons with arbitrary statistics and taking into account the change in the relaxation time in *2D* structures compared to bulk materials.

Formulation of the problem

Presentation of the main material. In semiconductor superlattices, in addition to the periodic potential of the crystal lattice, there is an additional one-dimensional potential, the period of which significantly exceeds the lattice constant. The presence of the potential of the superlattice significantly changes the energy spectrum, due to which it is possible to arbitrarily change its band structure. The physical properties of semiconductor SL are determined by their electronic spectrum. While the movement of current carriers in the direction perpendicular to the SL axis is almost free and corresponds to movement over a wide conduction band, the movement along its *0z* axis is limited.

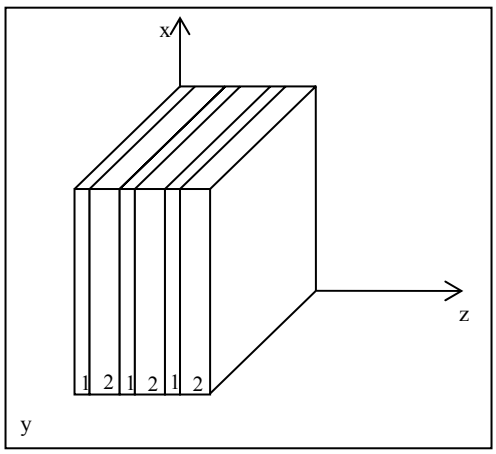

Fig.1. Schematic structure of a semiconductor superlattice. 1 - GaAs layer. 2 - AlAs layer.

In this direction, the electronic spectrum will have a miniband character. In the case of sufficiently narrow layers, which are quantum wells for electrons, all electrons will be located near the bottom of the lower miniband of dimensional quantization.

Within the framework of quasi-classical approximation

$$2\varepsilon_0 >> \hbar/\tau_{2D},\ eE_0,\ a\nabla_z k_0 T, \tag{2}$$

the dispersion law for electrons in the lower SL miniband looks like [13]

$$\varepsilon\left(\vec{k}\right) = \frac{\hbar^2 k_\perp^2}{2m_\perp} + 2\varepsilon_0\left(1 - \cos k_z a\right) \tag{3}$$

where $k_\perp = \left(k_x^2 + k_y^2\right)^{1/2}$, and k_z are the transverse and longitudinal to SL axis components of quasi-wave vector, $m_\perp$ is transverse effective mass close in value to the effective mass m^* of electrons of a semiconductor forming SL, a is SL period, $2\varepsilon_0$ is the width of the conduction band of SL in the direction k_z.

The longitudinal component of the relaxation time tensor of the electron gas in SL is written in the form [15]

$$\tau_{2D} = \frac{2\sqrt{2m_\perp k_0 T}}{3\pi\hbar} a\,\tau_{3D}\left(\frac{\varepsilon}{k_0 T}\right)^{1/2}, \tag{4}$$

where

$$\tau_{3D} = \tau_0\left(\frac{\varepsilon}{k_0 T}\right)^{r-1/2}, \tag{5}$$

is relaxation time in the bulk sample, τ_0 is independent of the electron energy constant, r is scattering parameter. The values of τ_0 and r for different scattering mechanisms are given in [16].

It is obvious that the differences in the power-law dependence of the relaxation time of the bulk sample - (r-1/2) and the superlattice - r, arise due to the different energy dependence of the density of quantum states.

It is known that at scattering of current carriers by acoustic phonons, point defects, and nonpolar optical phonons at high temperatures, the scattering parameter is the same, and is equal to $r = 0$. It is clear that under the action of the indicated scattering mechanisms, the longitudinal component of the relaxation time tensor does not depend on energy. Similar assumptions were made in [17] and a number of other works (see references in the same paper). The most convincing argument in favor of this statement is the results of [10], in which it was experimentally established that in SL *GaAs*/*AlAs* above the temperature 40K the relaxation time τ = const.

The nonequilibrium electron distribution function f is found in the approximation of the relaxation time from the Boltzmann kinetic equation

$$\vec{\upsilon}\frac{\partial f}{\partial \vec{r}} - e\vec{E}_0\frac{\partial f}{\hbar\partial \vec{k}} = -\frac{f_1}{\tau_{2D}}, \tag{6}$$

where $\vec{\upsilon} = \hbar^{-1} \partial\varepsilon\left(\vec{k}\right) / \partial\vec{k}$ is electron velocity, $\overrightarrow{E_0} = -\partial\varphi / \partial\vec{r}$ is electric field intensity, φ is electric potential, $f_1 = f - f_0$, $f_0 = \left[1 + \exp\left(\varepsilon - \varsigma\right)/k_0 T\right]$ is the equilibrium Fermi-Dirac distribution function with a variable in space temperature T and chemical potential ζ, k_0 is the Boltzmann constant.

Solving (6) in the approximation of the relaxation time for the nonequilibrium addition to the distribution function we obtain

$$f_1 = -\tau_{2D}\left(\frac{\partial f_0}{\partial\varepsilon}\right)\left[\frac{\varepsilon - \varsigma}{T}\vec{\upsilon}\cdot\nabla T - e\vec{\upsilon}\cdot\nabla\left(\varphi - \frac{\varsigma}{e}\right)\right], \tag{7}$$

The current density will be found from the ratio

$$\vec{j} = -\frac{2e}{(2\pi)^3}\int\vec{\upsilon}\left(\vec{k}\right)\cdot f_1\left(\vec{k},\vec{r}\right)d\vec{k}, \tag{8}$$

We assume that the vectors $\overrightarrow{E_0}$ and ∇T are directed along the SL axis which is compatible with the axis of the cylindrical coordinate system *0z*. Then, taking into account (7), for the current density we obtain

$$j = j_z = \sigma(\eta,\beta)\cdot\nabla_z\left(\frac{\varsigma}{e} - \varphi\right) - \alpha(\eta,\beta)\cdot\sigma(\eta,\beta)\nabla_z T \tag{9}$$

where α (η, β) and σ (η, β) are the Seebeck coefficient and electric conductivity along the SL axis.

The Seebeck coefficient will be found from relation [16]

$$\alpha(\eta,\beta) = \frac{\nabla_z\left(\frac{\varsigma}{e} - \phi\right)}{\nabla_z T}. \tag{10}$$

Assuming the current density in relation (9) equal to zero, for the Seebeck coefficient we obtain

$$\alpha(\eta,\beta) = -\frac{k_0}{e}\left[\frac{I_{1,2,0}(\eta,\beta) + \beta\, I_{0,2,2}(\eta,\beta)}{I_{0,2,0}(\eta,\beta)} - \eta\right]. \tag{11}$$

where

$$I_{k,l,m}(\eta,\beta) = \int_0^{\pi} F_k(\eta, z, \beta)\cdot(\sin z)^l\left(\sin\frac{z}{2}\right)^m dz, \tag{12}$$

$$F_k(\eta, z, \beta) = \int_0^{\infty}\frac{\exp\left(x - \eta + \beta\cdot\sin^2\frac{z}{2}\right)}{\left[1 + \exp\left(x - \eta + \beta\cdot\sin^2\frac{z}{2}\right)\right]^2}x^k dx, \tag{13}$$

three-parameter Fermi integrals $\varepsilon_\perp = \hbar^2 k_\perp^2 / 2m_\perp$, $x = \varepsilon_\perp / k_0 T$ is reduced energy, $\eta = \zeta / k_0 T$ is reduced chemical potential, $\beta = 2\varepsilon_0 / k_0 T$ is reduced width of the conduction miniband in the direction of the superlattice axis, $z = ak_z$.

Figs. 2 and 3 show the results of the numerical analysis of the obtained relations

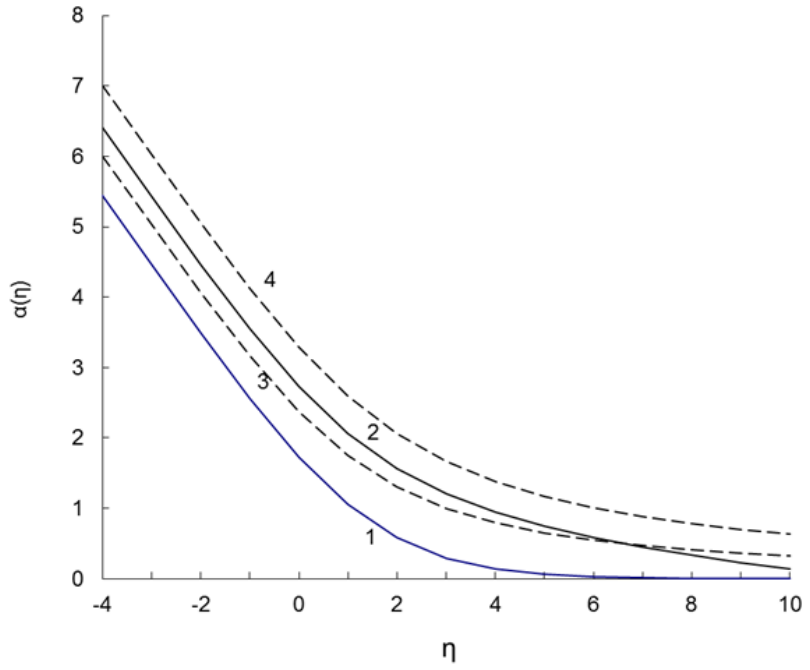

Fig. 2 Dependence of thermopower on the chemical potential at different values of the width of conduction miniband in the direction of the SL axis. 1 – at β = 1, 2 – at β = 10. Dashed curves correspond to the scattering of current carriers in a bulk material: by acoustic phonons - 3; by polar optical phonons - 4.

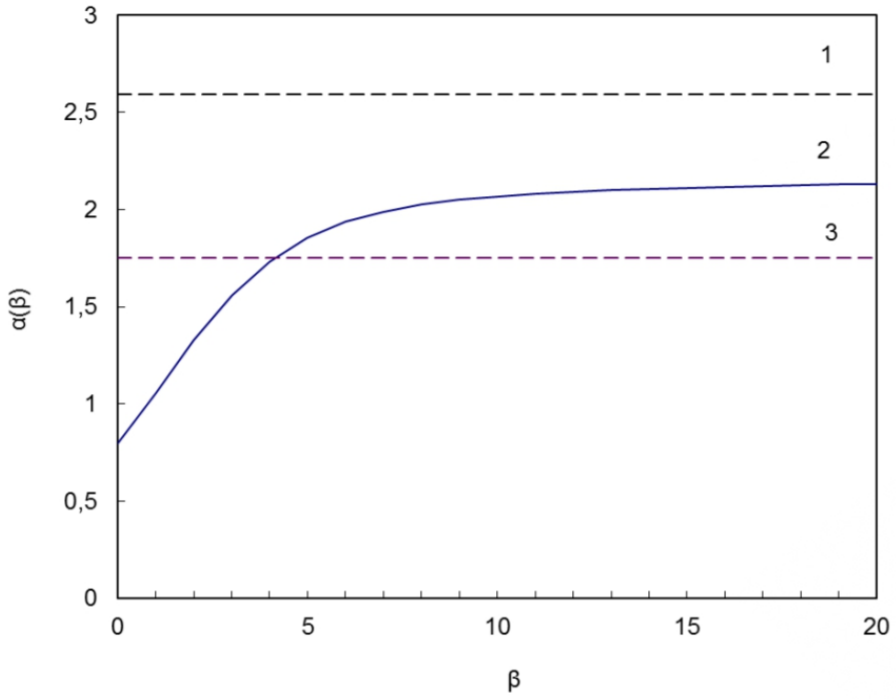

Fig. 3 Dependence of thermopower on the width of conduction miniband in the direction of the SL axis at η = 2. Dashed lines 1 and 3 correspond to the scattering of current carriers in a bulk material: 1 – by acoustic phonons; 3 – by polar optical phonons.

As follows from the analysis of relation (11), as the thickness of the superlattice layers decreases, the width of the conduction miniband in the direction k_z decreases, leading to a decrease in the Seebeck coefficient. If $\beta \to 0$, the value of the Seebeck coefficient asymptotically approaches the limit value

$$\alpha(\eta, 0) = -\frac{k_0}{e}\left[\frac{F_1(\eta)}{F_0(\eta)} - \eta\right], \tag{14}$$

and in the case of $\beta \to \infty$ to

$$\alpha(\eta, \infty) = -\frac{k_0}{e}\left[\frac{F_{5/2}(\eta)}{F_{3/2}(\eta)} - \eta\right], \tag{15}$$

where

$$F_k(\eta) = \int_0^\infty \frac{\exp(x-\eta)}{\left[1+\exp(x-\eta)\right]^2} x^k dx \quad , \tag{16}$$

one-parameter Fermi integrals of the *k-th* order [16].

An unlimited increase in β should be considered as an approximation of the width of the conduction miniband in the direction k_z to the width of the conduction band in the direction k . In this case, the movement of electrons along the SL axis approaches free one.

If $\eta < -4$, the electron gas of SL is nondegenerate, and (14) and (15) is converted to the form, respectively:

$$\alpha(\eta, 0) = -\frac{k_0}{e}[1-\eta]; \tag{17}$$

and

$$\alpha(\eta, \infty) = -\frac{k_0}{e}\left[\frac{5}{2} - \eta\right]. \tag{18}$$

For a bulk semiconductor whose composition is similar to the composition of the SL material at $\eta < -4$ relation (11) transforms into the well-known Pisarenko formula [16]

$$\alpha(\eta, \infty) = -\frac{k_0}{e}[2-\eta]. \tag{19}$$

Conclusions

As a result of calculation by the numerical methods, Figs. 2 and 3 show the graphical dependences of the thermopower (in units - k_0/e) on the chemical potential and the width of the conduction miniband in the direction of the *0z* axis (in units k_0T) for SL and bulk material. The analysis shows that the degeneracy of the SL electron gas sets in the faster, the narrower the width of the conduction miniband in the direction of its axis. Obviously, this is due to a decrease in the total number of quantum states in the conduction band. Moreover, at $\beta << 5$ the SL thermopower is less than the thermopower of the bulk samples made of the same material. As the width of the conduction miniband increases, the SL thermopower grows, asymptotically approaching the limiting value at $\beta \geq 10$ in the bulk samples, which is quite obvious, since in this case the top of the conduction band in the direction of the *0z* axis ceases to play any role. It is clear that within the accepted assumptions, the thermopower does not depend on the period of the semiconductor

SL. This is explained by the form of the dispersion law and the nature of the energy dependence of the relaxation time.

Although a decrease in the width of the conduction miniband in the direction of the SL axis leads to a decrease in the thermopower, there are a number of factors that have a positive effect on its increase. For example, the electron-phonon entrainment, which in semiconductor superstructures at low temperatures can be of crucial importance [17]. In addition, a slight decrease in thermopower in comparison with bulk materials does not exclude an increase in the thermoelectric figure of merit of SL as a whole, due to a decrease in the lattice component of thermal conductivity caused by intense scattering of phonons at the boundaries of the layers.

References

1. L.I.Anatychuk (1979). *Termoelementy i termoelektricheskiie ustroistva. Spravochnik. [Thermoelements and thermoelectric devices. Handbook]*. Kyiv: Naukova dumka [in Russian].
2. Bulat L.P., Zakordonets V.S. (1995). *Semiconductors,* 29 (10), 1743.
3. Hicks L.D., Dresselhaus M.S. (1993). *Phys. Rev*. B47, 12727.
4. Hicks L.D., Dresselhaus M.S. (1993). *Phys. Rev*. B47, 16631.
5. Hicks L.D., Harman T.C., Sun X., Dresselhaus M.S. (1996). *Phys. Rev*. B53, 10493.
6. Shick A.Ya. (1973). *Semiconductors*, 7(2), 261.
7. Askerov B.M., Gashimzade N.M., Panakhov M.M. (1987). *Semiconductors* 29(3),818.
8. Bulygin A.S., Shmelyov G.M., Maglevannyi I.I. (1999). *Semiconductors* 41(7), 1314.
9. Askerov B.M., Guliev B.I., Figarova S.R., Gadirova I.R. (1997). *Semiconductors*, 39(10), 1857.
10. Grahn H.T., von Klitzing K., Ploog K., Dőhler G.H. (1991). *Phys. Rev*. B 43, 14, 12095.
11. Fletcher R., Coleridge P.T., Feng Y. (1995). *Phys. Rev*. B 52, 4, 2823.
12. Bulayevskii L.N.(1975). *Uspekhi fizicheskikh nauk – Advances in Physical Sciences*, 116 (3), 449 [in Russian].
13. Tavger B.A., Demikhovskii V.Ya. (1968). *Uspekhi fizicheskikh nauk – Advances in Physical Sciences*, 96(1), 61[in Russian].
14. Silin A.P. (1985). *Uspekhi fizicheskikh nauk – Advances in Physical Sciences*, 147(3), 485 [in Russian].
15. Pshenai-Severin D.A., Ravich Yu.I. (2002). *Semiconductors*, 36(8), 974.
16. Askerov B.M. (1985). *Elektronnyie yavleniia perenosa v poluprovodnikakh [Electronic transport phenomena in semiconductors]*. Moscow: Nauka [in Russian].
17. Bass F.G., Bochkov V.S., Gurevich Yu.G. (1984). *Elektrony i phonony v ogranichennykh poluprovodnikakh [Electrons and phonons in confined semiconductors]*. Moscow: Nauka [in Russian].

Submitted 24.02.2021

Закордонець В.С. *канд. фіз.-мат. наук*

Тернопільський національно технічний університет
імені Івана Пулюя, вул. Руська, 56, Тернопіль, 46001,
Україна; *e-mail:wladim21@gmail.com*

ТЕРМОЕРС В НАПІВПРОВІДНИКОВИХ НАДГРАТКАХ ПРИ РОЗСІЮВАННІ НОСІЇВ СТРУМУ НА ФОНОНАХ І ТОЧКОВИХ ДЕФЕКТАХ

В квазікласичному одномінізонному наближені досліджена термоЕРС напівпровідникових надграток (НГ) у випадку довільної статистики та при розсіюванні носіїв струму на акустичних фононах, точкових дефектах і неполярних оптичних фононах з урахуванням зміни часу релаксації в порівнянні з об'ємними матеріалами. Встановлена аналітична залежність термоЕРС від приведеної ширини зони провідності в напрямку осі надгратки. Показано, що термоЕРС надгратки збільшується із збільшенням ширини мінізони провідності, асимптотично наближаючись до граничного значення при $\beta \geq 10$. *Бібл. 17, рис. 3.*

Ключові слова: коефіцієнт термоЕРС, добротність надгратки, термоЕРС.

Закордонец В.С., *канд. физ.-мат. наук*

Тернопольский национальный технический университет
имени Ивана Пулюя, ул. Русская, 56, Тернополь, 46001,
Украина; *e-mail*: *wladim21@gmail.com*

ТЕРМОЭДС В ПОЛУПРОВОДНИКОВЫХ СВЕРХРЕШЕТКАХ ПРИ РАССЕЯНИЯ НОСИТЕЛЕЙ ТОКА НА ФОНОНАХ И ТОЧЕЧНЫХ ДЕФЕКТАХ

В квазиклассическом одноминизонном приближении исследована термоЭДС полупроводниковых сверхрешеток (СР) в случае произвольной статистики и при рассеянии носителей тока на акустических фононах, точечных дефектах и неполярных оптических фононах с учетом изменения времени релаксации по сравнению с объемными материалами. Установлена аналитическая зависимость термоЭДС от приведенной ширины зоны проводимости β *в направлении оси сверхрешетки. Показано, что термоЭДС сверхрешетки увеличивается с увеличением ширины минизоны проводимости, асимптотически приближаясь к предельному значению при* $\beta \geq 10$. *Библ. 17, рис.3.*

Ключевые слова: коэффициент термоЭДС, добротность сверхрешоток, термоЭДС.

References

1. L.I.Anatychuk (1979). *Termoelementy i termoelektricheskiie ustroistva. Spravochnik. [Thermoelements and thermoelectric devices. Handbook]*. Kyiv: Naukova dumka [in Russian].
2. Bulat L.P., Zakordonets V.S. (1995). *Semiconductors,* 29 (10), 1743.
3. Hicks L.D., Dresselhaus M.S. (1993). *Phys. Rev*. B47, 12727.
4. Hicks L.D., Dresselhaus M.S. (1993). *Phys. Rev*. B47, 16631.
5. Hicks L.D., Harman T.C., Sun X., Dresselhaus M.S. (1996). *Phys. Rev*. B53, 10493.
6. Shick A.Ya. (1973). *Semiconductors*, 7(2), 261.
7. Askerov B.M., Gashimzade N.M., Panakhov M.M. (1987). *Semiconductors* 29(3),818.
8. Bulygin A.S., Shmelyov G.M., Maglevannyi I.I. (1999). *Semiconductors* 41(7), 1314.
9. Askerov B.M., Guliev B.I., Figarova S.R., Gadirova I.R. (1997). *Semiconductors*, 39(10), 1857.
10. Grahn H.T., von Klitzing K., Ploog K., Dőhler G.H. (1991). *Phys. Rev*. B 43, 14, 12095.
11. Fletcher R., Coleridge P.T., Feng Y. (1995). *Phys. Rev*. B 52, 4, 2823.
12. Bulayevskii L.N.(1975). *Uspekhi fizicheskikh nauk – Advances in Physical Sciences*, 116 (3), 449 [in Russian].
13. Tavger B.A., Demikhovskii V.Ya. (1968). *Uspekhi fizicheskikh nauk – Advances in Physical Sciences*, 96(1), 61[in Russian].
14. Silin A.P. (1985). *Uspekhi fizicheskikh nauk – Advances in Physical Sciences*, 147(3), 485 [in Russian].
15. Pshenai-Severin D.A., Ravich Yu.I. (2002). *Semiconductors*, 36(8), 974.
16. Askerov B.M. (1985). *Elektronnyie yavleniia perenosa v poluprovodnikakh [Electronic transport phenomena in semiconductors]*. Moscow: Nauka [in Russian].
17. Bass F.G., Bochkov V.S., Gurevich Yu.G. (1984). *Elektrony i phonony v ogranichennykh poluprovodnikakh [Electrons and phonons in confined semiconductors]*. Moscow: Nauka [in Russian].

Submitted 24.02.2021

Romaka V.A. *doc. tech. Science, professor*[1],
Stadnyk Yu.V. *cand. chem. Science*[2],
Romaka L.P. *cand. chem. Science*[2],
Pashkevych V.Z. *cand. tehn., docent*[1],
Romaka V.V. *doc. tech. Science*[3],
Horyn A.M. *cand. chem. Science*[2],
Demchenko P.Yu. *cand. chem. Science*[2]

[1]National University "Lvivska Politechnika", 12,
S. Bandera Str., Lviv, 79013, Ukraine, *e-mail: vromaka@polynet.lviv.ua*;
[2]Ivan Franko National University of Lviv, 6, Kyryla and Mefodiya Str.,
Lviv, 79005, Ukraine, *e-mail: lyubov.romaka@lnu.edu.ua*;
[3]Technische Universität Dresden, Bergstrasse 66,
01069 Dresden, Germany, *e-mail: vromakal@gmail.com*

STUDY OF STRUCTURAL, THERMODYNAMIC, ENERGY, KINETIC AND MAGNETIC PROPERTIES OF THERMOELECTRIC MATERIAL $Lu_{1-x}Zr_xNiSb$

The crystal and electronic structures, thermodynamic, kinetic, energy and magnetic properties of the thermoelectric material $Lu_{1-x}Zr_xNiSb$ in the ranges: T=80–400 K, x=0–0.10 were studied. Mechanisms of simultaneous generation of structural defects of acceptor and donor nature are established. It is shown that in the structure of the basic compound LuNiSb there are defects of acceptor nature as a result of vacancies in the crystallographic positions 4a and 4c of Lu and Ni atoms, respectively, which gave rise to acceptor levels (zones) in the band gap ε_g. Introduction of Zr impurity atoms into the structure of the LuNiSb compound by substitution of Lu atoms in position 4a generates structural defects of donor nature with simultaneous elimination of vacancies in positions 4a and 4c of Lu and Ni atoms, respectively (acceptor levels). The ratio of the concentrations of the available defects of donor and acceptor nature determines the location of the Fermi level ε_F and the conduction mechanisms in $Lu_{1-x}Zr_xNiSb$. The investigated solid solution $Lu_{1-x}Zr_xNiSb$ is a promising thermoelectric material. Bibl. 15, Fig. 9.

Keywords: electronic structure, electrical resistivity, thermopower coefficient.

Introducion

A new promising class of semiconductor thermoelectric materials with high efficiency of conversion of thermal energy into electricity are solid substitution solutions based on *RNiSb* compounds (*R* – rare earth metals of the yttrium subgroup) [1 – 4], which crystallize in the structural type *MgAgAs* (sp. group $F\bar{4}3m$) [5]. Thus, in [1 – 6], when studying the structural, kinetic and magnetic characteristics of *RNiSb* compounds, it was found that their crystal structure is defective, and the compounds themselves are semiconductors of the hole-type conductivity. Thus, in the crystal there is a mechanism for generating structural defects of acceptor nature. However, today there is no model of the structure of *RNiSb* and the mechanism of generating defects, which are adequate to the results of the experiment.

It is known that one of the ways to obtain thermoelectric materials with high values of thermoelectric quality factor Z is to generate in the crystal structural defects of donor and/or acceptor nature, which simultaneously leads to changes in the values of thermopower coefficient $\alpha(T, x)$ and thermal conductivity $\kappa(T, x)$, as well as the specific conductivity $\sigma(T, x)$ [7]. Therefore, to obtain a new thermoelectric material, a semiconductor solid solution of $Lu_{1-x}Zr_xNiSb$ obtained by doping a *LuNiSb* compound with *Zr* atoms by substituting *Lu* atoms at the crystallographic position 4*a* was investigated. In this case, structural defects of donor nature must be generated in the semiconductor, because the *Zr* atom ($4d^25s^2$) has a larger number of *d*-electrons than *Lu* ($5d^16s^2$).

On the other hand, without knowing the features of the spatial arrangement of atoms in *RNiSb* compounds and, in particular, in *LuNiSb*, it is almost impossible to understand the mechanism of entry of impurity atoms into the semiconductor matrix when obtaining a suitable solid solution. And this makes it unpredictable to obtain thermoelectric material with high values *Z*. Thus, the authors [4, 6] based on the results of calculating the density distribution of electronic states DOS *LuNiSb* for different variants of atoms in the nodes of the unit cell and the degree of occupancy of positions of own and/or foreign atoms suggested the existence of vacancies (~6%) in position 4*c* atoms *Ni*. In this case, structural defects of acceptor nature are generated in the crystal, and acceptor levels (zone) ε_A^1 appear in the band gap ε_g, which corresponds to the results of the experiment [6].

The following results of the study of structural, thermodynamic, kinetic, energy and magnetic characteristics of the semiconductor solid solution $Lu_{1-x}Zr_xNiSb$, $x = 0 – 0.10$, will clarify the crystal and electronic structure of the basic semiconductor *LuNiSb*. This will allow us to understand both the nature of *LuNiSb* defects and make the process of optimizing the characteristics of the thermoelectric material $Lu_{1-x}Zr_xNiSb$ predictable.

Research methods

The crystal structure, the distribution of the density of electronic states (DOS), and the magnetic, thermodynamic, kinetic, and energy characteristics of $Lu_{1-x}Zr_xNiSb$ have been studied. Samples of the solid solution $Lu_{1-x}Zr_xNiSb$ were synthesized by fusing the charge of the initial components in an electric arc furnace in an inert argon atmosphere followed by homogenizing annealing for 720 h at a temperature of 1073 K. Crystallographic parameters were calculated using the program Fullprof [8]. Diffraction data arrays were obtained using a powder diffractometer STOE STADI P ($Cu\text{K}\alpha_1$ radiation).. Calculations of the electronic structure, density distribution of electronic states (DOS), electron localization function (ELF), thermodynamic characteristics, as well as optimization of the crystal structure parameters of the $Lu_{1-x}Zr_xNiSb$ thermoelectric material were performed using the Koringa-Kon-Rostoker method as a method. Kohn-Rostoker (hereinafter KKR) in the Coherent Potential Approximation (CPA) and Local Density Approximation (LDA) approximation, as well as the Full Potential Linearized Augumented Plane Waves (FLAPW) method. KKR simulations were performed using AkaiKKR software packages [9] in the local density approximation for the exchange-correlation potential with parameterization Moruzzi, Janak, Williams (MJW) [10] in the semi-relativistic consideration of the core level and spin-orbit interaction. For calculations using the FLAPW method used in the software package Elk [11]. The simulation was performed for a 10×10×10 *k*-grid in both the local density (LDA) and generalized GGA gradient approximations. The Brillouin zone was divided into 1000 *k*-points, which were used to calculate the Bloch spectral function (band energy spectrum) and the density of electronic states. The width of the energy window was chosen so as to capture the semi-core states of *p*-elements. Visualization of volumetric data was performed using the program VESTA [12]. Topological analysis and interpretation of DOS and ELF were performed within the framework of Bader's theory [13]. The accuracy of calculations of the position

of the Fermi level $\varepsilon_F \pm 6$ meV. Temperature and concentration dependences of resistivity (ρ) and thermopower coefficient (α) with respect to copper and magnetic susceptibility (χ) (Faraday method) of $Lu_{1-x}Zr_xNiSb$ samples, $x = 0 – 0.10$, in the temperature range $T = 80 – 400$ K were measured.

Investigation of structural characteristics of $Lu_{1-x}Zr_xNiSb$

Microprobe analysis of the concentration of atoms on the surface of $Lu_{1-x}Zr_xNiSb$ samples established their correspondence to the initial compositions of the charge, and *X*-ray phase and structural analyzes showed that the diffraction patterns of samples including $x = 0 – 0.1$ are indexed in the structural type of *MgAgAs* [5] phases (Fig. 1*a*). With the help of structural studies, the change in the values of the period of the unit cell $a(x)$ $Lu_{1-x}Zr_xNiSb$ was established. Since the atomic radius *Lu* ($r_{Lu} = 0.173$ nm) is larger than *Zr*/($r_{Zr} = 0.160$ nm), it was logical to expect a decrease in the values of the period of the unit cell $a(x)$ when substituting Lu atoms at position 4*a* for *Zr* atoms. In this case, as mentioned above, structural defects of donor nature will be generated in the crystal, and impurity donor levels (zone) ε_D^1 will appear in the forbidden zone ε_g.

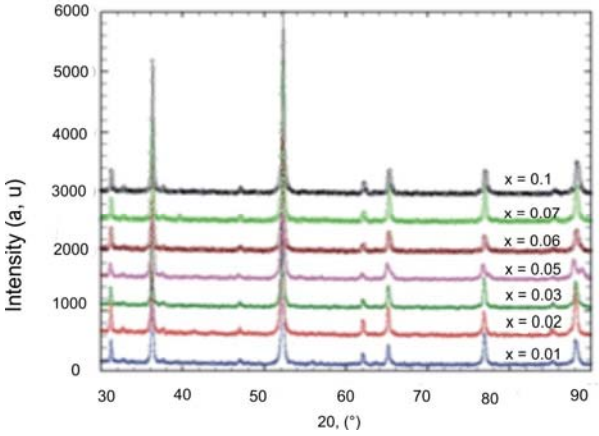

a)

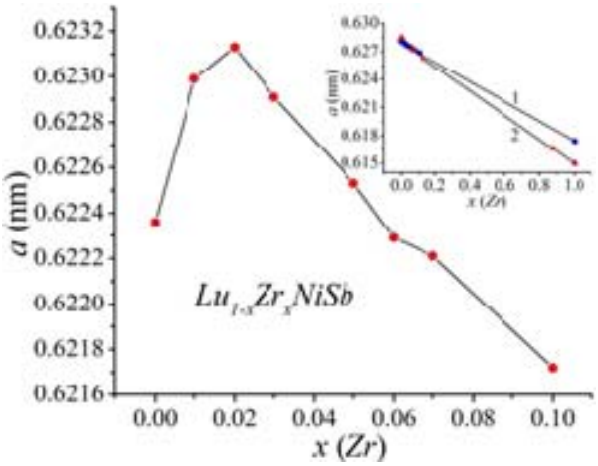

b)

Fig. 1. Diffractograms of samples (a) and change of values of the period of the unit cell a(x) (b) $Lu_{1-x}Zr_xNiSb$; insert: simulation a(x): 1 – using the program AkaiKKR, 2 – the program Elk

However, the results of the structural analysis of $Lu_{1-x}Zr_xNiSb$ show (Fig. 1*b*) that in the area of concentrations $x = 0 – 0.02$ the values of the period $a(x)$ increase rapidly, pass through the maximum and decrease just as rapidly at $x > 0.02$. In a related semiconductor solid solution $Er_{1-x}Zr_xNiSb$, we observed a similar behavior of the period of the unit cell $a(x)$: in the region $x = 0 – 0.02$ the values of $a(x)$ increased, and at concentrations $x > 0.05$ decreased [3].

The fact that in $Lu_{1-x}Zr_xNiSb$ there is a nonmonotonic change in the values of the period of the unit cell $a(x)$ (Fig. 1*b*) suggests that impurity *Zr* atoms introduced into the matrix of *LuNiSb* compounds not only replace *Lu* atoms in position 4*a*, but can also partially occupy both different crystallographic positions and generate the appearance of atoms in the tetrahedral voids of the structure, which make up ~24% of the volume of the unit cell [6].

Formally, based on geometric considerations, we can assume that the increase in the values of the period of the unit cell $a(x)$ $Lu_{1-x}Zr_xNiSb$ could cause partial occupation of the crystallographic position of 4*c Ni* atoms by *Zr* atoms. After all, the atomic radius of the Ni atom ($r_{Ni} = 0.124$ nm) is the smallest among the chemical elements $Lu_{1-x}Zr_xNiSb$ ($r_{Sb} = 0.159$ nm). However, such an assumption is unlikely due to the significant difference in the atomic radii of *Zr* and *Ni*. On the other hand, there is a high probability of returning *Ni* atoms to position 4*c* (filling vacancies of the *LuNiSb* compound [4, 6]), which can lead to an increase in the values of $a(x)$ and the elimination of vacancies. We also do not rule out the presence of vacancies in the crystallographic position 4*a*, which also generates structural defects of acceptor nature. The occupation of these vacancies by impurity *Zr* atoms also generates the appearance of structural defects of donor nature and leads to an increase in the values of $a(x)$ $Lu_{1-x}Zr_xNiSb$. However, the accuracy of *X*-ray structural studies does not allow to experimentally identify these vacancies.

Therefore, from the results of experimental results it follows that in the structure of $Lu_{1-x}Zr_xNiSb$ the following processes can occur simultaneously:

– substitution at position 4*a* of *Lu* atoms by *Zr* atoms, which generates structural defects of donor nature in the crystal and the appearance of donor levels (zone) ε_D^1 in the band gap ε_g;

– return of *Ni* atoms to position 4*c* and elimination of vacancies generates defects of donor nature, and impurity donor levels (zones) of ε_D^2 will appear in the forbidden zone. At the same time, the vacancy disappears and in the forbidden zone εg the corresponding acceptor level (zone) ε_A^1.

– occupation of vacancies in position 4*a* by *Zr* atoms simultaneously eliminates the structural defect of acceptor nature and now generates a defect of donor nature with the appearance of the corresponding donor level (zone) ε_D^3 in the forbidden zone ε_g.

To better understand the structural transformations in $Lu_{1-x}Zr_xNiSb$, we calculated the change in the values of the period of the unit cell $a(x)$ $Lu_{1-x}Zr_xNiSb$ using the software packages AkaiKKR [9] and Elk [11] (Fig. 1*b*, insert). The results of the calculation of the change in $a(x)$ $Lu_{1-x}Zr_xNiSb$ by both methods, in contrast to the experimental results, show only a monotonic decrease in the values of the cell period, which is quite logical and predictable provided that only *Lu* atoms are replaced by *Zr*.

From the insert of fig. 1*b* also shows that the values of the period of the unit cell of the *LuNiSb* compound, obtained by simulation by the software package AkaiKKR [9], are less than those obtained by implementing the software package Elk [11]. At the same time, the simulation result for the hypothetical compound *ZrNiSb* (the other side of the solid solution $Lu_{1-x}Zr_xNiSb$ for x=1) showed the opposite result: the values of period a of the compounds *ZrNiSb* obtained by AkaiKKR [9] are greater than those obtained by Elk [11]. Therefore, the course of the dependences $a(x)$ $Lu_{1-x}Zr_xNiSb$, obtained by different modeling methods, occurs according to different laws. In this case, the angles of inclination of the dependences $a(x)$ $Lu_{1-x}Zr_xNiSb$ are different. It turned out that the angle of change of the values of the period of the cell $a(x)$ $Lu_{1-x}Zr_xNiSb$, obtained from the experiment, coincides with that when using the software package Elk [11]. This result indicates a higher accuracy of modeling the structural characteristics of $Lu_{1-x}Zr_xNiSb$ by the FLAPW method compared to the KKR method.

Investigation of thermodynamic characteristics of $Lu_{1-x}Zr_xNiSb$

Based on the fact that there is no *ZrNiSb* compound with the structure of *MgAgAs*, and hence 100 % substitution of *Lu* atoms for *Zr* and vice versa, it is important to establish the limits of the possible existence of a solid solution of $Lu_{1-x}Zr_xNiSb$. For this purpose, modeling of thermodynamic characteristics for a hypothetical solid solution $Lu_{1-x}Zr_xNiSb$, $x = 0 – 1.0$, in the approximation of harmonic oscillations of atoms in the framework of the DFT density functional theory was performed. The change in the values of the enthalpy of mixing ΔH (Fig. 2*a*) and the total energy ΔE (Fig. 2*b*) $Lu_{1-x}Zr_xNiSb$, $x = 0 – 1.0$, suggests that the thermoelectric material exists as a solid substitution solution in the concentration range $x < 0.20$.

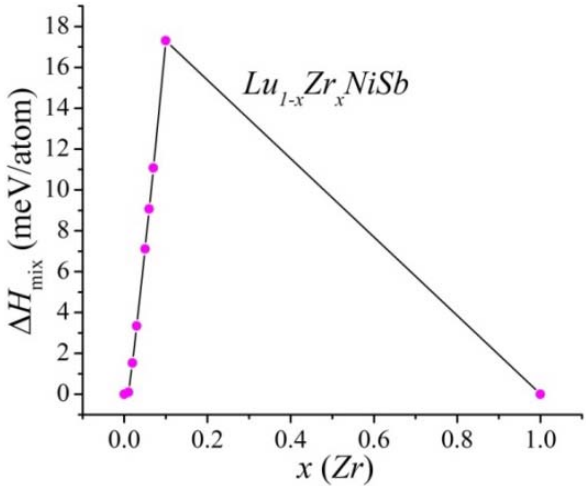

a)

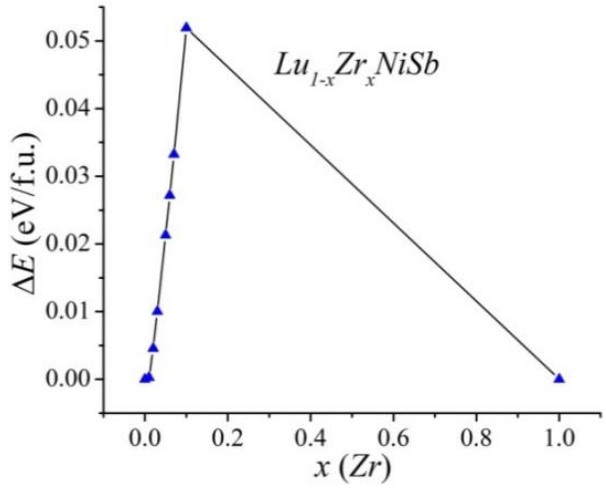

b)

Fig. 2. Calculation by Elk method of change of enthalpy values of mixing ΔH (a) and total energy ΔE (b) of solid solution $Lu_{1-x}Zr_xNiSb$

In this concentration region, the values of the enthalpy of mixing $\Delta H(x)$ and the total energy $\Delta E(x)$ increase, indicating the energy expediency of substituting *Lu* atoms for *Zr*. However, at higher concentrations of impurity atoms *Zr*, $x > 0.20$, the dependences $\Delta H(x)$ and $\Delta E(x)$ decrease, which indicates

the energy disadvantage of the formation of a solid substitution solution. Stratification (spinoidal phase decay) occurs and thermoelectric material does not exist. Therefore, the region of existence of the solid substitution solution $Lu_{1-x}Zr_xNiSb$ is limited by the concentration $x = 0.20$.

Investigation of electrokinetic and energy characteristics of $Lu_{1-x}Zr_xNiSb$

Temperature and concentration dependences of specific electrical resistance ρ and thermopower coefficient α of samples $Lu_{1-x}Zr_xNiSb$, $x = 0 – 0.10$, are shown in Fig. 3 – 7.

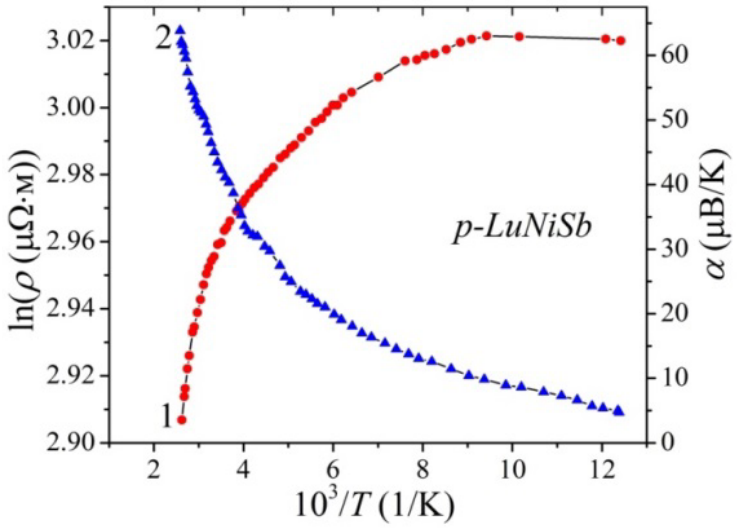

a)

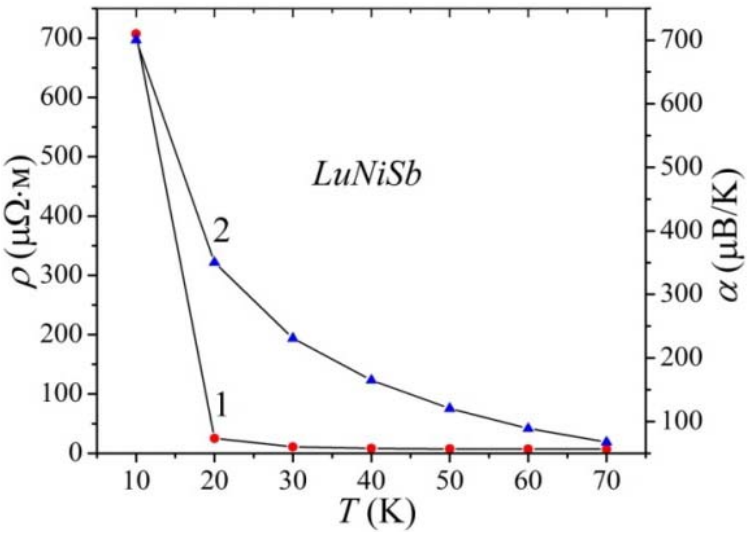

b)

Fig. 3. Temperature dependences of specific electrical resistance ρ (1) and thermo-emf coefficient α (2) LuNiSb; a – the results of the experiment, b – the calculation in the range T = 4.2–70 K

As we can see from Fig. 3, for the basic compound *LuNiSb* the dependence ln(ρ(1/*T*)) is characteristic of semiconductors [14] and is approximated by the known relation (1):

$$\rho^{-1}(T) = \rho_1^{-1} \exp\left(-\frac{\varepsilon_1^{\rho}}{k_B T}\right) + \rho_3^{-1} \exp\left(-\frac{\varepsilon_3^{\rho}}{k_B T}\right), \quad (1)$$

where the first high-temperature term describes the activation of current carriers ε_1^{ρ} from the Fermi level ε_F to the level of continuous energy zones, and the second, low-temperature term, the hopping conductivity at impurity donor states ε_3^{ρ} with energies close to the Fermi level ε_F. Calculations showed that in the *p-LuNiSb* semiconductor the Fermi level ε_F is located at a distance ε_1^{ρ} = 10.2 meV from the ceiling of the valence band ε_V.

Temperature dependences of the thermopower coefficient α(1/*T*) *p-LuNiSb* (Fig. 3*a*) are described by the known expression (2) [15]:

$$\alpha = \frac{k_B}{e}\left(\frac{\varepsilon_i^{\alpha}}{k_B T} - \gamma + 1\right), \quad (2)$$

where γ is a parameter that depends on the nature of the scattering mechanism. From the high- and low-temperature activation regions of the α(1/*T*) dependence, the values of activation energies ε_1^{α} = 35.3 meV and ε_3^{α} = 1.9 meV were calculated, which, as shown in [6], are proportional to the amplitude of large-scale fluctuations of continuous energy and small-scale zones. of fluctuations of strongly doped and highly compensated semiconductor [14].

The presence of a high-temperature activation region on the temperature dependence of the resistivity ln(ρ(1/*T*)) *p-LuNiSb* indicates the location of the Fermi level ε_F in the band gap ε_g of the semiconductor, and positive values of the thermopower coefficient α(*T*) at these temperatures specify its position – near the valence band ε_V. Therefore, holes are the main carriers of electric current. The obtained values of activation energies ε_1^{ρ} and ε_1^{α} for *p-LuNiSb* are consistent with the results of previous studies [4, 6].

Modeling of temperature dependences of kinetic characteristics of *LuNiSb* compound in the temperature range *T* = 4.2 – 70 K shows a rapid decrease in the values of resistivity ρ(*T*) in the range *T* = 4.2 – 20 K (Fig. 3*b*). This behavior ρ(*T*) is characteristic of semiconductors when there is an increase in the number of free current carriers due to their activation from the Fermi level ε_F. Such carriers are holes, which is indicated by positive values of the thermo-emf coefficient α(*T*) *LuNiSb*, and this is consistent with the results of the experiment.

The introduction of *Zr* atoms into the structure of the *LuNiSb* compound by substituting *Lu* atoms at position 4*a* generates structural defects of donor nature in $Lu_{1-x}Zr_xNiSb$. Simulation of the change in the values of resistivity ρ(*x*,*T*) at the lowest concentration of *Zr* atoms (*x* = 0.01) shows two fundamentally different areas: at temperatures *T* = 4.2 – 20 K, the values of ρ(*T*) decrease, which is characteristic of semiconductors, and with increasing temperatures – increase, indicating the metallic type of conductivity (Fig. 4). The values of the thermopower coefficient α(*T*) $Lu_{0.99}Zr_{0.01}NiSb$ decrease rapidly from the values of $\alpha_{4.2\ K}$ = 225 μV/K to $\alpha_{70\ K}$ = -20 μV/K. The change in the sign of the thermopower coefficient α(*T*) indicates a change in the type of conductivity when the main current carriers are electrons. The Fermi level ε_F is located in the conduction band ε_C.

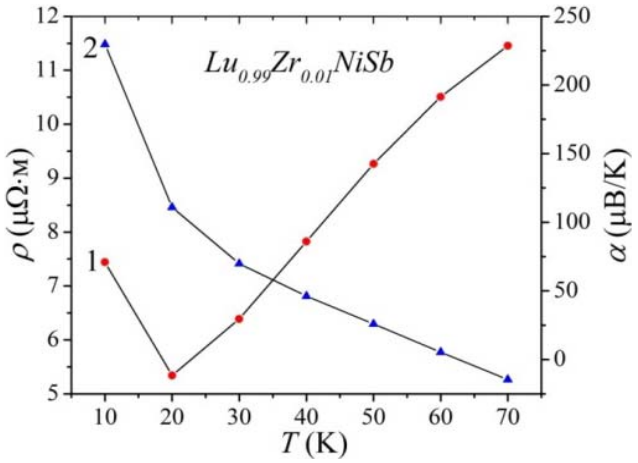

a)

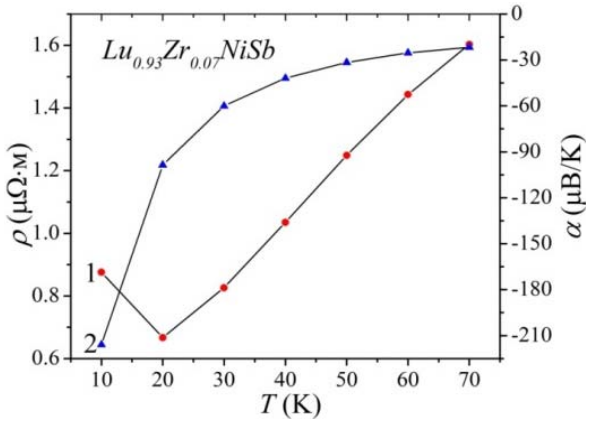

b)

Fig. 4. Results of modeling the temperature dependences of the resistivity ρ (T, x) (1) and the thermo-emf coefficient α (T, x) (2) Lu1-xZrxNiSb at temperatures T = 4.2–70

At an even higher concentration of *Zr* atoms ($x = 0.07$ and $x = 0.10$) in the temperature range $T = 4.2 – 70$ K, the sign of the thermopower coefficient α(T) remains negative, and the nature of the change in resistivity values ρ(T) is similar, as for the case when the concentration of *Zr* atoms was $x = 0.01$ (Fig. 4). The fact that at all concentrations of *Zr* atoms in the temperature range $T = 4.2 – 20$ K the values of the resistivity ρ(T,x) $Lu_{1-x}Zr_xNiSb$ decrease indicates the depth of occurrence in the band gap ε_g of the donor states. At low temperatures ($T < 20$ K), the thermal energy is insufficient for the activation of electrons in the conduction band ε_C. However, at temperatures $T > 20$ K the concentration of free electrons becomes significant and the Fermi level ε_F enters the conduction band ε_C, indicating the transition of the conductivity of the dielectric metal, which is the Anderson transition [15].

Doping *p-LuNiSb* with the smallest in the experiment concentration of *Zr* atoms ($x = 0.01$) radically changes both the nature of the behavior of temperature dependences of resistivity ρ(T, x) and the thermopower coefficient α(T,x), and the type of main carriers of electric current (Fig. 5*a*, 6*a*). The metallic nature of the behavior of the temperature dependences of the resistivity ρ(T, x) $Lu_{1-x}Zr_xNiSb$ (Fig. 5*a*) indicates that the Fermi level ε_F has left the band gap ε_g and is in the zone of continuous energies. The fact

that such a zone is a conduction band ε_C can be stated on the basis of negative values of the thermopower coefficient $\alpha(T, x)$ (Fig. 6*a*) at all concentrations and temperatures. It is clear that the increase in the values of $\rho(T, x)$ $Lu_{1-x}Zr_xNiSb$ with increasing temperature is due to the current carriers in the semiconductor scattering mechanisms.

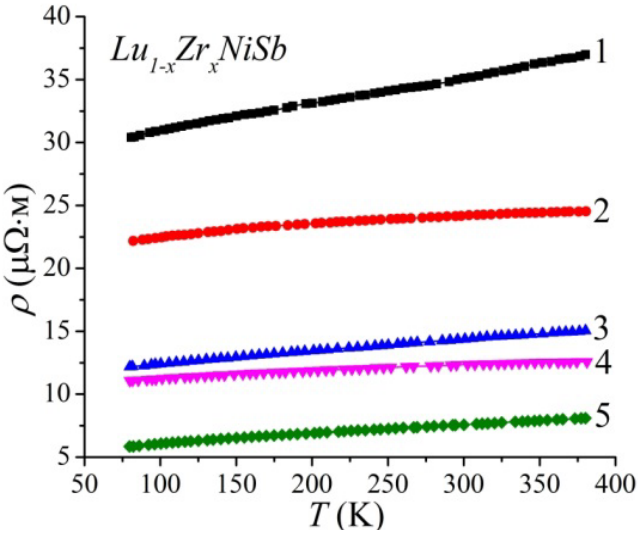

a)

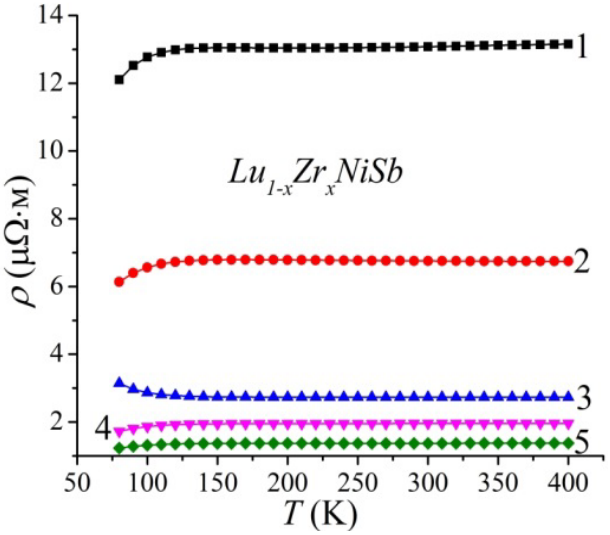

b)

Fig. 5. Temperature dependences of resistivity $\rho(T,x)$ $Lu_{1-x}Zr_xNiSb$:
a – experimental results, b – calculation;
1 – x = 0.01; 2 – x = 0.02; 3 – x = 0.05; 4 – x = 0.07; 5 – x = 0.1

Thus, from the above we can note the closeness of the results of experimental studies and calculations of changes in the values of the kinetic characteristics of the semiconductor solid solution $Lu_{1-x}Zr_xNiSb$ (Fig. 4 – 6). This is evidence of both the correctness of the experiment and the chosen method of modeling.

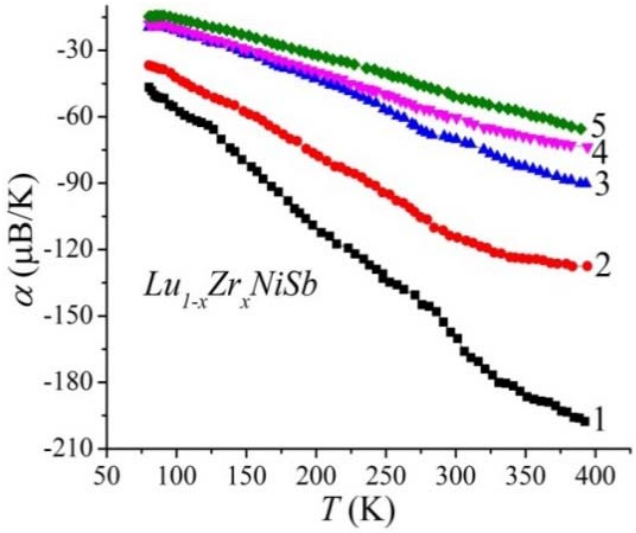

a)

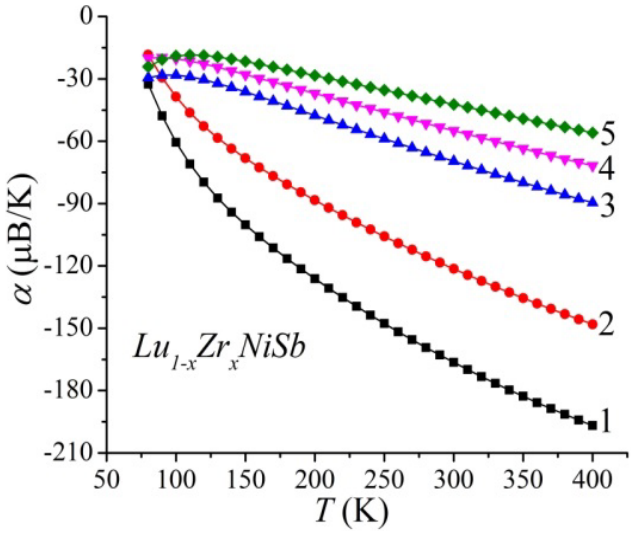

b)

Fig. 6. Temperature dependences of the thermopower coefficient α(*T,x*) *Lu1-xZrxNiSb: a – experimental results, b – calculation; 1 – x = 0.01; 2 – x = 0.02; 3 – x = 0.05; 4 – x = 0.07; 5 – x = 0.1*

The nature of the change in the values of the resistivity ρ(*x, T*) *Lu1-xZrxNiSb* at all temperatures turned out to be unexpected (Fig. 7*a*). It is known that if two types of electric current carriers are present in a semiconductor at the same time, then the maximum on the dependence ρ(*x, T*) indicates that the concentrations of the available ionized acceptors and donors are balanced. Available in Fig. 7*a*, the maximum on the dependence ρ(*x, T*) *Lu1-xZrxNiSb* on $x \approx 0.01$ has a different nature. After all, for $x = 0$ we have a semiconductor of *p*-type conductivity, when the Fermi level ε_F lies at a distance of 10.2 meV near the valence band ε_V. And at a concentration of $x = 0.01$ it is located deep in the conduction band ε_C and electrons are the main carriers. The same applies to the nature of the change in the values of the thermopower coefficient α(*T, x*) *Lu1-xZrxNiSb*, in particular, the available minimum at $x \approx 0.01$ (Fig. 7*b*). It is correct to talk only about the increase in the values of ρ(*x, T*) and α(*x,T*) *Lu1-xZrxNiSb* at all

temperatures in the concentration range $0.01 \le x \le 0.10$ (Fig. 7*a*), when the Fermi level ε_F is located in the conduction band ε_C. And the reason for this behavior $\rho(x,T)$ and $\alpha(x,T)$ $Lu_{1-x}Zr_xNiSb$ is the increase in the concentration of free electrons and the density of states at the Fermi level ε_F. This is understandable, because *Zr* atoms, replacing *Lu*, generate structural defects of donor nature, which supply electrons to the semiconductor.

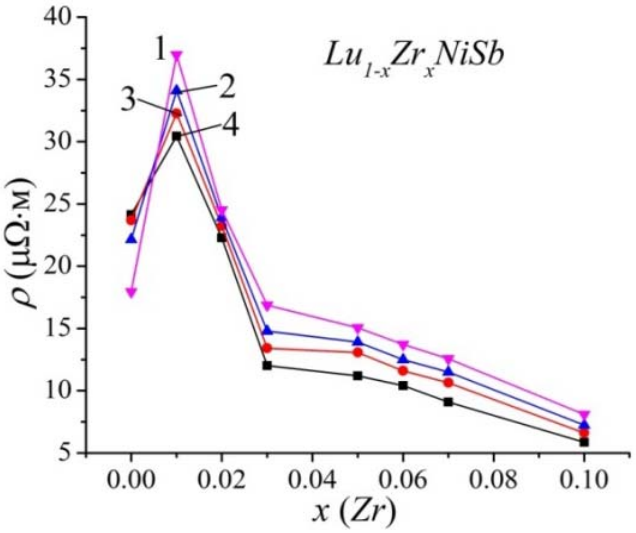

a)

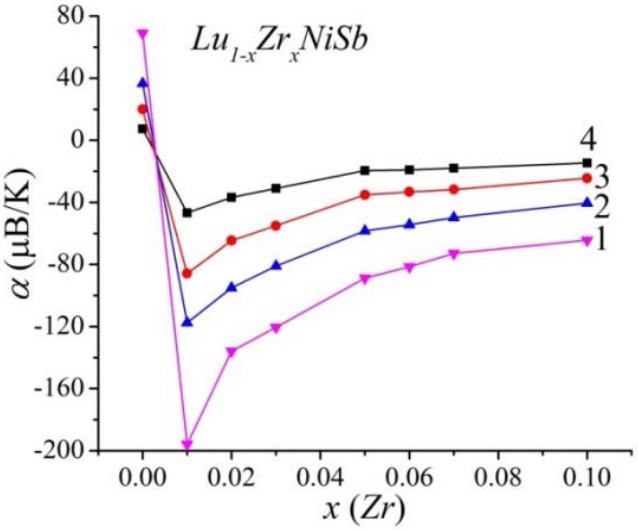

b)

Fig. 7. Change in the values of resistivity ρ(x,T) (a) and the thermopower coefficient α(T,x) (b) $Lu_{1-x}Zr_xNiSb$ at different temperatures: 1 – T = 380 K; 2 – T = 250 K; 3 – T = 160 K; 4 – T = 80 K

Extremely interesting and informative were the results of calculation from low-temperature activation regions of $\alpha(1/T)$ $Lu_{1-x}Zr_xNiSb$ dependences of activation energies $\varepsilon_1^{\alpha}(x)$ (Fig. 8*a*), the values of which are proportional to the amplitude of large-scale fluctuations in the zones of continuous energy in the

crystal space of charged centers, in particular, ionized acceptors and donors [14]. And the higher the degree of compensation of the semiconductor (the ratio of ionized acceptors and donors), the greater the distortion of the zones and the value of the modulation amplitude of the zones of continuous energies.

It should be noted at once that it is correct to analyze the behavior of the activation energy $\varepsilon_1^{\alpha}(x)$ $Lu_{1-x}Zr_xNiSb$ only at the concentration range $0.01 \le x \le 0.10$, when the conductivity of the semiconductor determines one type of basic carriers. After all, for $x = 0$ we have a semiconductor of hole type of conductivity, and for $0.01 \le x$ – electronic. From fig. 8*a*, it follows that at concentrations of $0.01 \le x \le 0.10$ the values of the activation energy $\varepsilon_1^{\alpha}(x)$ $Lu_{1-x}Zr_xNiSb$ rapidly decrease, indicating the predominance of the concentration of one type of electric current carrier over another. Since the main carriers of $Lu_{1-x}Zr_xNiSb$ current at $0.01 \le x$ are electrons and their concentration is much higher than that of holes, the ratio of donors to holes increases with increasing impurity concentration (the degree of compensation decreases).

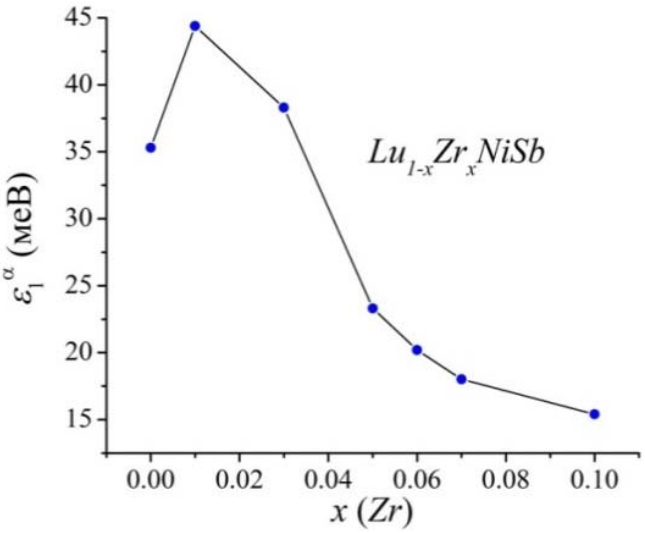

a)

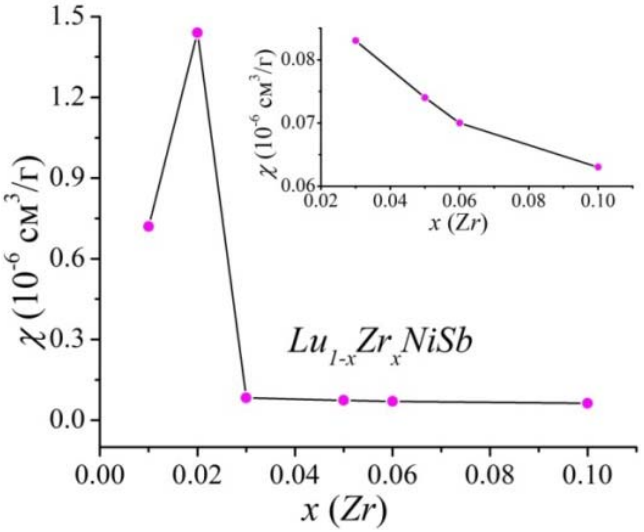

b)

Fig. 8. Change in the values of activation energy $\varepsilon_1^{\alpha}(x)$ (a) and specific magnetic susceptibility $\chi(x)$ (b) $Lu_{1-x}Zr_xNiSb$ for T = 293 K

In the classical case of doping, for example, a *p*-type semiconductor with a donor impurity, it first leads to the capture of free electrons by acceptors (ionization of acceptors) to concentrations when the number of acceptors corresponds to the number of ionized donors. At higher concentrations, when all acceptors are ionized, the donor electrons become collectivized (free) and participate in electrical conductivity. That is, first the electrons are captured by the acceptors present in the semiconductor [14]. In the case of $Lu_{1-x}Zr_xNiSb$, this compensation mechanism is absent.

The question of the reason for such nonclassical behavior of the kinetic characteristics of $Lu_{1-x}Zr_xNiSb$ seems logical. That is, what structural changes in $Lu_{1-x}Zr_xNiSb$ could have caused such a significant effect on the electronic system of the semiconductor, which is reflected in the above electrokinetic characteristics?

Recall that in the structure of *p-LuNiSb* there are vacancies at position 4*c* of *Ni* atoms, which generates structural defects of acceptor nature, and in the band gap ε_g appears the corresponding acceptor level (band) ε_A^1 [3, 6]. In addition, structural studies of $Lu_{1-x}Zr_xNiSb$ found that one of the reasons for the increase in the values of the period of cell $a(x)$ in the area of concentrations $x = 0 – 0.02$ (Fig. 1*b*) is the return to the 4*c* position of *Ni* atoms (elimination of vacancies). At the same time, position 4*c* generates structural defects of donor nature and eliminates structural defects of acceptor nature (namely, elimination of vacancies, not their ionization during electron capture). At the same time, the donor level (zone) ε_D^2 appears in the forbidden zone ε_g $Lu_{1-x}Zr_xNiSb$ and the corresponding acceptor level (zone) ε_A^1 disappears.

However, the simultaneous disappearance of acceptors and the activation of donor generation mechanisms, in particular when *Zr* atoms replace *Lu* atoms at position 4*a* and the return of *Ni* atoms to position 4*c*, cannot cause a giant concentration of donors to appear in the $Lu_{1-x}Zr_xNiSb$ semiconductor. the conduction band ε_C at the lowest concentration ($x = 0.01$). We can assume the existence of another, not described above, the mechanism of donor generation in $Lu_{1-x}Zr_xNiSb$, which is associated with changes in the concentration of Zr atoms.

Experimental studies of the magnetic susceptibility of $\chi(x)$ have shown that samples of both *LuNiSb* compounds and $Lu_{1-x}Zr_xNiSb$ solid solutions at all concentrations are Pauli paramagnetics (Fig. 8*b*). In this case, the synchrony of the behavior of the dependences of the resistivity $\rho(x,T)$ (Fig. 7*a*), the thermopower coefficient $\alpha(T,x)$ (Fig. 7*b*) and the magnetic susceptibility $\chi(x)$ (Fig. 8*b*), associated with a change in the density of states at the Fermi level ε_F.

Therefore, the study of a semiconductor solid solution of $Lu_{1-x}Zr_xNiSb$ obtained by doping a *LuNiSb* compound with *Zr* atoms by substituting Lu atoms in the crystallographic position 4*a* showed the complex nature of the impurity atoms entering the compound matrix when changes occur in several positions simultaneously. The first and most important step in modeling the electronic structure of $Lu_{1-x}Zr_xNiSb$, in particular the behavior of the Fermi level ε_F, is to understand the features of the spatial arrangement and electronic structure of the basic semiconductor *p-LuNiSb*. It is these features that determine the way in which impurity atoms enter the semiconductor matrix, which determines the formation of structural defects of different nature and the appearance in the forbidden zone of the corresponding energy levels..

Refinement of electronic and crystal structures of the basic *p-LuNiSb* semiconductor

If we take as a basis an ordered model of the crystal structure of the *LuNiSb* compound, in which all crystallographic positions are occupied by atoms according to the structural type of *MgAgAs* [5], then modeling of the electronic structure of *LuNiSb* shows that the compound is an *n*-type semiconductor (Fig. 9). Accordingly, the Fermi level ε_F (dashed line) lies near the conduction band ε_C, which in the experiment will give negative values of the thermopower coefficient $\alpha(T)$. However, this

simulation result does not agree with the results of experimental studies (Fig. 3*a*), where positive values of the thermopower coefficient α(*T*) were obtained.

The inconsistency of the results of experimental studies of the basic *p-LuNiSb* semiconductor and modeling of its electronic structure for an ordered model of the crystal structure indicates its disorder. Therefore, in the crystal structure of the compound *LuNiSb* there is a partial occupation of atoms of foreign positions, and it is also possible to have vacancies in different crystallographic positions. After all, in the case of doping the *LuNiSb* with impurity atoms, the presence of vacancies will determine the ways of formation of structural defects and energy levels in the band gap ε_g. That is why it is important to establish the features of the crystal structure of the *p-LuNiSb* semiconductor.

To clarify the crystal structure of the compound *LuNiSb*, as close as possible to the results of experimental measurements (Fig. 3*a*), modeling of its electronic structure for different variants of the spatial arrangement of atoms and the availability of vacancies. In Fig. 9 shows the distribution of the DOS electron density for an ordered model of the crystal structure of the *LuNiSb* compound (all atoms occupy their own positions), but the crystallographic positions of 4*a Lu* atoms and 4*c Ni* atoms contain a certain number of vacancies.

Thus, in the hypothetical compound $Lu_{0.99}NiSb$ the Fermi level ε_F will change its position and is located at the edge of the valence band ε_V: the dielectric-metal conductivity transition will occur (Fig. 9), and free holes become the main current carriers. The location of the Fermi level ε_F near the edge of the valence band ε_V or in the band itself is understandable, because the absence of the *Lu* atom at position 4*a* generates a structural defect of acceptor nature and the corresponding acceptor level (band). In this experiment we will have positive values of the thermopower coefficient α(*T*) $Lu_{0.99}NiSb$, and the intersection of the Fermi level ε_F and the valence band ε_V will change the conductivity from activation to metallic: the values of resistivity ρ will increase with temperature.

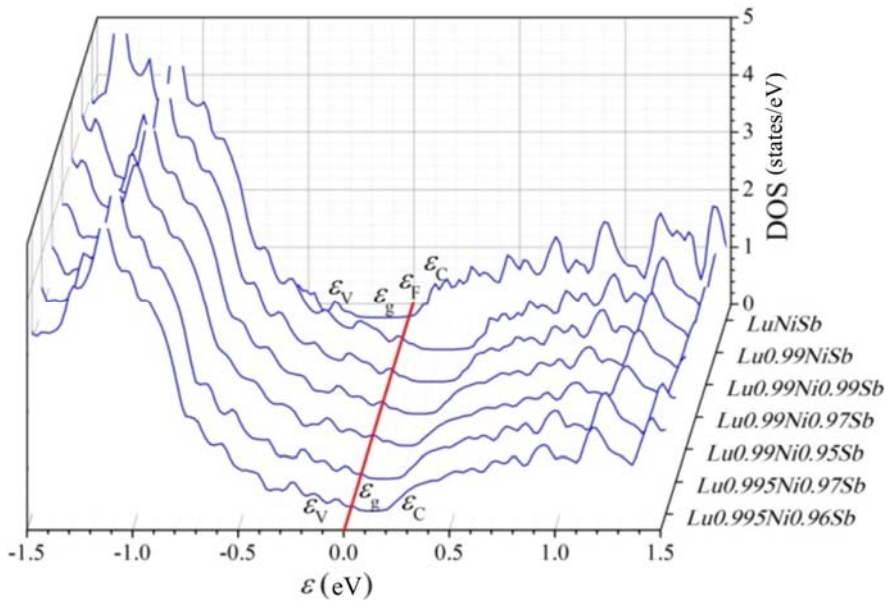

Fig. 9. Calculation of the density distribution of electronic states of DOS for different employment options of the crystallographic positions of the compound LuNiSb

Such simulation results with respect to the type of main electric current carriers correspond to the experimental results (Fig. 3*a*). However, experimental studies have shown that the temperature dependences of the resistivity ρ(*T*) of *LuNiSb* contain high- and low-temperature activation regions,

indicating the activation of holes from the Fermi level ε_F to the edge of the valence band ε_V. Therefore, the Fermi level ε_F in the real crystal is located in the band gap ε_g of the semiconductor, and not the edge of the valence band ε_V, as shown by the simulation results for the case $Lu_{0.99}NiSb$.

The most acceptable results of experimental studies are the model of the electronic structure of the compound *LuNiSb*, which assumes the presence of vacancies in the crystallographic positions of 4*a* *Lu* atoms (~0.005) and 4*c* Ni atoms (~0.04) (Fig. 9). In this model $Lu_{0.995}Ni_{0.96}Sb$ the spatial arrangement of atoms and the presence of vacancies at positions 4*a* and 4*c*, the compound is a hole-type semiconductor semiconductor in which the Fermi level ε_F is located in the band gap near the edge of the valence band ε_V. Under this model of the electronic structure of *p-LuNiSb* on the temperature dependences of the resistivity $\rho(T)$ will be present high- and low-temperature activation sites, and the value of the thermopower coefficient $\alpha(T)$ corresponds to the results of the experiment (Fig. 3*a*).

Thus, doping of the *LuNiSb* semiconductor with donor *Zr* impurities introduced into the structure by substituting Lu atoms at position 4*a* revealed defects of acceptor nature in the structure of the base compound as a result of vacancies at crystallographic positions 4*a* and 4*c* of *Lu* and *Ni* atoms, respectively, the corresponding acceptor levels (zones). The ratio of the concentrations of donor and acceptor levels present in the structure of the *LuNiSb* compound determines the location of the Fermi level ε_F in the semiconductor, and its doping with *Zr* donors will change the mechanisms and type of conductivity $Lu_{1-x}Zr_xNiSb$.

Conclusions

The result of a comprehensive study of the crystal and electronic structures, thermodynamic, kinetic, energy and magnetic properties of the thermoelectric material $Lu_{1-x}Zr_xNiSb$ is the establishment of the nature of structural defects of donor and acceptor nature. It is shown that the structure of the basic compound *LuNiSb* has defects of acceptor nature as a result of vacancies in the crystallographic positions 4*a* and 4*c* of *Lu* and *Ni* atoms, respectively, which gave rise to acceptor levels (zones) in the band gap ε_g. Introduction of *Zr* impurity atoms into the structure of the *LuNiSb* compound by substitution of *Lu* atoms in position 4*a* generates structural defects of donor nature with simultaneous elimination of vacancies in positions 4*a* and 4*c* of *Lu* and *Ni* atoms, respectively (acceptor levels). The ratio of the concentrations of available donors and acceptors determines the location of the Fermi level ε_F and the conduction mechanisms in $Lu_{1-x}Zr_xNiSb$. The investigated solid solution $Lu_{1-x}Zr_xNiSb$ is a promising thermoelectric material. The investigated solid solution $Lu_{1-x}Zr_xNiSb$ is a promising thermoelectric material, but requires additional research.

References

1. Karla I., Pierre J., Skolozdra R.V. (1998). Physical properties and giant magnetoresistance in *RNiSb* compounds. *J. Alloys Compd*., 265, 42–48. (DOI: https://doi.org/10.1016/S0925-8388(97)00419-2).
2. Romaka V.V., Romaka L., Horyn A., Rogl P., Stadnyk Yu., Melnychenko N., Orlovskyy M., Krayovskyy V. (2016). Peculiarities of thermoelectric half-Heusler phase formation in *Gd-Ni-Sb* and *Lu-Ni-Sb* ternary systems. *J. Solid State Chem*., 239, 145–152. (DOI: https://doi.org/10.1016/j.jssc.2016.04.029).
3. Romaka V.A, Stadnyk Yu., Romaka L., Krayovskyy V., Klyzub P., Pashkevych V., Horyn A., Garanyuk P. (2021). Synthesis and Electrical Transport Properties of $Er_{1-x}Sc_xNiSb$ Semiconducting Solid Solution. *J. Phys. and Chem. Sol. State*, 22(1), 146-152. (DOI: 10.15330/pcss.22.1.146-152).
4. Stadnyk Yu., Romaka V.A, Horyn A., Romaka V.V., Romaka L., Klyzub P., Pashkevych V., Garanyuk P. Modeling of Structural and Energetic Parameters of $p\text{-}Er_{1-x}Sc_xNiSb$ Semiconductor.

J. Phys. and Chem. Sol. State, 22(3), 509-515. (DOI: 10.15330/pcss.22.3.509-515).

5. Romaka V.V., Romaka L.P., Krayovskyy V.Ya., Stadnyk Yu.V. (2015). *Stanidy ridkisnozemelnykh ta perekhidnykh metaliv* [*Stannides of rare earth and transition metals*] Lviv: Lvivska Polytechnika [in Ukrainian].
6. Romaka V.A., Stadnyk Yu.V., Krayovskyy V.Ya., Romaka L.P., Guk O.P., Romaka V.V., Mykyuchuk M.M., Horyn A.M. (2020). *Novitni termochutlyvi materialy ta peretvoriuvachi temperatury* [*New thermosensitive materials and temperature converters*]. Lviv, Lvivska Polytechnika [in Ukrainian].
7. Anatychuk L.I. (1979). *Termoelementy i termoelectricheskiie ustroistva. Spravochnik.* [*Thermoelements and thermoelectric devices*. *Reference book*]. Kyiv: Naukova dumka [in Russian].
8. Roisnel T., Rodriguez-Carvajal J. (2001). WinPLOTR: a windows tool for powder diffraction patterns analysis. *Mater. Sci. Forum*, Proc. EPDIC7 378–381, 118–123.
9. Akai H. (1989). Fast Korringa-Kohn-Rostoker coherent potential approximation and its application to FCC *Ni-Fe* systems. *J. Phys.: Condens. Matter*., 1, 8045–8063.
10. Moruzzi V.L., Janak J.F., Williams A.R. (1978). *Calculated electronic properties of metals.* NY: Pergamon Press.
11. Savrasov S.Y. (1996). Linear-response theory and lattice dynamics: A muffin-tin-orbital approach. *Phys. Rev. B*, 54(23), 16470–16486.
12. Momma K., Izumi F. (2008). VESTA: a three-dimensional visualization system for electronic and structural analysis. *J. Appl. Crystallogr*., 41, 653–658.
13. Bader R.F.W. (1994). *Atoms in Molecules: A Quantum Theory*. Oxford: Clarendon press.
14. Shklovskii B.I. and Efros A.L. (1984). *Electronic properties of doped semiconductors* NY: Springer; (1979) Moscow: Nauka.
15. Mott N.F., Davis E.A. (1979). *Electron processes in non-crystalline materials.* Oxford: Clarendon Press.

Submitted 12.03.2021

Ромака В.А. *докт. техн.наук, професор*[1]**,**
Стадник Ю.В. *канд. хім. наук*[2]**,**
Ромака Л.П. *канд. хім. наук*[2]**,**
Пашкевич В.З. *канд. техн. наук, доцент*[1]**,**
Ромака В.В. *докт. техн.наук,*
канд. хім. наук, професор[3]**,**
Горинь А.М. *канд. хім. наук*[2]**,**
Демченко П.Ю. *канд. хім. наук*[2]

[1]Національний університет "Львівська політехніка", вул. С. Бандери,
12, Львів, 79013, Україна, *e-mail: vromaka@polynet.lviv.ua*;

[2]Львівський національний університет ім. І. Франка, вул. Кирила і Мефодія, 6, Львів, 79005, Україна, *e-mail: lyubov.romaka@lnu.edu.ua*;
[3]Дрезденський технічний університет, Бергштрассе 66, Дрезден, 01069 Німеччина, *e-mail: vromakal@gmail.com*

ДОСЛІДЖЕННЯ СТРУКТУРНИХ, ТЕРМОДИНАМІЧНИХ, ЕНЕРГЕТИЧНИХ, КІНЕТИЧНИХ ТА МАГНІТНИХ ВЛАСТИВОСТЕЙ ТЕРМОЕЛЕКТРИЧНОГО МАТЕРІАЛУ $Lu_{1-x}Zr_xNiSb$

Досліджено кристалічну та електронну структури, термодинамічні, кінетичні, енергетичні та магнітні властивості термоелектричного матеріалу $Lu_{1-x}Zr_xNiSb$ у діапазонах: T = 80–400 K, x = 0–0.10. Встановлено механізми одночасного генерування структурних дефектів акцепторної та донорної природи. Показано, що у структурі базової сполуки LuNiSb присутні дефекти акцепторної природи як результат наявності вакансій у кристалографічних позиціях 4a та 4c атомів Lu та Ni відповідно, що обумовило появу у забороненій зоні ε_g акцепторних рівнів (зон). Уведення до структури сполуки LuNiSb домішкових атомів Zr шляхом заміщення у позиції 4a атомів Lu генерує структурні дефекти донорної природи з одночасною ліквідацією вакансій у позиціях 4a та 4c атомів Lu та Ni відповідно (акцепторних рівнів). Співвідношення концентрацій наявних дефектів донорної та акцепторної природи визначає у $Lu_{1-x}Zr_xNiSb$ розташування рівня Фермі ε_F та механізми провідності. Досліджений твердий розчин $Lu_{1-x}Zr_xNiSb$ є перспективним термоелектричним матеріалом. Бібл. 15, рис. 9.
Ключові слова: електронна структура, електроопір, коефіцієнт термоЕРС.

Ромака В.А. *докт. техн.наук, професор*[1],
Стадник Ю.В. *канд. хим. наук*[2],
Ромака Л.П. *канд. хим. наук*[2],
Пашкевич В.З. *канд. техн. наук, доцент*[1],
Ромака В.В. *докт. техн.наук, канд. хим. наук, профессор*[3],
Горынь А.М. *канд. хим. наук*[2],
Демченко П.Ю. *канд. хим. наук*[2]

[1]Национальный университет "Львовская политехника", ул. С. Бандеры, 12, Львов, 79013, Украина, *e-mail: vromaka@polynet.lviv.ua*;
[2]Львовский национальный университет им. И. Франко, ул. Кирилла и Мефодия, 6, Львов, 79005, Украина, *e-mail: lyubov.romaka@lnu.edu.ua*;
[3]Дрезденский технический университет, Бергштрассе 66, Дрезден, 01069 Германия, *e-mail: vromakal@gmail.com*

ИССЛЕДОВАНИЕ СТРУКТУРНЫХ, ТЕРМОДИНАМИЧЕСКИХ, ЭНЕРГЕТИЧЕСКИХ, КИНЕТИЧЕСКИХ И МАГНИТНЫХ СВОЙСТВА ТЕРМОЭЛЕКТРИЧЕСКИХ МАТЕРИАЛОВ $Lu_{1-x}Zr_xNiSb$

Исследованы кристаллическая и электронная структуры, термодинамические, кинетические, энергетические и магнитные свойства термоэлектрического материала $Lu_{1-x}Zr_xNiSb$ в диапазонах: T = 80-400 K, x = 0-0.10.Установлены механизмы одновременного генерирования структурных дефектов акцепторной и донорной природы. Показано, что в структуре базового соединения LuNiSb присутствуют дефекты акцепторной природы как результат наличия вакансий в кристаллографических позициях 4a и 4c атомов Lu и Ni соответственно, что обусловило появление в запрещенной зоне ε_g акцепторных уровней (зон). Введение в структуру соединения LuNiSb примесных атомов Zr путем замещения в позиции 4a атомов Lu генерирует структурные дефекты донорной природы с одновременной ликвидацией вакансий в позициях 4a и 4c атомов Lu и Ni соответственно (акцепторных уровней). Соотношение концентраций имеющихся дефектов донорной и акцепторной природы определяет в $Lu_{1-x}Zr_xNiSb$ положение уровня Ферми ε_F и механизмы проводимости. Исследованный твердый раствор $Lu_{1-x}Zr_xNiSb$ является перспективным термоэлектрическим материалом. Библ. 15, рис. 9.

Ключевые слова: Электронная структура, электросопротивление, коэффициент термоЭДС.

References

1. Karla I., Pierre J., Skolozdra R.V. (1998). Physical properties and giant magnetoresistance in *RNiSb* compounds. *J. Alloys Compd*., 265, 42–48. (DOI: https://doi.org/10.1016/S0925-8388(97)00419-2).
2. Romaka V.V., Romaka L., Horyn A., Rogl P., Stadnyk Yu., Melnychenko N., Orlovskyy M., Krayovskyy V. (2016). Peculiarities of thermoelectric half-Heusler phase formation in *Gd-Ni-Sb* and *Lu-Ni-Sb* ternary systems. *J. Solid State Chem*., 239, 145–152. (DOI: https://doi.org/10.1016/j.jssc.2016.04.029).
3. Romaka V.A, Stadnyk Yu., Romaka L., Krayovskyy V., Klyzub P., Pashkevych V., Horyn A., Garanyuk P. (2021). Synthesis and Electrical Transport Properties of $Er_{1-x}Sc_xNiSb$ Semiconducting Solid Solution. *J. Phys. and Chem. Sol. State*, 22(1), 146-152. (DOI: 10.15330/pcss.22.1.146-152).
4. Stadnyk Yu., Romaka V.A, Horyn A., Romaka V.V., Romaka L., Klyzub P., Pashkevych V., Garanyuk P. Modeling of Structural and Energetic Parameters of p-$Er_{1-x}Sc_xNiSb$ Semiconductor. *J. Phys. and Chem. Sol. State*, 22(3), 509-515. (DOI: 10.15330/pcss.22.3.509-515).
5. Romaka V.V., Romaka L.P., Krayovskyy V.Ya., Stadnyk Yu.V. (2015). *Stanidy ridkisnozemelnykh ta perekhidnykh metaliv* [*Stannides of rare earth and transition metals*] Lviv: Lvivska Polytechnika [in Ukrainian].
6. Romaka V.A., Stadnyk Yu.V., Krayovskyy V.Ya., Romaka L.P., Guk O.P., Romaka V.V., Mykyuchuk M.M., Horyn A.M. (2020). *Novitni termochutlyvi materialy ta peretvoriuvachi temperatury* [*New thermosensitive materials and temperature converters*]. Lviv, Lvivska Polytechnika [in Ukrainian].
7. Anatychuk L.I. (1979). *Termoelementy i termoelectricheskiie ustroistva. Spravochnik.* [*Thermoelements and thermoelectric devices*. *Reference book*]. Kyiv: Naukova dumka [in Russian].
8. Roisnel T., Rodriguez-Carvajal J. (2001). WinPLOTR: a windows tool for powder diffraction patterns analysis. *Mater. Sci. Forum*, Proc. EPDIC7 378–381, 118–123.
9. Akai H. (1989). Fast Korringa-Kohn-Rostoker coherent potential approximation and its application to FCC *Ni-Fe* systems. *J. Phys.: Condens. Matter*., 1, 8045–8063.
10. Moruzzi V.L., Janak J.F., Williams A.R. (1978). *Calculated electronic properties of metals.* NY: Pergamon Press.
11. Savrasov S.Y. (1996). Linear-response theory and lattice dynamics: A muffin-tin-orbital approach. *Phys. Rev. B*, 54(23), 16470–16486.
12. Momma K., Izumi F. (2008). VESTA: a three-dimensional visualization system for electronic and

structural analysis. *J. Appl. Crystallogr*., 41, 653–658.

13. Bader R.F.W. (1994). *Atoms in Molecules: A Quantum Theory*. Oxford: Clarendon press.
14. Shklovskii B.I. and Efros A.L. (1984). *Electronic properties of doped semiconductors* NY: Springer; (1979) Moscow: Nauka.
15. Mott N.F., Davis E.A. (1979). *Electron processes in non-crystalline materials.* Oxford: Clarendon Press.

Submitted 12.03.2021

Anatychuk L.I. *acad. of the NAS of Ukraine* [1,2]
Yuryk O.E. *doc. med. sciences*[3],
Strafun S.S. *doc. med. sciences, professor,*
National Academy
of medical sciences of Ukraine[3],
Stashkevych A.T.[3],
Kobylianskyi R.R. *cand. phys.-math. sciences*[1,2]
Cheviuk A.D.[1,2], **Yuryk N.E.**[3], **Duda B.S.**[3]

[1]Institute of Thermoelectricity of the NAS and MES of Ukraine,
1, Nauky str., Chernivtsi, 58029, Ukraine,
e–mail: anatych@gmail.com;
[2]Yu.Fedkovych Chernivtsi National University,
2, Kotsiubynskyi str., Chernivtsi, 58012, Ukraine;
[3]State Institution "Institute of Traumatology and
Orthopedics of the National Academy of Medical Sciences
of Ukraine", Kyiv, Ukraine, *e–mail: olhayuryk01@gmail.com*

THERMOMETRIC INDICATORS IN PATIENTS WITH CHRONIC LOWER BACK PAIN

The paper presents the results of the development of a thermoelectric device for the diagnosis of inflammatory processes and pain syndrome in degenerative-dystrophic diseases of the lumbosacral spine. Such a device makes it possible to store, process and visualize measurement results in real time. The results of preliminary clinical trials are presented, in particular, the determination of thermometric indicators in the lumbosacral region of the spine in persons with chronic pain syndrome against the background of degenerative-dystrophic pathology of the spine in the presence of hernias and protrusions of intervertebral discs. The effectiveness of using the proposed thermoelectric device in medical practice has been confirmed. Bibl. 33, Fig. 2, Tabl. 3.
Key words: heat flux density, temperature, thermometric indicators, spinal osteochondrosis, thermoelectric device.

Introduction

General characterization of the problem. Degenerative-dystrophic pathologies of the spine and their neurological manifestations are one of the urgent problems of modern medicine. This is due to the wide prevalence of pathology in the active working age, the frequent predisposition of the disease to a stable and prolonged course, the steady progression of the number of such patients with age. An important place in this list is occupied by neurological manifestations of osteochondrosis of the lumbar spine, which account for 60-70 % of all diseases of the peripheral nervous system and are the cause of more than 70 % of cases of temporary disability. The prevalence of this pathology in Ukraine is 10 thousand people per 100 thousand population. It should be noted that many aspects of this pathology

have not yet been studied, modern methods of diagnosis and treatment of this disease need further improvement [1 – 5].

The Institute of Traumatology and Orthopedics of the National Academy of Medical Sciences of Ukraine has established [6 – 10] that determining the pathophysiological mechanisms of back pain based on clinical and paraclinical methods of examination of the patient is the main step towards prescribing the most effective and safe therapy and predicting the disease. The most common cause of low back pain is a herniated disc – a disease of the musculoskeletal system which occurs due to rupture of the fibrous ring (upper disc) and squeezing out the pulpal ring (inner part of the disc). The main clinical signs of intervertebral disc herniation can be manifested alone or in combination with the following syndromes: local pain (lumbar pain), reflected pain (lumbosciatica), radicular syndrome (radiculopathy), spinal cord injury syndrome (myelopathy).

The development of modern diagnostic methods, such as magnetic resonance imaging, computed tomography, makes it possible to determine the level, localization of hernia or protrusion of the intervertebral disc. Today there are already many works [11 – 13], which showed the absence of a direct relationship between the presence or severity of degenerative-dystrophic changes in the spine and the presence or intensity of pain in the back. That is, there is an urgent problem of studying other peripheral mechanisms that cause back pain. The mechanisms of back pain in the first hours/days of its occurrence in degenerative-dystrophic pathology of the spine, especially in its lumbosacral region, which is most common in the clinical practice of neurologist and orthopedist, have not been studied at all. Medical practice also requires the introduction of new highly informative, portable devices for functional diagnostics, which would allow in the first hours/days to reveal the nature of neurological damage in degenerative-dystrophic pathology of the spine and assess the degree of pain in this pathology [14 – 17].

Semiconductor thermoelectric heat flux sensors [18 – 27], which combine miniature size, high sensitivity, stability of parameters in a wide range of operating temperatures and are consistent with modern recording equipment [28 – 31], are promising for the study of local human heat release. Use of such sensors allows one to achieve high locality and accuracy of thermometric measurements. This, in turn, makes it possible to obtain information about the characteristics of objects under study and analyze them in detail in order to identify in the early stages the inflammatory processes in the human body.

Therefore, *the purpose of this work* is to study the thermometric indicators in patients with chronic low back pain using a thermoelectric device for the diagnosis of inflammatory processes and pain in degenerative-dystrophic diseases of the lumbosacral spine.

Design and technical characteristics of the device

The Institute of Thermoelectricity of the National Academy of Sciences and the Ministry of Education and Science of Ukraine has developed a thermoelectric device for diagnosing inflammatory processes and pain in degenerative-dystrophic diseases of the lumbosacral spine [32, 33] (Fig. 1). Technical characteristics of the device are given in Table 1.

The device comprises control unit 1 and thermoelectric temperature and heat flux sensors 2. Temperature and heat flux density are measured simultaneously by two thermoelectric sensors with recording of measurement results on a MicroSD memory card and computer display on a personal computer (PC). Special computer program "TermoMonitor" was also developed to process measurement results, their accumulation and reproduction in a given form on a PC.

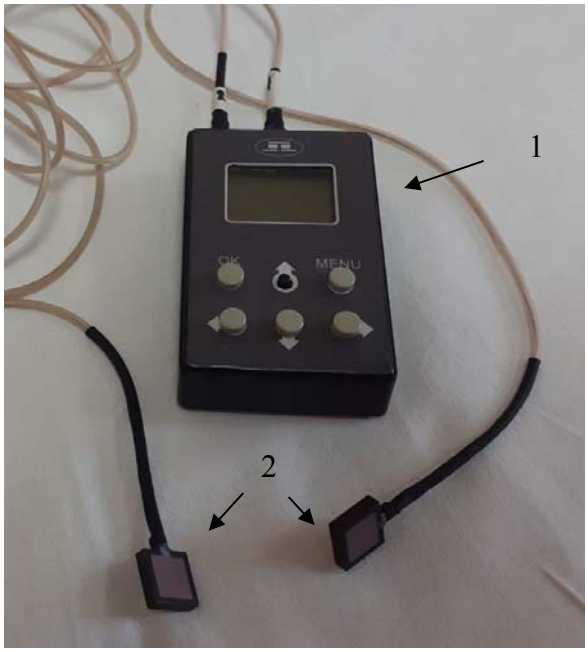

Fig. 1. Thermoelectric device for diagnosing inflammatory processes and pain degenerative-dystrophic diseases of human lumbosacral spine: 1 – control unit, 2 – thermoelectric temperature and heat flux sensor

Table 1

Technical characteristics of the device

№	Technical characteristics	Parameter values
1.	Heat flux density measurement range	(1 ÷ 100) mW/cm^2
2.	Maximum error in measuring heat flux density	5 %
3.	Operating temperature range of thermoelectric sensor	(0 ÷ +50) °C
4.	Temperature measurement accuracy	± 0.1 °C
5.	Number of thermoelectric sensors	2
6.	Overall dimensions of thermoelectric sensor	(14 × 14 × 3) mm
7.	Thermoelectric sensor weight	0.020 kg
8.	Overall dimensions of control unit	(90 × 55 × 25) mm
9.	Device weight	0.150 kg
10.	Time of continuous operation of the device	48 hours

The operating principle of the device consists in converting the heat flux and temperature of the human body using two thermoelectric heat flux density and temperature sensors into equivalent electrical signals, which are shown on the digital display of the control unit in units of heat flux density (mW/cm^2) and temperature (°C).

On the upper wall there are two connectors for thermoelectric temperature and heat flux sensors and a power button. On the right side wall there is a slot for a microSD memory card and a miniUSB-

connector for connecting the device to a PC. The device battery is also powered via the miniUSB connector.

Mounted on the front wall of the case is a liquid crystal display, which displays the values of the heat flux density of the relevant parts of the human body and the temperature values in the form of graphs. Thus, the obtained measurement results can be analyzed directly from the graphs shown on the display. The presence of two thermoelectric sensors in the device at the same time allows one to compare the results of measuring the sick and healthy parts of the human body surface.

In addition, on the front wall of the device there are 6 buttons to control the operation of the device − "LEFT", "RIGHT", "UP", "DOWN", "OK", "MENU". The purpose of the “MENU” items of the device is as follows:

– "START RECORDING" / "STOP RECORDING" – the device starts recording the measurement results in a new file, stops the corresponding recording and saves the information on the memory card;
– "MODE SELECTION" – calls the sub-menu to select one of 9 modes of displaying information in the form of real-time graphs;
- "RECORDING PERIOD" – is used to select the period of time after which the measured results will be recorded in a file on a memory card and shown on the display of the device;
– "TIME/DATE" – switch to time and date setting mode;
– "BATTERY" – displays the voltage on the battery of the device;
– "HELP" – displays information about the device.

The block-diagram of the device (Fig. 2) consists of the following functional units: thermoelectric heat flux sensor with built-in temperature sensor, analog-to-digital converter (ADC) for converting analog sensor signals to digital, multiplexer for switching digital signals from ADC and their alternate transmission to microcontroller. It is used for processing digital signals, their storage on a memory card, graphical visualization of information on the display and PC.

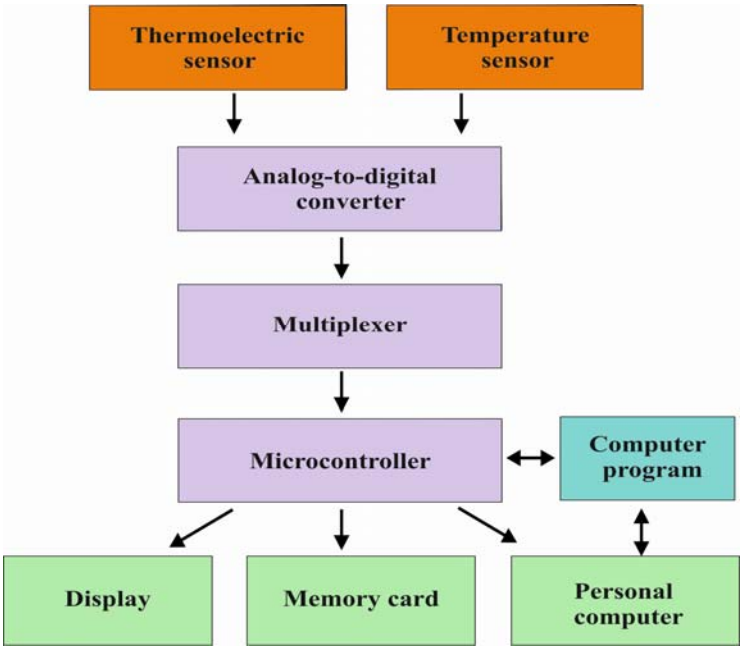

Fig. 2. Block-diagram of thermoelectric device

The main functional unit of the control unit is a microcontroller that operates at a frequency of up to 20 MHz and provides a high speed of processing signals from thermoelectric temperature and heat flux sensor. Personal computer helps to program the microcontroller, which, in turn, controls the work of other functional units of the device.

The device contains its own power supply in order to be able to use it offline with a patient. This, in turn, allows one to expand the functionality of the device. The device is powered by a lithium-ion battery with a capacity of 1200mA/h, which provides 48 hours of continuous operation of the device.

Methods of clinical trials

The purpose of preliminary clinical trials was to investigate thermometric parameters in patients with chronic low back pain using a thermoelectric device to diagnose inflammation and pain in degenerative-dystrophic diseases of the lumbosacral spine, and to confirm the effectiveness of such a device in medical practice. Clinical trials were conducted in the laboratory of neuro-orthopedics and pain problems and in the rehabilitation department of the Institute of Traumatology and Orthopedics of the National Academy of Medical Sciences of Ukraine.

This study included 55 patients with chronic lumbosacral pain. The pain was constant, radiated to one of the lower extremities, significantly limited their daily activities and intensified at night. Along with the use of nonsteroidal anti-inflammatory drugs, patients were forced to use anticonvulsants and antidepressants. The duration of the disease was 1 – 5 years. Age of patients: 49 ± 3.5 years. All patients were divided into two clinical groups.

Clinical group I included 39 people with unilateral lumbosciatica in the presence of hernias and protrusions of intervertebral discs with signs of linear instability of the lumbosacral spine, which were subject to conservative treatment (main group).

Clinical group II included 16 patients with unilateral lumbosciatica with hernias and protrusions of intervertebral discs without signs of linear instability of the lumbosacral spine, which were also subject to conservative treatment (comparison group).

The control group consisted of 10 people with no pain, in the presence of hernias and protrusions of the intervertebral discs, without signs of linear instability of the lumbosacral spine.

In all patients, the level of pain intensity was assessed using a verbal-analog scale (VAS). We used a scale of 100 mm length with millimeter divisions, which additionally every 20 mm contains words that characterize the intensity of pain: 0 – means no pain (starting point of the line), 20 mm – corresponds to the descriptor "weak", 40 mm – "moderate" , 60 mm – "strong", 80 mm – "extremely strong", 100 mm – "intolerable" (end point of the line). The intensity of pain was estimated in millimeters [10].

In the room where the examination was carried out, the temperature was constantly maintained in the range of 20 – 22 °C and the relative humidity of 50 – 60 %. On the eve of the examination, the patients were canceled all physiotherapeutic and warming procedures, as well as anti-inflammatory, antipyretic, sudinosilicidal or vasoconstrictive medications. Patients had to stop smoking 3 – 4 hours before the examination. 2 – 3 hours before the examination, patients were removed from various ointment applications and the skin surface was degreased with a mixture of 40 % ethyl alcohol and ether (in a ratio of 4: 1). Immediately before the examination, patients underwent temperature adaptation for 15 – 20 minutes. At this time, they were at rest, without static and dynamic muscle tension. The measurement of thermometric parameters from the patient's skin surface was carried out in real time for 3 min. using the above thermoelectric device. During the measurements, the time of thermal adaptation (in seconds) was recorded – t (the time from the beginning of the examination until the main parameters of the device reached “saturation”), the temperature and heat flux density at “saturation”. Thermoelectric sensors were

applied in the spine region symmetrically on both sides paravertebrally at the level of the spinous processes of the $L_4 - L_5$ vertebrae. In addition to measuring thermometric parameters, heart rate variability was determined simultaneously, as both of these parameters are regulated by the autonomic nervous system, and the main centres of regulation of heat exchange and vascular tone are located nearby in the brain stem.

Spectral analysis of the heart rhythm made it possible to identify high-frequency respiratory waves (HF – high frequency), reflecting the tone of the parasympathetic nervous system, low-frequency waves (LF – low frequency), reflecting the state of segmental baroreflex regulatory sympathetic mechanisms and very low-frequency slow waves (VLF), reflecting the degree of activation of cerebral ergotropic systems. Additionally, time characteristics were also analyzed: for the parasympathetic nervous system (RMSSD and Pnn 50 %), sympathetic nervous system (SDNN), cerebral metabolic fluctuations (SDANN), and the ratio of autonomic balance was determined by the formula of this ratio LF/HF. The obtained results were processed using the computer software package STATISTIKA 6.0.

Results of preliminary clinical trials

Patients of clinical group I complained of heartburn and pain in the lower back, lower extremities, trophic disorders. Their backs were fixed in a bent position. Unilateral tension symptoms were positive, and 23 % of patients had the overlapping Lasegue sign. There was also a decrease in the volume of movements in the lumbar spine, lumbar muscle tension, pain on palpation and percussion of the paravertebral points, a sharp restriction of inclinations towards the lesion. In the supine position and with bent lower limbs in the hip joints, the pain decreased. The pain was pulling in nature, accompanied by numbness and running creeps in the lower extremities. The skin was pale, cold to the touch, dry with signs of hyperkeratosis. White dermographism was noted. The severity of the pain syndrome on the VAS scale was 76.2 ± 4.1 mm.

In persons of clinical group II, the pain was also unilateral, sometimes at night it tended to be bilateral, increased with flexion or extension of the spine and prolonged sitting, decreased at rest. Movements in the lumbar spine were not limited, but painful, especially when bending. At a symptom of a tension there was a back pain. Pale skin, burning sensation, distension, asymmetry of white and red dermographism in the lower extremities were noted. Cyanosis, "marbling" of skin, mainly in feet was noted. Concomitant diseases were detected: varicose veins of the lower extremities and hemorrhoidal veins, which indicated systemic weakness of the venous apparatus. The intensity of the pain syndrome on the VAS scale was 49.4 ± 3.9 mm.

In the control group (10 persons), uniform indicators of temperature and heat flux density were recorded on both sides within the range: $T_0 = 33.2 \pm 0.5$ °C, $q_0 = 171.3 \pm 0.6$ mW/cm^2.

In the main group I (39 people) there was a symptom of "scissors" on the pain side (intersecting temperature and heat flux density on the pain side), with a significant decrease in heat flux density and a moderate increase in temperature on the injured side. Indicators of temperature in the paravertebral region on the pain side were $T_1 = 34.2 \pm 1.7$ °C, and heat flux density $q_1 = 26.8 \pm 4.9$ mW/cm^2 (Table 2). In our opinion, the appearance of the scissors symptom in the examined individuals can be explained based on the well-known experimental studies of P. Veselovsky (1982), who found that when the peripheral nerve fiber is damaged, cold receptors, which are 2 – 2.5 times more numerous than thermal, are the first to suffer.

In comparison group II (16 people), a moderate decrease in the heat flux density and a slight increase in temperature on the pain side were revealed. The main thermometric parameters are as follows: $T_2 = 39.8 \pm 6.3$ °C, $q_2 = 120.6 \pm 99.2$ mW/cm^2 (Table 3).

The analysis of the obtained results showed that in persons of the main and clinical group the severity of long-term chronic pain process is due to the high degree of activity of metabolic processes both at the cellular level and at the level of cerebral ergotropic systems; there is a relative activation of both

sympathetic and parasympathetic autonomic nervous system. In addition, a balanced combination of drugs helped to maintain a balanced autonomic balance between the sympathetic and parasympathetic nervous systems.

Table 2

Parameters of spectral and time characteristics of vegetovascular reactions in group I

$N = 39$	$M \pm m$	$T_1 = 34.2 \pm 1.7$ °C	$q_1 = 26.8 \pm 4.9$ mW/cm^2
		Correlation ratio, r	
Indicators (spectral characteristics)			
VLF, ms^2	13768.07±7361.08	0.65	0.28
LF, ms^2	23417.68±14962.65	0.76	0.37
HF, ms^2	32919.18±21321.92	0.84	0.44
LF/HF, conventional units	2.01±0.55	- 0.15	0
LFn, %	54.86±4.37	- 0.2	- 0.3
HFn, %	45.14±4.37	0.2	0.3
Indicators (time characteristics)			
SDNN, ms	156.11±61.38	0.76	0.41
Pnn 50, %	18.35±7.01	0.65	0.57
RMSSD, ms	186.58±86.67	0.81	0.46

Table 3

Parameters of spectral and time characteristics of vegetovascular reactions in group II

$N = 16$	$M \pm m$	$T_2 = 39.8 \pm 6.3$ °C	$q_2 = 120.6 \pm 99.2$ mW/cm^2
		Correlation ratio, r	
Indicators (spectral characteristics)			
VLF, ms^2	21608.2±11315.41	- 0.09	- 0.10
LF, ms^2	60093.9±31361.08	- 0.06	- 0.11
HF, ms^2	114969.2±60523.87	- 0.07	- 0.10
LF/HF, conventional units	1.0±0.37	- 0.13	- 0.14
LFn, %	37.4±3.57	- 0.17	- 0.28
HFn, %	60.5±3.72	0.21	0.30
Indicators (time characteristics)			
SDNN, ms	287.5±108.02	- 0.02	- 0.06
Pnn 50, %	54.0±22.07	0.08	- 0.08
RMSSD, ms	383.7±153.47	- 0.02	- 0.04

According to correlation analysis, in patients of clinical group I a high degree of correlation with the indicators of skin temperature fluctuations in the superficial paravertebral areas in the lumbar region was recorded. A high degree of correlation was also observed when measuring the heat flux density. However, these correlative changes indicated that patients undergo more significant changes in the deep nervous processes with a tendency to predominant activity of the parasympathetic part of the nervous system. This was indicated by the ratio of the LF/HF coefficient, when a high correlation was found between this indicator and the heat flux density; the reliability was $p < 0.05$.

In the comparison group (clinical group II), all negative weak correlations between the heat flux density and heart rate variability were found, except for the HFn indicator, which also indicated the role of parasympathetic reactions in the formation of heat flux density indicators in patients with signs of lumboischialgia in the absence of linear instability in lumbar spine.

Thus, preliminary clinical trials provide an opportunity to diagnose inflammatory processes, in particular in the neurological manifestations of spinal osteochondrosis, and to monitor the effectiveness of conservative treatment in degenerative-dystrophic diseases of the lumbosacral spine.

Thus, the statistical set of clinical material will improve the method of automatic processing of the results, which in the future will introduce the proposed thermoelectric device in the primary care at the level of family doctor's office and automatically diagnose people with neurological vertebrogenic disorders without costly diagnostics.

Conclusions

1. A thermoelectric device for the diagnosis of inflammatory processes and pain syndrome in degenerative-dystrophic diseases of the lumbosacral spine has been developed and manufactured. Such a device makes it possible to store, process and visualize measurement results in real time.
2. On the basis of preliminary clinical trials it was established that determination of thermometric parameters in the lumbosacral region of the spine in persons with chronic pain syndrome against the background of degenerative-dystrophic pathology of the spine in the presence of hernias and protrusions of intervertebral discs makes it possible to improve the diagnosis of neurological manifestations of this pathology, to predict the course of this disease and choose an effective method of treatment.
3. The efficiency of using the proposed thermoelectric device in medical practice has been confirmed, which, in the future, at the level of a family doctor’s office, will automatically make a diagnosis for persons with neurological vertebrogenic disorders without the use of expensive radiation diagnostic devices.

References

1. Veselovskiy V.P, Mikhailov M.K., Samitov O.Sh. (1990). *Diagnostika sindromov osteokhondroza pozvonochnika [Diagnostics of the spinal osteochondrosis syndromes]*. Kazan: Kazan University Publ. [in Russian].
2. Gioiev P.M. (2003). Kompleksnoie lecheniie zabolevanii poiasnichnogo otdela pozvonochnika [Complex treatment of diseases of the lumbar spine]. St-Petersburg: IPTP [in Russian].
3. Yepifanov V.A., Rolik I.S., Yepifanov A.V. (2000). *Osteokhodroz pozvonochnika (diagnostika, lecheniie, profilaktika [Spinal osteochondrosis (diagnosis, treatment, prevention)]*. Moscow [in Russian].
4. Zhuk P.M., Stelmakh I.N., Nychik A.Z. (2003). *Osteokhondroz pozvonochnika. Lecheniie i profilaktika [Spinal osteokhondrozis. Treatment and prevention]*. Kiev: Kniga-plus [in Russian].
5. Yaremenko D.A., Shevchenko E.G., Golubeva I.V. et al. (2006). Disability due to spinal osteochondrosis and unused reserves in its prevention. *Orthopaedics, Traumatology and Prosthetics*,

4, 63-67.

6. Popelianskiy Ya. Yu. (1989). *Bolezni perifericheskoi nervnoi sistemy (rukovodstvo dlia vrachei) [Diseases of the peripheral nervous system (a guide for doctors)]*. Moscow: Meditsina [in Russian].
7. Macheret E.L., Dovhyi I.L., Korkushko O.O. (2006). Osteokhondroz poperekovoho viddilu khrebta, uskladnenyi hryzhamy dyskiv. T.I. [Osteochondrosis of the lumbar spine, complicated by disc herniation. Vol. I.] Kyiv: Try krapky [in Ukrainian].
8. Kogan O.G., Shmidt I.R., Tolstokorov A.A. (1983). *Metodologicheskiie osnovy dispanserizatsii pri zabolevaniiakh nervnoi sistemy [Methodlogical foundations of clinical examination for diseases of the nervous system]*. Novosibirsk [in Russian].
9. Kolosova T.V., Golovchenko Yu.I. (2009). Features of the complex therapy of vertebrogenic pain syndromes of the lumbosacral region. *International Neurological Journal*, 3, 89-95.
10. Macheret E.L., Dovhyi I.L., Korkushko O.O. (2006). *Osteokhondroz poperekovoho viddilu khrebta, uskladnenyi hryzhamy dyskiv: pidruchnyk [Osteochondrosis of the lumbar spine, complicated by disc herniation: textbook]*. Kyiv. Vol.1. – 256 p.; Vol.2. – 480 p. [in Ukrainian].
11. Jensen M.P., Dworkin R.H., Gammaitoni A.R. (2005). Assessment of pain quality in chronic neuropathic and nociceptive pain clinical trials with the Neuropathic Pain Scale. *J. Pain*, 6 (2), 98-106.
12. Kovacs F.M., Arana E., Royuela A, (2012). Vertebral endplate changes are not associated with chronic low back pain among Southern European subjects: a case control study. *Am. J. Neuroradiol*., 33 (8), 1519-1524.
13. Suri P., Boyko E.J., Goldberg J. et al. (2014). Longitudinal associations between incident lumbar spine MRI findings and chronic low back pain or radicular symptoms: retrospective analysis of data from the longitudinal assessment of imaging and disability of the back (LAIDBACK). *BMC Musculoskeletal Disorders,* 15, 52.
14. Fedoseiev S.V. (2005). Spinal instability: modern methods of diagnosis and treatment, standardization of diagnostic and treatment-and-prophylactic measures. *Orthopaedics, Traumatology and Prosthetics,* 1, 98-103.
15. Liev A.A. (2009). Vertebroneurology: formation, problems, prospects. *International Neurological Journal*, 3, 12-17.
16. Khodarev S.V., Gavrishev S.V., Molchanovskiy V.V. et al. (2001). *Printsypy i metody lecheniia bolnykh s vertebronevrologicheskoi patologiei: uchebnoie posobiie [Principles and methods of treatment of patients with vertebral neurological pathology: textbook]*. Rostov on Don: Feniks [in Russian].
17. Yurik O.E. (2001). *Nevrologichni proiavy osteokhondrozu: patogenez, klinika, likuvannia [Neurological manifestations of osteochondrosis: pathogenesis, clinic, treatment]*. Kyiv: Zdorovia [in Ukrainian].
18. Anatychuk L.I. (1979). *Termoelementy i termoelektricheskiie ustroistva: spravochnik [Thermoelements and thermoelectric devices: handbook]*. Kyiv: Naukova dumka [in Russian].
19. Anatychuk L.I., Lozinskiy N.G., Mykytiuk P.D., Rozver Yu.Yu. (1983). Termoelektricheskiy poluprovodnikovyi teplomer [Thermoelectric semiconductor heat meter]. *Pribory i Tekhnika Eksperimenta – Instruments and Experimental Techniques,* 5, 236 [in Russian].
20. Anatychuk L.I., Bulat L.P., Gutsal D.D., Miagkota A.P. (1989). Termoelektricheskii teplomer [Thermoelectric heat meter]. Pribory i Tekhnika Eksperimenta - *Instruments and Experimental Techniques*, 4, 248 [in Russian].
21. Ladyka R.B., Moskal D.N., Didukh V.D. (1992). Poluprodnikovyie teplomery v diagnostike i lechenii zabolevanii sustavov [Semiconductor heat meters in the diagnosis and treatment of joint diseases].

Meditsinskaia tekhnika – Biomedical Engineering, 6, 34-35 [in Russian].

22. Ladyka R.B., Dakaliuk O.N., Bulat L.P., Miagkota A.P. (1996). Primeneniie poluprovodnikovykh teplomerov v diagnostike i lechenii [Application of semiconductor heat meters in diagnostics and treatment] - *Biomedical Engineering*, 6, 36-37 [in Russian].
23. Demchuk B.M., Kushneryk L.Ya, Rublenyk I.M. (2002). Thermoelectric sensors for orthopedics. *J.Thermoelectricity*, 4, 80-85.
24. *Patent of Ukraine 53104 A* (2003). Ashcheulov A.A., Klepikovskiy A.V., Kushneryk L.Ya., Rarenko A.I., Cherchenko V.I. Sensor for preliminary diagnosis of inflammatory processes of the mammary glands [in Ukrainian].
25. Ashcheulov A.A., Kushneryk L.Ya. (2004). Termoelektricheskiy pribor dlia mediko-biologicheskoi ekspress-diagnostiki [Thermoelectric device for medical and biological express diagnostics]. *Tekhnologiia i Konstruirovaniie v Elektronnoi Apparature*, 4, 38-39 [in Russian].
26. Anatychuk L.I., Kobylianskyi R.R., Konstantynovych I.A. (2014). Hraduiuvannia termoelektrychnykh sensoriv teplovoho potoku [Calibration of thermoelectric heat flow sensors]. *Pratsi XV Mizhnarodnoi naukovo-praktychnoi konferentsii "Suchasni informatsiini ta elektronni tekhnologii" – Proc. of XV International scientific and practical conference "Modern Information and Electronic Technologies"* (Ukraine, Odesa, May 26-30, 2014. (Vol. 2, pp. 30-31) [in Ukrainian].
27. Kobylianskyi R.R., Boichuk V.V. (2015). Vykorystannia termoelektrychnykh teplomiriv u medychnii diagnostytsi [Use of thermoelectric heat meters in medical diagnostics]. *Naukovy visnyk Chernivetskoho Universytetu. Fizyka. Elektronika – Scientific Bulletin of Chernivtsi University. Physics. Electronics, 4(1), 90-96.*
28. Gischuk V.S. (2012). Electronic recorder of signals from human heat flux sensors. *J.Thermoelectricity*, 4, 105-108.
29. Gischuk V.S. (2013). Electronic recorder with processing signals from heat flux thermoelectric sensor. *J. Thermoelectricity*, 1, 82-86.
30. Gischuk V.S. (2013). Modernized device for human heat flux measurements. *J. Thermoelectricity*, 2, 91-95.
31. Anatychuk L.I., Ivaschuk O.I., Kobylianskyi R.R., Postevka I.D., Bodiaka V.Yu., Gushul I.Ya. (2016). Thermoelectric device for temperature and heat flux density measurement "ALTEC-10008". *J.Thermoelectricity*, 1, 76-84.
32. Anatychuk L.I., Yuryk O.E., Kobylianskyi R.R., Roi I.V., Fischenko Ya.V., Slobodianiuk N.P., Yuryk N.E., Duda B.S. (2017). Thermoelectric device for the diagnosis of inflammatory processes and neurological manifestations of human vertebral osteochondrosis. *J.Thermoelectricity*, 3, 54-67.
33. Yuryk O.E., Anatychuk L.I., Roi I.V., Kobylianskyi R.R., Fischenko Ya.V., Slobodianiuk N.P., Yuryk N.E., Duda B.S. (2017). Osoblyvosti teplovoho obminu u patsientiv z nevrologichnymy proiavamy osteokhondrozu v poperekovo-kryzhovomu viddili khrebta [Features of heat exchange in patients with neurological manifestations of osteochondrosis in the lumbosacral spine]. *Trauma*, 18 (6).

Submitted 18.03.2021

Анатичук Л.І. *акад. НАН України*[1,2]
Юрик О.Є. *докт. мед. наук* [3]
Страфун С.С. *докт. мед. наук, професор,*
чл.-корр. НАМН України[3],
Сташкевич А.Т.[3]
Кобилянський Р.Р. *канд. фіз.-мат. наук* [1,2]
Чев'юк А.Д.[1,2], **Юрик Н.Є.**[3], **Дуда Б.С.**[3]

[1]Інститут термоелектрики НАН і МОН України, вул. Науки, 1,
Чернівці, 58029, Україна; *e–mail: anatych@gmail.com*
[2]Чернівецький національний університет ім. Юрія Федьковича,
вул. Коцюбинського 2, Чернівці, 58000, Україна
[3]ГУ «Інститут травматології і ортопедії АМН України»,
Київ, Україна, *e–mail: olhayuryk01@gmail.com*

ТЕПЛОМЕТРИЧНІ ПОКАЗНИКИ У ПАЦІЄНТІВ З ХРОНІЧНИМ БОЛЕМ У ПОПЕРЕКУ

У роботі наведено результати розробки термоелектричного приладу для діагностики запальних процесів та больового синдрому при дегенеративно-дистрофічних захворюваннях попереково-крижового відділу хребта. Такий прилад дає можливість збереження, обробки і візуалізації результатів вимірювань у режимі реального часу. Наведено результати попередніх клінічних досліджень, зокрема визначення теплометричних показників у попереково-крижовій ділянці хребта у осіб з хронічним больовим синдромом на фоні дегенеративно-дистрофічної патології хребта за наявності гриж і протрузій міжхребцевих дисків. Підтверджено ефективність застосування запропонованого термоелектричного приладу у медичній практиці. Бібл. 33, рис. 2, табл. 3.

Ключові слова: густина теплового потоку, температура, теплометричні показники, остеохондроз хребта, термоелектричний прилад.

Анатычук Л.И., *акад. НАН Украины*[1,2]
Юрык О.Е., *докт. мед. наук* [3]
Страфун С.С. *докт. мед. наук, профессор,*
чл.-корр. НАМН Украины[3],
Сташкевич А.Т.[3]
Кобылянскый Р.Р., *канд. физ.-мат. наук* [1,2]
Чевьюк А.Д.[1,2], **Юрык Н.Е.**[3], **Дуда Б.С.**[3]

[1]Институт термоэлектричества НАН и МОН Украины,
ул. Науки, 1, Черновцы, 58029, Украина,
e–mail: anatych@gmail.com;
[2]Черновицкий национальный университет
им. Юрия Федьковича, ул. Коцюбинского, 2,
Черновцы, 58012, Украина;
[3]ГУ «Институт травматологии и ортопедии АМН Украины»,
Киев, Украина, *e–mail: olhayuryk01@gmail.com*

ТЕПЛОМЕТРИЧЕСКИЕ ПОКАЗАТЕЛИ У ПАЦИЕНТОВ С ХРОНИЧЕСКОЙ БОЛЬЮ В ПОЯСНИЦЕ

В работе приведены результаты разработки термоэлектрического прибора для диагностики воспалительных процессов и болевого синдрома при дегенеративно-дистрофических заболеваниях пояснично-крестцового отдела позвоночника. Такой прибор дает возможность хранения, обработки и визуализации результатов измерений в режиме реального времени. Приведены результаты предыдущих клинических исследований, в частности определение теплометрических показателей в пояснично-крестцовой области позвоночника у лиц с хроническим болевым синдромом на фоне дегенеративно-дистрофических патологий позвоночника при наличии грыж и протрузий межпозвонковых дисков. Подтверждена эффективность применения предложенного термоэлектрического устройства в медицинской практике. Библ. 33, рис. 2, табл. 3.

Ключевые слова: плотность теплового потока, температура, теплометрические показатели, остеохондроз позвоночника, термоэлектрический прибор.

References

1. Veselovskiy V.P, Mikhailov M.K., Samitov O.Sh. (1990). *Diagnostika sindromov osteokhondroza pozvonochnika [Diagnostics of the spinal osteochondrosis syndromes]*. Kazan: Kazan University Publ. [in Russian].
2. Gioiev P.M. (2003). Kompleksnoie lecheniie zabolevanii poiasnichnogo otdela pozvonochnika [Complex treatment of diseases of the lumbar spine]. St-Petersburg: IPTP [in Russian].
3. Yepifanov V.A., Rolik I.S., Yepifanov A.V. (2000). *Osteokhodroz pozvonochnika (diagnostika, lecheniie, profilaktika [Spinal osteochondrosis (diagnosis, treatment, prevention)]*. Moscow [in Russian].
4. Zhuk P.M., Stelmakh I.N., Nychik A.Z. (2003). *Osteokhondroz pozvonochnika. Lecheniie i profilaktika [Spinal osteokhondrozis. Treatment and prevention]*. Kiev: Kniga-plus [in Russian].
5. Yaremenko D.A., Shevchenko E.G., Golubeva I.V. et al. (2006). Disability due to spinal osteochondrosis and unused reserves in its prevention. *Orthopaedics, Traumatology and Prosthetics*, 4, 63-67.
6. Popelianskiy Ya. Yu. (1989). *Bolezni perifericheskoi nervnoi sistemy (rukovodstvo dlia vrachei) [Diseases of the peripheral nervous system (a guide for doctors)]*. Moscow: Meditsina [in Russian].
7. Macheret E.L., Dovhyi I.L., Korkushko O.O. (2006). Osteokhondroz poperekovoho viddilu khrebta, uskladnenyi hryzhamy dyskiv. T.I. [Osteochondrosis of the lumbar spine, complicated by disc herniation. Vol. I.] Kyiv: Try krapky [in Ukrainian].
8. Kogan O.G., Shmidt I.R., Tolstokorov A.A. (1983). *Metodologicheskiie osnovy dispanserizatsii pri zabolevaniiakh nervnoi sistemy [Methodlogical foundations of clinical examination for diseases of the*

nervous system]. Novosibirsk [in Russian].

9. Kolosova T.V., Golovchenko Yu.I. (2009). Features of the complex therapy of vertebrogenic pain syndromes of the lumbosacral region. *International Neurological Journal*, 3, 89-95.
10. Macheret E.L., Dovhyi I.L., Korkushko O.O. (2006). *Osteokhondroz poperekovoho viddilu khrebta, uskladnenyi hryzhamy dyskiv: pidruchnyk [Osteochondrosis of the lumbar spine, complicated by disc herniation: textbook]*. Kyiv. Vol.1. – 256 p.; Vol.2. – 480 p. [in Ukrainian].
11. Jensen M.P., Dworkin R.H., Gammaitoni A.R. (2005). Assessment of pain quality in chronic neuropathic and nociceptive pain clinical trials with the Neuropathic Pain Scale. *J. Pain*, 6 (2), 98-106.
12. Kovacs F.M., Arana E., Royuela A, (2012). Vertebral endplate changes are not associated with chronic low back pain among Southern European subjects: a case control study. *Am. J. Neuroradiol*., 33 (8), 1519-1524.
13. Suri P., Boyko E.J., Goldberg J. et al. (2014). Longitudinal associations between incident lumbar spine MRI findings and chronic low back pain or radicular symptoms: retrospective analysis of data from the longitudinal assessment of imaging and disability of the back (LAIDBACK). *BMC Musculoskeletal Disorders,* 15, 52.
14. Fedoseiev S.V. (2005). Spinal instability: modern methods of diagnosis and treatment, standardization of diagnostic and treatment-and-prophylactic measures. *Orthopaedics, Traumatology and Prosthetics,* 1, 98-103.
15. Liev A.A. (2009). Vertebroneurology: formation, problems, prospects. *International Neurological Journal*, 3, 12-17.
16. Khodarev S.V., Gavrishev S.V., Molchanovskiy V.V. et al. (2001). *Printsypy i metody lecheniia bolnykh s vertebronevrologicheskoi patologiei: uchebnoie posobiie [Principles and methods of treatment of patients with vertebral neurological pathology: textbook]*. Rostov on Don: Feniks [in Russian].
17. Yurik O.E. (2001). *Nevrologichni proiavy osteokhondrozu: patogenez, klinika, likuvannia [Neurological manifestations of osteochondrosis: pathogenesis, clinic, treatment]*. Kyiv: Zdorovia [in Ukrainian].
18. Anatychuk L.I. (1979). *Termoelementy i termoelektricheskiie ustroistva: spravochnik [Thermoelements and thermoelectric devices: handbook]*. Kyiv: Naukova dumka [in Russian].
19. Anatychuk L.I., Lozinskiy N.G., Mykytiuk P.D., Rozver Yu.Yu. (1983). Termoelektricheskiy poluprovodnikovyi teplomer [Thermoelectric semiconductor heat meter]. *Pribory i Tekhnika Eksperimenta – Instruments and Experimental Techniques,* 5, 236 [in Russian].
20. Anatychuk L.I., Bulat L.P., Gutsal D.D., Miagkota A.P. (1989). Termoelektricheskii teplomer [Thermoelectric heat meter]. Pribory i Tekhnika Eksperimenta - *Instruments and Experimental Techniques*, 4, 248 [in Russian].
21. Ladyka R.B., Moskal D.N., Didukh V.D. (1992). Poluprodnikovyie teplomery v diagnostike i lechenii zabolevanii sustavov [Semiconductor heat meters in the diagnosis and treatment of joint diseases]. *Meditsinskaia tekhnika – Biomedical Engineering*, 6, 34-35 [in Russian].
22. Ladyka R.B., Dakaliuk O.N., Bulat L.P., Miagkota A.P. (1996). Primeneniie poluprovodnikovykh teplomerov v diagnostike i lechenii [Application of semiconductor heat meters in diagnostics and treatment] - *Biomedical Engineering*, 6, 36-37 [in Russian].
23. Demchuk B.M., Kushneryk L.Ya, Rublenyk I.M. (2002). Thermoelectric sensors for orthopedics. *J.Thermoelectricity*, 4, 80-85.
24. *Patent of Ukraine 53104 A* (2003). Ashcheulov A.A., Klepikovskiy A.V., Kushneryk L.Ya., Rarenko A.I., Cherchenko V.I. Sensor for preliminary diagnosis of inflammatory processes of the mammary

glands [in Ukrainian].

25. Ashcheulov A.A., Kushneryk L.Ya. (2004). Termoelektricheskiy pribor dlia mediko-biologicheskoi ekspress-diagnostiki [Thermoelectric device for medical and biological express diagnostics]. *Tekhnologiia i Konstruirovaniie v Elektronnoi Apparature*, 4, 38-39 [in Russian].
26. Anatychuk L.I., Kobylianskyi R.R., Konstantynovych I.A. (2014). Hraduiuvannia termoelektrychnykh sensoriv teplovoho potoku [Calibration of thermoelectric heat flow sensors]. *Pratsi XV Mizhnarodnoi naukovo-praktychnoi konferentsii "Suchasni informatsiini ta elektronni tekhnologii" – Proc. of XV International scientific and practical conference "Modern Information and Electronic Technologies"* (Ukraine, Odesa, May 26-30, 2014. (Vol. 2, pp. 30-31) [in Ukrainian].
27. Kobylianskyi R.R., Boichuk V.V. (2015). Vykorystannia termoelektrychnykh teplomiriv u medychnii diagnostytsi [Use of thermoelectric heat meters in medical diagnostics]. *Naukovy visnyk Chernivetskoho Universytetu. Fizyka. Elektronika – Scientific Bulletin of Chernivtsi University. Physics. Electronics, 4(1), 90-96.*
28. Gischuk V.S. (2012). Electronic recorder of signals from human heat flux sensors. *J.Thermoelectricity*, 4, 105-108.
29. Gischuk V.S. (2013). Electronic recorder with processing signals from heat flux thermoelectric sensor. *J. Thermoelectricity*, 1, 82-86.
30. Gischuk V.S. (2013). Modernized device for human heat flux measurements. *J. Thermoelectricity*, 2, 91-95.
31. Anatychuk L.I., Ivaschuk O.I., Kobylianskyi R.R., Postevka I.D., Bodiaka V.Yu., Gushul I.Ya. (2016). Thermoelectric device for temperature and heat flux density measurement "ALTEC-10008". *J.Thermoelectricity*, 1, 76-84.
32. Anatychuk L.I., Yuryk O.E., Kobylianskyi R.R., Roi I.V., Fischenko Ya.V., Slobodianiuk N.P., Yuryk N.E., Duda B.S. (2017). Thermoelectric device for the diagnosis of inflammatory processes and neurological manifestations of human vertebral osteochondrosis. *J.Thermoelectricity*, 3, 54-67.
33. Yuryk O.E., Anatychuk L.I., Roi I.V., Kobylianskyi R.R., Fischenko Ya.V., Slobodianiuk N.P., Yuryk N.E., Duda B.S. (2017). Osoblyvosti teplovoho obminu u patsientiv z nevrologichnymy proiavamy osteokhondrozu v poperekovo-kryzhovomu viddili khrebta [Features of heat exchange in patients with neurological manifestations of osteochondrosis in the lumbosacral spine]. *Trauma*, 18 (6).

Submitted 18.03.2021

L.I. Anatychuk *acad. National Academy of sciences of Ukraine*[1]
A.M. Kibak[1]


L.I. Anatychuk

[1]Institute of Thermoelectricity
of the NAS and MES of Ukraine,
1, Nauky str., Chernivtsi, 58029, Ukraine;
e-mail: anatych@gmail.com
[2]Yu.Fedkovych Chernivtsi National University,
2, Kotsiubynskyi str., Chernivtsi, 58000, Ukraine


A.M. Kibak

INDIVIDUAL AIR-CONDITIONERS FOR DOCTORS' CLOTHES

The paper discusses the possibility of using individual conditioners for doctors' clothes. Their use will improve the temperature conditions for the stay of medical personnel during long-term operations. To determine the most rational options for using these air conditioners, their physical models have been developed, and the advantages and disadvantages of the known options for individual conditioners for doctors' clothes have been analyzed. The paper also considers the prospects for the use of thermoelectric air conditioners.
Key words: air-conditioner for clothes, thermoelectric air-conditioner, thermal conditions, phase transition, doctor's clothes.

Introduction

General characterization of the problem. In recent years, extensive research has been pursued on the study of individual air conditioners for humans. Thus, in [1] their classification by air conditioning method and purpose was carried out. As a result of this classification, almost 20 new design features of air conditioners have been found, which can be useful in the development of air conditioners for both mass and special purposes. From the proposed classification, depending on the areas of application, individual air conditioners for doctors were identified as particularly promising. At the same time, their detailed study was not carried out in the work.

With the development of medical technology, modern methods of performing operations without incisions (radiosurgery, angiography, laparoscopy, etc.) are becoming more widespread [2]. At the same time, surgeons, nurses and technologists working with X-ray control methods are increasingly exposed to radiation hazards. To protect against radiation, medical personnel use special radiation-protective clothing [3]. With long-term use of such clothing, a problem arises that due to the lack of ventilation between the body and clothing, a significant overheating of the body occurs, which leads to increased fatigue and the inability to perform the assigned work [4].

To solve this problem, individual air conditioners are used. In [5 – 7], various options for the implementation of air conditioning are considered depending on the type of refrigeration or various design features. The most common options for providing air conditioning for medical staff are the use of phase transition and ambient air, on the basis of which real air conditioners are developed [8]. Also promising is

the use of air conditioning with thermoelectric converters. This is due to the presence of a number of advantages in such converters, namely: high reliability, the ability to provide both cooling and heating, the absence of harmful refrigerants, low maintenance costs, the ability to adjust the temperature in a wide range [9]. But with all these advantages, this type of conditioning has no real application.

Analysis of the literature. Today, the problem of air conditioning of clothes is solved by various methods. In particular, the known methods are based on the use of substances with high heat capacity; on the phase transition of a liquid (evaporation of water); on the use of ambient air and on cooling and heating due to thermoelectric effects.

In [4], a project is presented, the purpose of which was to develop a cooling vest using phase change material to increase the thermal comfort of the surgeon. This air conditioner provided some improvement in temperature conditions, but all results were based only on the subjective assessments of the surveyed medical workers. In addition, the design of such a vest was imperfect due to the low cooling efficiency and the need for constant replacement of the cooled elements.

In [5], designs of radiation protective clothing were proposed in which the solution to the problem of the level of protection against radiation, rather than the efficiency of cooling, is described in more detail. Therefore, there is a need for further study of this issue.

In [10], clothes with cooling for doctors are described, based on the absorption of thermal energy as a result of the phase transition of a substance. Such clothes are designed in the form of vests with channels filled with a special liquid (water, gel, etc.). Cooling in this case is carried out by evaporation of the liquid through a special porous outer surface of the air conditioner.

In [11], the method of cooling the body by blowing it with ambient air was used. Such an air conditioner is produced in the form of overalls with channels for the passage of air, which is forced into the clothes by an electric fan.

In [12 – 14] the possibility of using thermoelectric conditioners for clothes is considered. In most cases, such air conditioners are Peltier modules located in clothes (or in special devices that are attached to clothes), which cool or heat clothes depending on the direction of the electric current.

All of these options for individual conditioners for doctors' clothes have their own advantages and disadvantages. Therefore, it is important to consider the known methods of conditioning the clothes of doctors and determine the most promising of them.

The purpose of the proposed work is to determine the most rational options for known individual air conditioners for doctors' clothes and to study the possibility of using thermoelectric air conditioners.

Known options of individual air-conditioners for doctors' clothes

The most defining feature that distinguishes individual air conditioners from each other is the type of heat or cold sources. The efficiency of air conditioners depends on them in the first place. Among the main options are: the use of *heat and cold accumulators* (*with the presence of phase transitions of substances*); use of *ambient air* (*with the presence of electric fans*); use of an *electric heater*; use of a *catalytic heater*; the use of a *compression heat pump*; and the use of a *thermoelectric heat pump.* It is also possible to combine the above sources of heat and cold [1].

Today there are a number of companies that develop individual conditioners for doctors' clothes. Basically, these air conditioners use three types of cooling: the use of *heat and cold accumulators*; using *ambient air* and using *liquid cooling in combination with a heat pump*.

To determine the most rational options for individual conditioners for doctors' clothes, we will consider their real implementations and carry out a comparative analysis of their main parameters.

The Japanese company Kuchofuku Co. Ltd develops cooling clothing based on the intensification of heat exchange by air fans. The main product is an air-conditioned shirt. The use of such a shirt makes it possible for a long time to provide comfortable conditions for medical personnel, since the fans are connected to a lithium-ion battery pack, which can operate for up to 24 hours on a single charge, depending on the cooling mode [15]. The physical model of such clothing is shown in Fig. 1.

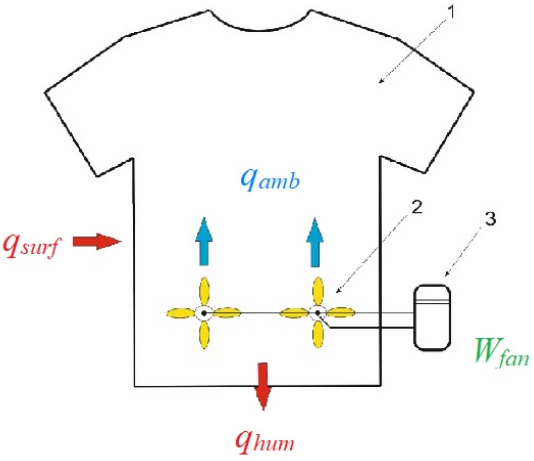

Fig. 1. Physical model of air conditioner for clothes using ambient air (fans): 1 - conditioned clothes; 2 - a system of electrically coupled fans; 3-power supply.

Where q_{hum} is the power of heat release from the human body; $q_{amb.}$ is the power of heat release from the ambient; $q_{surf.}$ is thermal power removed to the ambient; W_{fan} is power of the fan.

There are samples of special clothes for doctors, developed by the American company Coolshirt Systems. Their products are vests that are connected to special cooling systems. Further, these systems supply water with adjustable temperature to the vest to create optimal temperature conditions [16]. Such products are ideal for surgeons and medical staff while working in any operating room.

The products of the American company Polar Products are developed in a similar way. A special system for the surgeon's cooling consists of a cooling vest in which more than 15 meters of thin tubes are connected, through which the flow of cooling water passes. The system also includes a waterproof cooling tank, special couplings and insulated water pipes. For convenience, when transporting the tank, a wheeled cart is used [17]. The physical model of such variants of individual conditioners for doctors' clothes is shown in Fig. 2.

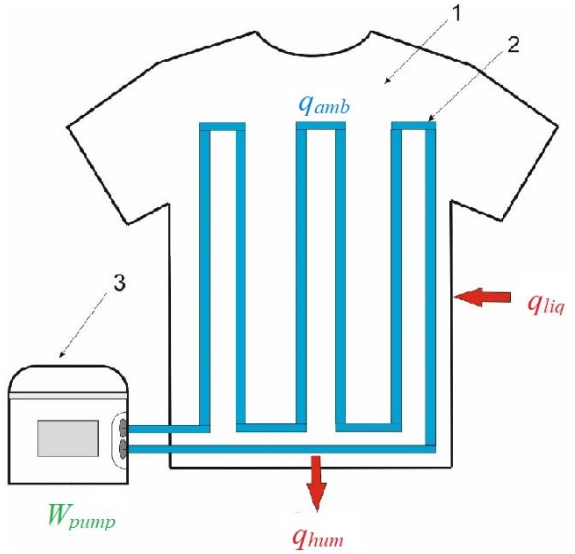

Fig. 2. Physical model of air conditioner for clothes using a circulating fluid system: 1 - conditioned clothes; 2 - a system of pipes through which chilled liquid circulates; 3 - a cooling tank with a pump.

Where q_{hum} is the power of heat release from the human body; q_{amb} is the power of heat release from the ambient; q_{liq} is thermal power removed to the ambient; W_{pump} is the power of the pump.

The most common type of cooling is the use of phase transition of the substance (Fig. 3). The following companies use this method: the German company E.COOLINE [18], the American company TechNiche [19], the Dutch company INUTEQ B.V [20] and the American company StacoolVEST [21]. Although the products of such companies have the same type of cooling, but the parameters of air conditioners can be quite different. First of all it depends on the working substance which will be used by conditioners, and also on the design features.

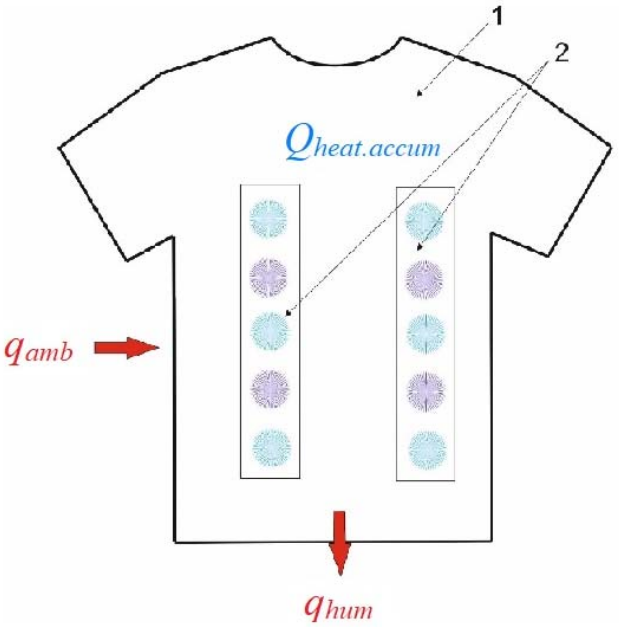

Fig. 3. Physical model of air conditioner for clothes using phase transition (cooling mode): 1 – conditioned clothes; 2 – cooling packages with a working substance (heat accumulator).

In Fig. 3: q_{hum} is the power of heat release from the human body; q_{amb} is the power of heat release from the ambient; $Q_{heat.accum}$ is the amount of heat absorbed by the working substance (heat accumulator).

Based on the products of the companies reviewed, Table 1 was created, which contains the main parameters of individual conditioners for doctors' clothes. As you can see, the parameters of various air conditioners can vary both within wide limits and in an insignificant range. One of the main parameters, the cooling temperature, in all the options presented is almost the same. That is, each air conditioner can provide approximately 10 °C cooling, which is sufficient. Despite this, there is a significant difference in weight, operating time and cost of air conditioners.

The *Coolshirt Systems* and *Polar Products* options are the most expensive, but they can still provide continuous cooling as they can be operated directly from an outlet. If necessary, there is a possibility of autonomous operation from batteries with a working time of about 6 hours. The weight of such air conditioners is not the largest, even taking into account the tubes that are located over the area of the clothing. A version of the air conditioner from Kuchofuku Co. Ltd is the most rational choice when considering cost and weight, as these figures are the smallest compared to others. At the same time, the operating time of such air conditioners is also one of the highest among those reviewed.

A wide range of phase change refrigeration air conditioners can compete with other options primarily due to cost and weight, and also due to the simplicity and reliability of the design itself. One of the significant drawbacks is the operating time, which strongly depends on environmental conditions (temperature, humidity).

Table 1

Parameters of individual air-conditioners for doctors' clothes

№	Companies that develop air-conditioners	Cooling type	Cooling type	Working time (h)	Mass (kg)	Cooling temperature (°C)	Working range (°C)	Electric components	Price ($)
1	Kuchofuku Co. Ltd (Japan) [15]	Air-conditioning using ambient air (with the availability of fans).	Body	8-24	0.5	5-10	15-35	Battery (6500 mA)	200
2	INUTEQ B.V. (Netherlands) [20]	Liquid cooling (working substance - water).	Body	8-48	0.7	5-10	20-25	-	150
3	E.COOLINE (Germany) [18]	Evaporative cooling	Body	2-24	1	Up to 12	24-32	-	150-200
4	TechNiche (USA) [19]	Liquid cooling with the use of a pump	Abdomen, chest, back	from 6	1	5-10	15-30	Power supply (12 V and 3 A)	1000
5	TechNiche (США) [19]	Cooling based on phase transition	Body	2-3	1-1.5	Up to 10	from 14	-	400
6	COOLSHIRT SYSTEMS (USA) [16]	Liquid cooling with the use of a pump.	Body	from 6	1.5-2	5-8	18-32	2A / 12B	1500
7	StacoolVEST (USA) [21]	Cooling based on phase transition	Body	1-3	2-2.5	5-10	20-30	-	190

Thermoelectric air-conditioners for doctors' clothes

As noted above, thermoelectric conditioners for doctors' clothes have no real use in practice. At the same

time, work is underway to make it possible to manufacture various design options for such air conditioners. It follows from the analysis of the literature that only three possible variants of thermoelectric air conditioners for doctors' clothes are mainly considered. All of them differ in the arrangement of thermoelectric converters - in a special backpack behind clothes, over the entire surface of clothes and in a device that acts only on the corresponding part of the human body. To further determine the advantages and disadvantages of each of the options, we will consider them in more detail based on known works.

Option A

The arrangement of thermoelectric converters in a special backpack behind clothes was studied in [22]. The air conditioner belongs to a surgical suit that provides a high degree of cooling and sterility. It includes a hood and vest that are loosely attached to the user's head and body, respectively. The hood has a large visor through which the user can see freely. The body is located above the user's head and under the hood. At the same time, it carries a significant part of the weight of the hood and is supported above the user's head by means of vertically extended support rods that are connected to the backpack. The casing houses a fan and a thermoelectric module. An exhaust fan is part of the backpack and forces air to be drawn in through the filter and then flow past the user's face. A fan in the backpack draws air downward around the user's upper body and expels it out of the vest through a filter.

This air conditioner is quite difficult to implement. At the same time, it is inappropriate to use it together with radiation-protective clothing. First, it is quite large, which is a significant disadvantage, as it is an additional burden on the surgeon, who already wears heavy radiation-protective clothing. Secondly, the cooling in this embodiment occurs from the outside of the user, which is inefficient for the torso, which is under clothing. The latter problem is solved by supplying cooled air from the backpack directly under the clothes, using a system of special channels. But at the same time it is necessary to understand the complexity of such a design in the implementation.

Option B

The next possibility of realizing a thermoelectric air conditioner for doctors' clothes is the use of thermoelectric converters, which are placed directly in the clothes. The physical model of this option is shown in Fig. 4. Where q_{hum} is the power of heat release from the human body; q_{amb} is the power of heat release from the ambient; q_x is thermal power absorbed on the cold side of thermoelectric converter; $W_{t/e}$ is the power supplied to thermoelectric module.

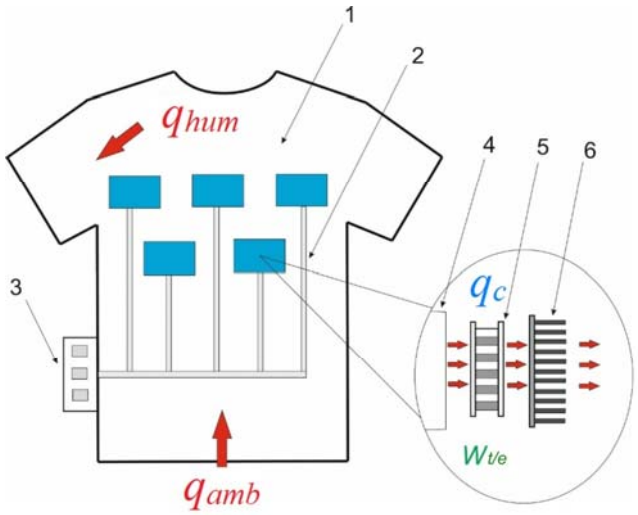

Fig. 4. Physical model of air conditioner for clothes using thermoelectric modules located on the area of conditioned clothes (cooling mode): 1 – conditioned clothes; 2 – electric connections; 3 – power supply; 4 – element for providing thermal contact; 5 – thermoelectric module; 6 – air heat exchanger.

The cooling system contains several thermoelectric modules, which are located in the area required by the user. They are then electrically connected to a DC power supply. On the cold side, the thermoelectric module is connected to the element to ensure thermal contact, and on the hot side - to the air heat exchanger to dissipate unnecessary heat into the environment.

The disadvantage of this air conditioning option is primarily associated with the removal of excess heat, since for high cooling efficiency it is assumed to use a thermoelectric air conditioner under radiation protective clothing. In this case, unnecessary heat from the hot surface of the module will not be dissipated into the environment, which negatively affects the overall cooling effect. In this case, the use of thermoelectric air conditioning on top of radiation-protective clothing will also lose in cooling efficiency. It is impractical to change the design of the radiation-protective clothing. For example, if you make extra holes in such clothes, you can solve the problem of removing excess heat. But it should be understood that this will reduce the ability of such clothing to perform its basic functions, namely the protection of medical personnel from radiation.

Option C

The third option of thermoelectric air conditioning is to create a special air conditioner that will cool only the relevant part of the human body. First of all, this means conditioning the head or neck.

Figs. 5 and 6 show physical models of thermoelectric device for cooling the neck and head of a person, respectively. Where q_{hum} is the power of heat release from human body; q_{amb} is the power of heat release from the ambient; q_c is thermal power absorbed on the cold side of thermoelectric converter; $W_{t/e}$ is the power supplied to thermoelectric module.

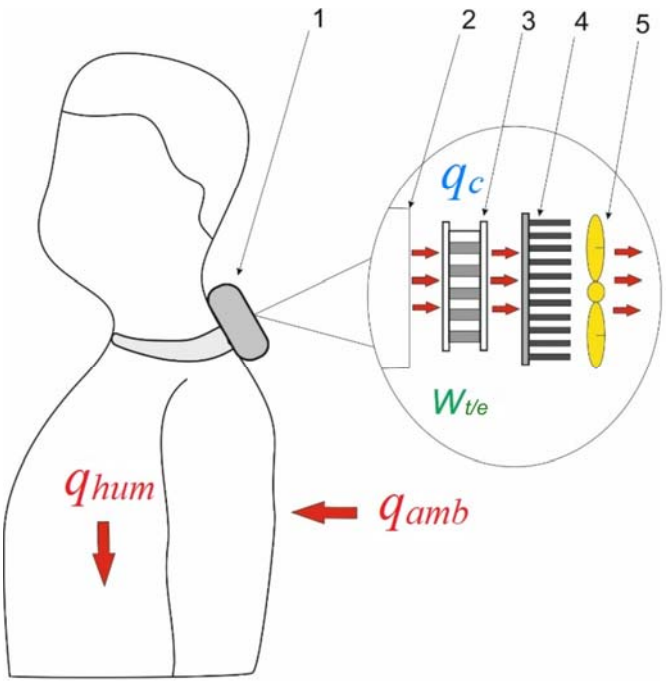

Fig. 5. Physical model of air conditioner for clothes using thermoelectric device with a directed action on neck area (cooling mode):
1 – thermoelectric device; 2 – element for providing thermal contact;
3 – thermoelectric module; 4 – air heat exchanger; 5 – fan.

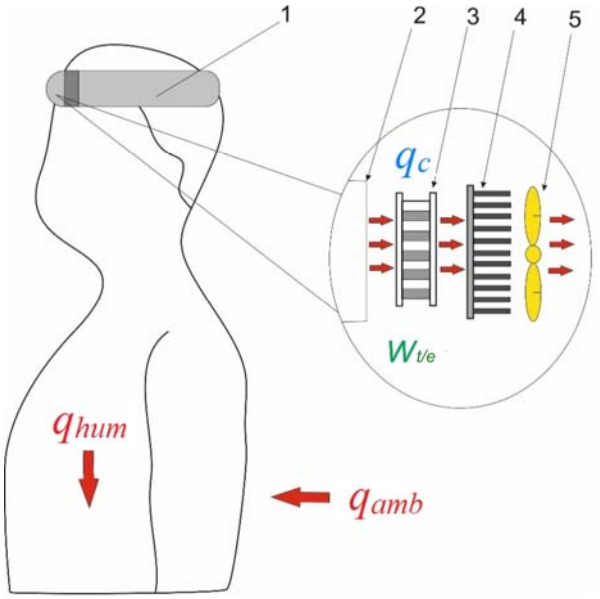

Fig. 6. Physical model of air conditioner for clothes using thermoelectric device with a directed action on head area (cooling mode): 1 – thermoelectric device; 2 – element for providing thermal contact; 3 – thermoelectric module; 4 – air heat exchanger; 5 – fan.

The thermoelectric device consists of a heat dissipation element that fits around the user's neck. The thermoelectric module, operating at low current and low voltage, is thermally connected on one side to the rear surface of the element, and on the other to an air heat exchanger. The presence of a fan allows efficient heat dissipation to the environment. A battery can be used to power the thermoelectric module.

The work [23] studied a thermoelectric device that corresponds to this option. The invention is a self-contained device that can be sized to fit the user's neck or forehead (or other body part) to provide cooling or heating. The device operates in a dry state, that is, without the need for any external coolant. It includes a thermal contact element that absorbs or dissipates heat. The surface of this element is directed towards the user and is pressed against the corresponding area of the human body. The Peltier thermoelectric module is in thermal contact with the surface of this element. The device preferably includes a power supply from a low voltage battery, a fan and the corresponding electronic circuits, and also provides temperature control on the element that absorbs / dissipates heat to select the operating mode. There is also an air heat exchanger, which allows you to effectively dissipate unnecessary heat. The device operates at low voltage and low current, but achieves a fairly efficient operation. The electronic circuits that are housed in this invention control the precise degree of heating or cooling and make compensatory changes, if necessary, in the power supply to reach a user-selected temperature. In cooling mode, the thermoelectric device will dissipate heat, thus cooling the user. The fan diverts heat flow from the air heat exchanger, which, in turn, leads to greater cooling of the surface returned to the user. As a result, effective cooling of the corresponding area of the human body is achieved.

Another variant of head cooling was studied in [24]. The invention relates to a new and useful personal protective system, such as the type of system used to provide a sterile barrier between medical staff and the patient. In this case, the system can operate in cooling mode, which is realized through the use of a

cooling strip located in the headdress. Such a strip includes Peltier thermoelectric modules that are attached to a flexible strip. There are also conductors, which are built into a flexible tape, through which current is supplied to thermoelectric modules. The presence of two sensors allows you to control the surface temperatures of the modules. The use of radiators and fans provides greater cooling efficiency. The modules and fans are powered by the battery. If necessary, the cooling strip can be placed not only in the hat, but also in other possible clothing options.

In [25], a personal heat control device is considered. The invention has many application aspects. It can be a stand-alone device or integrated into an accessory. One of the options for its use is to cool the human head. The device is made in the form of a helmet and contains thermoelectric modules, which are attached to the user's head thanks to an elastic band. At the same time, the cooling surfaces of the modules are directed towards the user's head, and the heating surfaces are directed away from the head. The heat pipes are thermally connected to the hot side of the modules at one end and to the heatsink at the other. They provide heat transfer from one place to another with minimal losses. The design of the device also provides a place for one or more power sources. Current is supplied to thermoelectric modules through electrical conductors, which can travel the same path as heat pipes.

The use of option C as thermoelectric cooling allows solving the problems that arose in the previous two options. At the same time, the cooling efficiency will be less, but still sufficient to ensure optimal conditions for the stay of medical personnel.

In general, the development of a thermoelectric air conditioner for doctors' clothes is very promising. All variants of such air conditioners considered in the work have their own advantages and disadvantages. To cool medical personnel who use radiation-protective clothing, it is most appropriate to choose a thermoelectric conditioner for clothing with conditioning only a certain part of the human body. At the same time, solving some of the described shortcomings of options A and B will allow to obtain air conditioners that will be on a par with the known individual air conditioners, or even outweigh them.

Conclusions

1. The use of liquid-cooled air conditioners is the most rational for the development of a self-contained and efficient air conditioning system that can be used by medical personnel in any operating room. This is achieved due to continuous running time and low cooling temperature. At the same time, their price is higher than the other options considered. Therefore, it is rational to use air conditioners based on phase transitions and air conditioners with air cooling, which are less efficient in air conditioning, but win in price.
2. Among the thermoelectric conditioners for doctors' clothes, the most expedient from the point of view of general efficiency is option C. Such a conditioner allows solving the shortcomings related to the mass and removal of excess heat from the hot side of the thermoelectric module.
3. It is also expedient to study thermoelectric air conditioners, which are presented by options A and B. Today, their efficiency is not high enough, but solving these problems will allow such air conditioners to compete with other individual air conditioners, or even outperform them.

References

1. Prybyla A.V. (2016). Physical models of individual air-conditioners (part one). *J.Thermoelectricity*, 1, 16 – 40.
2. https://www.tokb.ru/novosti/rentgenokhirurgiya-operatsii-bez-skalpelya-i-narkoza-vozvrashchayut-

zdorove-vzroslym-i-detyam/
3. https://ukrvet.ua/ua/dlya-chego-nuzhna-rentgenozashchitnaya-odezhda/
4. Lango Thomas, Nesbakken Ragnhild, Farevik Hilde, Holbo Kristine, Reitan Jarl, Yavuz Yunus, Mervik Ronald (2009). Cooling vest for improving surgeons' thermal comfort: A multidisciplinary design project. *Minimally Invasive Therapy,* 18:1, 1–10.
5. *Pat. US8710477B1* (2011). Robert L. Marchione. Radiation protective garment with forced ventilation and method.
6. *Pat. US6349412B1* (2000). W. Clark Dean. Medical cooling vest and system employing the same.
7. *Pat. US2007007982 9A1* (2005). Derek Duke. Medical garment ventilation system.
8. https://www.amazon.com/s?k=COMPCOOLER&ref=bl_dp_s_web_19826386011
9. *Pat. US2017002705 3A1* (2016). Joshua E. Moczygemba. Thermoelectric device cooling system.
10. *Pat. US10842205B2* (2017). Hoon Joo Lee, Matthew D. Nordstrom. Apparel thermo-regulatory system.
11. *Pat. US 20060191270 A1* (2006). Ray Warren. Air conditioning system for a garment.
12. *Pat. US 2002/0156509 A1* (2002). John A. Baker. Thermal control suit.
13. *Pat. US 2010/0107657 A1* (2010). Kranthi K. Vistakula. Apparel with heating and cooling capabilities.
14. http://dhamainnovations.com/
15. https://www.japantrendshop.com/kuchofuku-airconditioned-cooling-work-shirt-p-1202.html
16. https://coolshirt.com/
17. https://www.polarproducts.com/polarshop/pc/home.asp
18. https://www.e-cooline.com/
19. https://www.techniche-intl.com/products/
20. https://inuteq.com/
21. https://stacoolvest.com/
22. *Pat. US5655374A* (1996). Albert N. Santilli Jeffrey M. Kalman Richard O. McCarthy. Surgical suit.
23. *Pat. US6125636A* (1999). Charles E. Taylor Shek Fai Lau. Thermo-voltaic personal cooling/heating device.
24. *Pat. WO2017053232* (2017). Bryan Ulmer, Brian Vanderwoude, Beau Kidman, David Goldenberg. Personal protection system with a cooling strip.
25. *Pat. US8087254B2* (2005). Anthony Peter Arnold. Personal heat control device and method.

Submitted 15.02.2021

Анатичук Л.І. *акад. НАН України*[1,2]
Кібак А.М.[1]

[1]Інститут термоелектрики НАН і МОН України,
вул. Науки, 1, Чернівці, 58029, Україна;
e–mail: anatych@gmail.com
[2]Чернівецький національний університет
ім. Юрія Федьковича, вул. Коцюбинського 2,
Чернівці, 58000, Україна

ІНДИВІДУАЛЬНІ КОНДИЦІОНЕРИ ДЛЯ ОДЯГУ ЛІКАРІВ

У роботі розглядаються можливості використання індивідуальних кондиціонерів для одягу лікарів. Їх застосування дозволить покращити температурні умови перебування медичного персоналу під час проведення довготривалих операцій. Для визначення найбільш раціональних варіантів використання даних кондиціонерів розроблено їх фізичні моделі, а також проаналізовані переваги та недоліки відомих варіантів індивідуальних кондиціонерів для одягу лікарів. Також у роботі розглянуто перспективи використання термоелектричних кондиціонерів. Бібл. 25, рис 6, табл. 1

Ключові слова: кондиціонер для одягу, термоелектричний кондиціонер, теплові умови, фазовий перехід, одяг для лікарів.

Анатычук Л.И., *акад. НАН Украины*[1,2]
Кибак А.М.[1]

[1]Институт термоэлектричества НАН и МОН Украины,
ул. Науки, 1, Черновцы, 58029, Украина;
e–mail: anatych@gmail.com
[2]Черновицкий национальный университет
им. Юрия Федьковича, ул. Коцюбинского 2,
Черновцы, 58000, Украина

ИНДИВИДУАЛЬНЫЕ КОНДИЦІОНЕРЫ ДЛЯ ОДЕЖДЫ ВРАЧЕЙ

В работе рассматриваются возможности использования индивидуальных кондиционеров для одежды врачей. Их использование поможет улучшить температурные условия пребывания медицинского персонала в лечебных учреждениях во время проведения длительных операций. Для определения наиболее рациональных вариантов использования данных кондиционеров разработаны их физические модели, а также проанализированы преимущества и недостатки известных вариантов индивидуальных кондиционеров для одежды врачей. Также в работе рассмотрены перспективы використання термоэлектрических кондиционеров. Библ. 25, рис 6, табл. 1

Ключевые слова: кондиционер для одежды, термоэлектрический кондиционер, тепловые условия, фазовый переход, одежда для врачей.

References

1. Prybyla A.V. (2016). Physical models of individual air-conditioners (part one). *J.Thermoelectricity*, 1, 16 – 40.
2. https://www.tokb.ru/novosti/rentgenokhirurgiya-operatsii-bez-skalpelya-i-narkoza-vozvrashchayut-zdorove-vzroslym-i-detyam/
3. https://ukrvet.ua/ua/dlya-chego-nuzhna-rentgenozashchitnaya-odezhda/
4. Lango Thomas, Nesbakken Ragnhild, Farevik Hilde, Holbo Kristine, Reitan Jarl, Yavuz Yunus, Mervik Ronald (2009). Cooling vest for improving surgeons' thermal comfort: A multidisciplinary design project. *Minimally Invasive Therapy,* 18:1, 1–10.
5. *Pat. US8710477B1* (2011). Robert L. Marchione. Radiation protective garment with forced ventilation and method.
6. *Pat. US6349412B1* (2000). W. Clark Dean. Medical cooling vest and system employing the same.
7. *Pat. US2007007829A1* (2005). Derek Duke. Medical garment ventilation system.
8. https://www.amazon.com/s?k=COMPCOOLER&ref=bl_dp_s_web_19826386011
9. *Pat. US2017002705 3A1* (2016). Joshua E. Moczygemba. Thermoelectric device cooling system.
10. *Pat. US10842205B2* (2017). Hoon Joo Lee, Matthew D. Nordstrom. Apparel thermo-regulatory system.
11. *Pat. US 20060191270 A1* (2006). Ray Warren. Air conditioning system for a garment.
12. *Pat. US 2002/0156509 A1* (2002). John A. Baker. Thermal control suit.
13. *Pat. US 2010/0107657 A1* (2010). Kranthi K. Vistakula. Apparel with heating and cooling capabilities.
14. http://dhamainnovations.com/
15. https://www.japantrendshop.com/kuchofuku-airconditioned-cooling-work-shirt-p-1202.html
16. https://coolshirt.com/
17. https://www.polarproducts.com/polarshop/pc/home.asp
18. https://www.e-cooline.com/
19. https://www.techniche-intl.com/products/
20. https://inuteq.com/
21. https://stacoolvest.com/
22. *Pat. US5655374A* (1996). Albert N. Santilli Jeffrey M. Kalman Richard O. McCarthy. Surgical suit.
23. *Pat. US6125636A* (1999). Charles E. Taylor Shek Fai Lau. Thermo-voltaic personal cooling/heating device.
24. *Pat. WO2017053232* (2017). Bryan Ulmer, Brian Vanderwoude, Beau Kidman, David Goldenberg. Personal protection system with a cooling strip.
25. *Pat. US8087254B2* (2005). Anthony Peter Arnold. Personal heat control device and method.

Submitted 15.02.2021

NEWS
OF INTERNATIONAL THERMOELECTRIC ACADEMY

ANUKHIN ANATOLIY IVANOVICH

(Dedicated to 70th birthday)

On January 25, 2021, Anatoly Ivanovich Anukhin, a Corresponding Member of the International Thermoelectric Academy, a well-known specialist in the development of new thermoelectric materials, celebrated his 70th birthday.

A.I. Anukhin was born in Karelia; in 1952, together with his parents, he moved to Ukraine.

In 1974 he graduated from the Physics Department of Taras Shevchenko Kyiv State University (specialization - cryogenic materials science).

After graduation, he was sent to work at the “Saturn” Research Institute in the laboratory of thermoelectricity, where he was engaged in X-ray structural analysis of thermoelectric materials and epitaxial films on leucosapphire of refractory metals such as molybdenum, tungsten, vanadium and rhenium. At the “Saturn” Research Institute" A.I. Anukhin worked from 1974 to 1993 as an engineer, senior engineer, leading engineer. Since 1978, he led a group of developers of technology for obtaining high-performance thermoelectric materials. The technology was introduced at the pilot plant of the institute in the town of Glukhov, Sumy region. During the same period of time, he was engaged in the development of new thermoelectric materials for work in the low-temperature region (150-180 K).

The main directions of scientific research and practical developments of A.I. Anukhin include thermoelectric modules and thermoelectric semiconductor materials.

In 1991 he defended his Ph.D. thesis devoted to studies of the properties of low-temperature thermoelectric materials.

From 1995 to 2011 he worked in the research and production company "Modul".

A.I. Anukhin is the author of over 30 scientific papers and two inventions in the field of thermoelectricity.

The International Thermoelectric Academy, Institute of Thermoelectricity, “Journal of Thermoelectricity” Editorial Board congratulate the esteemed Anatoly Ivanovich Anukhin on his jubilee and wish him good health, happiness and further creative success.

IVANOVA IIDIIA DMITRIEVNA

(Dedicated to 80th birthday)

January 24, 2021 marks the 80th birthday of Lidiia Dmitrievna Ivanova, a Corresponding Member of the International Thermoelectric Academy, a well-known specialist in the field of physical and chemical analysis of semiconductors and the creation of new thermoelectric materials, leading researcher of the laboratory of semiconductor materials at the A. Baikov Institute of Metallurgy and Materials Science (IMET) of the Russian Academy of Sciences.

Lidiia Dmitrievna Ivanova was born on January 24, 1941 in Moscow. She began her career in 1960 in the laboratory of semiconductor materials at IMET.

In 1965 L.D.Ivanova graduated from the Faculty of Physics (Department of Semiconductors) of M. Lomonosov Moscow State University; in 1973 she defended her dissertation for the degree of Candidate of Technical Sciences.

Lidiia Dmitrievna is constantly working in the field of physical and chemical materials science and technology of thermoelectric materials. Under her leadership, research is being carried out on the development of new materials for various temperature levels for thermoelectric refrigerators and generators. Various methods have been developed for obtaining materials, both in the form of fine-crystalline materials and in the form of perfect single crystals. Comprehensive studies of thermoelectric, mechanical, X-ray structural, optical and transport properties of various thermoelectric materials are carried out. A number of studies were carried out jointly with scientists from various cities of Russia and different countries, both of near (Ukraine, Belarus, Georgia) and far abroad (Germany, France, USA). The obtained scientific results are published in scientific articles and reported at scientific conferences.

The main directions of scientific research and practical developments of L.D. Ivanova include materials science, growing of single crystals of thermoelectric materials, physicochemical analysis of thermoelectric materials.

Lidiia Dmitrievna is the author of about 140 scientific works, 6 certificates of authorship and patents for manufacturing methods, structure and composition of thermoelectric materials.

The method of growing single crystals based on solid solutions of bismuth and antimony chalcogenides was introduced at the Chernivtsi State University and at the Phonon LLC enterprise (Voronezh).

At the present time, Lidiia Dmitrievna is pursuing research in the field of a new direction in thermoelectricity, namely, the possibility of using nanotechnology to obtain highly efficient thermoelectric materials.

The International Thermoelectric Academy, “Journal of Thermoelectricity” Editorial Board congratulate the esteemed Lidiia Dmitrievna Ivanova on her jubilee and sincerely wish her good health, happiness and new creative achievements.

ARTICLE SUBMISSION GUIDELINES

For publication in a specialized journal, scientific works are accepted that have never been printed before. The article should be written on an actual topic, contain the results of an in-depth scientific study, the novelty and justification of scientific conclusions for the purpose of the article (the task in view).

The materials published in the journal are subject to internal and external review which is carried out by members of the editorial board and international editorial board of the journal or experts of the relevant field. Reviewing is done on the basis of confidentiality. In the event of a negative review or substantial remarks, the article may be rejected or returned to the author(s) for revision. In the case when the author(s) disagrees with the opinion of the reviewer, an additional independent review may be done by the editorial board. After the author makes changes in accordance with the comments of the reviewer, the article is signed to print.

The editorial board has the right to refuse to publish manuscripts containing previously published data, as well as materials that do not fit the profile of the journal or materials of research pursued in violation of ethical norms (for instance, conflicts between authors or between authors and organization, plagiarism, etc.). The editorial board of the journal reserves the right to edit and reduce the manuscripts without violating the author's content. Rejected manuscripts are not returned to the authors.

Submission of manuscript to the journal

The manuscript is submitted to the editorial office of the journal in paper form in duplicate and in electronic form on an electronic medium (disc, memory stick). The electronic version of the article shall fully correspond to the paper version. The manuscript must be signed by all co-authors or a responsible representative.

In some cases it is allowed to send an article by e-mail instead of an electronic medium (disc, memory stick).

English-speaking authors submit their manuscripts in English. Russian-speaking and Ukrainian-speaking authors submit their manuscripts in English and in Russian or Ukrainian, respectively. Page format is A4. The number of pages shall not exceed 15 (together with References and extended abstracts). By agreement with the editorial board, the number of pages can be increased.

To the manuscript is added:

1. Official recommendation letter, signed by the head of the institution where the work was carried out.

2. License agreement on the transfer of copyright (the form of the agreement can be obtained from the editorial office of the journal or downloaded from the journal website – Dohovir.pdf). The license agreement comes into force after the acceptance of the article for publication. Signing of the license agreement by the author(s) means that they are acquainted and agree with the terms of the agreement.

3. Information about each of the authors – full name, position, place of work, academic title, academic degree, contact information (phone number, e-mail address), ORCID code (if available). Information about the authors is submitted as follows:

authors from Ukraine - in three languages, namely Ukrainian, Russian and English;

authors from the CIS countries - in two languages, namely Russian and English;

authors from foreign countries – in English.

4. Medium with the text of the article, figures, tables, information about the authors in electronic

form.

5. Colored photo of the author(s). Black-and-white photos are not accepted by the editorial staff. With the number of authors more than two, their photos are not shown.

Requirements for article design

The article should be structured according to the following sections:

- *Introduction*. Contains the problem statement, relevance of the chosen topic, analysis of recent research and publications, purpose and objectives.
- *Presentation of the main research material* and the results obtained.
- *Conclusions* summing up the work and the prospects for further research in this direction.
- *References*.

The first page of the article contains information:

1) in the upper left corner – UDC identifier (for authors from Ukraine and the CIS countries);

2) surname(s) and initials, academic degree and scientific title of the author(s);

3) the name of the institution where the author(s) work, the postal address, telephone number, e-mail address of the author(s);

4) article title;

5) abstract to the article – not more than 1 800 characters. The abstract should reflect the consistent logic of describing the results and describe the main objectives of the study, summarize the most significant results;

6) key words – not more than 8 words.

The text of the article is printed in Times New Roman, font size 11 pt, line spacing 1.2 on A4 size paper, justified alignment. There should be no hyphenation in the article.

Page setup: "mirror margins" – top margin – 2.5 cm, bottom margin – 2.0 cm, inside – 2.0 cm, outside – 3.0 cm, from the edge to page header and page footer – 1.27 cm.

Graphic materials, pictures shall be submitted in color or, as an exception, black and white, in .opj or .cdr formats, .jpg or .tif formats being also permissible. According to author's choice, the tables and partially the text can be also in color.

Figures are printed on separate pages. The text in the figures must be in the font size 10 pt. On the charts, the units of measure are separated by commas. Figures are numbered in the order of their arrangement in the text, parts of the figures are numbered with letters – a, b, .. On the back of the figure, the title of the article, the author (authors) and the figure number are written in pencil. Scanned images and graphs are not allowed to be inserted.

Tables are provided on separate pages and must be executed using the MSWord table editor. Using pseudo-graph characters to design tables is inadmissible.

Formulae shall be typed in Equation or MatType formula editors. Articles with formulae written by hand are not accepted for printing. It is necessary to give definitions of quantities that are first used in the text, and then use the appropriate term.

Captions to figures and tables are printed in the manuscript after the references.

Reference list shall appear at the end of the article. References are numbered consecutively in the order in which they are quoted in the text of the article. References to unpublished and unfinished works are inadmissible.

Attention! In connection with the inclusion of the journal in the international bibliographic abstract database, the reference list should consist of two blocks: CITED LITERATURE and REFERENCES (this requirement also applies to English articles):

CITED LITERATURE – sources in the original language, executed in accordance with the Ukrainian standard of bibliographic description DSTU 8302:2015. With the aid of VAK.in.ua

(http://vak.in.ua) you can automatically, quickly and easily execute your "Cited literature" list in conformity with the requirements of State Certification Commission of Ukraine and prepare references to scientific sources in Ukraine in understandable and unified manner. This portal facilitates the processing of scientific sources when writing your publications, dissertations and other scientific papers.

REFERENCES – the same cited literature list transliterated in Roman alphabet (recommendations according to international bibliographic standard APA-2010, guidelines for drawing up a transliterated reference list "References" are on the site http//www.dse.org.ua, section for authors).

To speed up the publication of the article, please adhere to the following rules:

- in the upper left corner of the first page of the article – the UDC identifier;
- family name and initials of the author(s);
- academic degree, scientific title;

begin a new line, Times New Roman font, size 12 pt, line spacing 1.2, center alignment;

- name of organization, address (street, city, zip code, country), e-mail of the author(s);

begin a new line 1 cm below the name and initials of the author(s), Times New Roman font, size 11 pt, line spacing 1.2, center alignment;

- the title of the article is arranged 1 cm below the name of organization, in capital letters, semi-bold, font Times New Roman, size 12 pt, line spacing 1.2, center alignment. The title of the article shall be concrete and possibly concise;
- the abstract is arranged 1 cm below the title of the article, font Times New Roman, size 10 pt, in italics, line spacing 1.2, justified alignment in Ukrainian or Russian (for Ukrainian-speaking and Russian-speaking authors, respectively);
- key words are arranged below the abstract, font Times New Roman, size 10 pt, line spacing 1.2, justified alignment. The language of the key words corresponds to that of the abstract. Heading "Key words" - font Times New Roman, size 10 pt, semi-bold;
- the main text of the article is arranged 1 cm below the abstract, indent 1 cm, font Times New Roman, size 11 pt, line space spacing 1.2, justified alignment;
- formulae are typed in formula editor, fonts Symbol, Times New Roman. Font size is "normal" – 12 pt, "large index" – 7 pt, "small index" – 5 pt, "large symbol" – 18 pt, "small symbol" – 12 pt. The formula is arranged in the text, center aligned and shall not occupy more than 5/6 of the line width, formulae are numbered in parentheses on the right;
- dimensions of all quantities used in the article are represented in the International System of Units (SI) with the explication of the symbols employed;
- figures are arranged in the text. The figures and pictures shall be clear and contrast; the plot axes – parallel to sheet edges, thus eliminating possible displacement of angles in scaling; figures are submitted in color, black-and-white figures are not accepted by the editorial staff of the journal;
- tables are arranged in the text. The width of the table shall be 1 cm less than the line width. Above the table its ordinary number is indicated, right alignment. Continuous table numbering throughout the text. The title of the table is arranged below its number, center alignment;
- references should appear at the end of the article. References within the text should be

enclosed in square brackets behind the text. References should be numbered in order of first appearance in the text. Examples of various reference types are given below.

Examples of LITERATURE CITED

Journal articles

Anatychuk L.I., Mykhailovsky V.Ya., Maksymuk M.V., Andrusiak I.S. Experimental research on thermoelectric automobile starting pre-heater operated with diesel fuel. *J.Thermoelectricity*. 2016. №4. P.84–94.

Books

Anatychuk L.I. *Thermoelements and thermoelectric devices. Handbook.* Kyiv, Naukova dumka, 1979. 768 p.

Patents

Patent of Ukraine № 85293. Anatychuk L.I., Luste O.J., Nitsovych O.V. Thermoelement.

Conference proceedings

Lysko V.V. *State of the art and expected progress in metrology of thermoelectric materials.* Proceedings of the XVII International Forum on Thermoelectricity (May 14-18, 2017, Belfast). Chernivtsi, 2017. 64 p.

Authors' abstracts

Kobylianskyi R.R. *Thermoelectric devices for treatment of skin diseases*: extended abstract of candidate's thesis. Chernivtsi, 2011. 20 p.

Examples of REFERENCES

Journal articles

Gorskiy P.V. (2015). Ob usloviakh vysokoi dobrotnosti i metodikakh poiska perspektivnykh sverhreshetochnykh termoelektricheskikh materialov [On the conditions of high figure of merit and methods of search for promising superlattice thermoelectric materials]. *Termoelektrichestvo - J.Thermoelectricity,* 3, 5 – 14 [in Russian].

Books

Anatychuk L.I. (2003). *Thermoelectricity. Vol.2. Thermoelectric power converters*. Kyiv, Chernivtsi: Institute of Thermoelectricity.

Patents

Patent of Ukraine № 85293. Anatychuk L. I., Luste O.Ya., Nitsovych O.V. Thermoelements [In Ukrainian].

Conference proceedings

Rifert V.G. Intensification of heat exchange at condensation and evaporation of liquid in 5 flowing-down films. In: *Proc. of the 9th International Conference Heat Transfer.* May 20-25, 1990, Israel.

Authors'abstracts

Mashukov A.O. *Efficiency hospital state of rehabilitation of patients with color carcer.* PhD (Med.) Odesa, 2011 [In Ukrainian].